Hyperspectral Remote Sensing of Individual Gravesites –

Exploring the effects of Cadaver Decomposition on Vegetation and Soil Spectra

Eva Snirer

Department of Geography

McGill University, Montreal

August 2013

A thesis submitted to McGill University in partial fulfillment of the requirements of the degree of Masters of Science.

Abstract

The detection of clandestine graves is an emerging tool in hyperspectral remote sensing. Though previous studies have demonstrated that it is possible to use hyperspectral remote sensing techniques in detection of mass graves, there is a lack of studies demonstrating the feasibility to utilize this same technology for the detection of individual burial sites. This thesis summarizes the first year of a multi-year study to ascertain the detectable changes to vegetation and soil spectra caused by the chemicals released from a single decomposing body.

Eighteen pig (*Sus scrofa*) carcasses were buried in a temperate environment in Ottawa, ON. Three scenarios were examined; surface body deposition, 30 cm, and 90 cm soil cover. A Twin Otter aircraft with hyperspectral sensors covering the visible to shortwave infrared range was used to collect the imagery. In addition to the airborne sensor, a portable spectroradiometer was used to collect plant and soil spectra in the lab (the soil and plant samples were collected coincidentally with the airborne imagery).

Through chemical analysis of the soil collected both before site set up and coincidentally with the airborne imagery, I was able to determine the changes in chemistry and spectra caused by decomposing cadavers rather than just soil disturbance. Statistical analysis of the Chlorophyll and Carotenoids extraction demonstrates separability of vegetation into three categories: 1) background, 2) disturbed soil, shallow and deep graves, and 3) surface burials. Statistical analysis of the vegetation spectra corresponded to the chemical analysis in differentiating between background, disturbed soil, shallow and deep graves, and surface burials, as well analysis of the soil spectra allowed for separation into disturbed soil, shallow and deep graves, and surface burials.

Résumé

La détection des fosses clandestines (tombes) est un domain d'étude récent (un nouvel outil) dans la télédétection hyperspectrale. Bien que des études antérieures ont démontrés qu'il est possible d'utiliser des techniques de télédétection hyperspectrale pour la localisation des fosses communes, il y a un manque d'études démontrant la faisabilité d'utiliser cette même technologie pour la détection des tombes individuelles. Cette thèse se porte sur la première année d'une étude a long terme, elle constate que des changements sont détectables au niveau de la réponse spectrale de la végétation et de du sol. Ces changements sont causés par les produits chimiques libérées par un corps en décomposition. Dix-huit carcasses de porc (*Sus scrofa*) ont été enterrées dans un environnement tempéré à Ottawa, ON. Trois scénarios ont été examinés: la décomposition d'un corps déposé en surface, un corps enterré à 30 cm dans le sol, et un corps enterré à 90 cm dans le sol. Un avion Twin Otter avec des capteurs hyperspectrales couvrant les ondes visible à l'infrarouge du spectre électromagnétique ont été utilisés pour recueillir des images aériennes du site. En plus, un spectroradiomètre portable a été utilisé pour recueillir des signatures spectrales des plantes et du sol en laboratoire (les échantillons ont été collectés en même temps que l'imagerie aérienne). Grâce à l'analyse chimique du sol faite avant et après l'établissement du site, ainsi qu'en même temps que l'imagerie aérienne, j'ai déterminer que certains changements chimiques ainsi que des changements dans la réflectance sont causés par la décomposition des cadavres plutôt que par la perturbation du sol. L'analyse statistique des niveaux de chlorophylle et des caroténoïdes démontre une séparabilité de la végétation en trois catégories: 1) le fond, 2) les sols perturbés, les tombes peu profondes et les tombes profondes, et 3) les corps déposé en surface. L'analyse statistique des signatures spectrales de la végétation confirme à l'analyse chimique pour différencier entre le fond, le sol perturbé, les tombes peu profondes et profondes, et les corps décomposant en surface. L'analyse des signatures spectres de sol a aussi permis de séparer entre un sol perturbé, une tombe peu profonde ou profonde, ou un « enterrement » de surface.

Acknowledgements

I would like to express my gratitude to my supervisor, Dr. Margaret Kalacska, whose expertise, understanding, and limitless patience, considerably added to my graduate experience. By giving me the intellectual freedom to purse my research, for engaging me in new ideas, encouraging me to attend a number of conferences, and in demanding a high standard in all my academic endeavours, she contributed so much to my success. I would also like to thank Dr. Gail Chmura for her useful comments, observations, and over all engagement throughout the classwork and research that when into this master's thesis. In addition, I express my appreciation to Dr. Rick Parent from School of Criminology at Simon Fraser University, for taking time out from his research and teaching duties to serve as my external reader. I would like to offer my special thanks to the Flight Research Laboratory of the NRC Institute for Aerospace Research, without their support this project would not be possible. I wish to acknowledge the help provided by the members of the Service de police de la Ville de Montréal (SPVM) and Sûreté du Québec (QC) in the various stages of this project.

This research would not have been possible without their financial support of my supervisor; Teaching Assistantships, Graduate Research Scholarships, and Travel Grants awarded by the Department of Geography at McGill University, and McGill Financial Services for the Bursaries and Loans. Additionally the funding provided by the Canadian Police Research Centre (CPRC) facilitated in putting this project in motion. This support contributed the completion of this thesis and I gratefully acknowledge their support.

I would like to thank my fellow lab mates and officemates, especially after the 'computer tower dropped on foot' incident that impeded my ability to stand and walk for a few weeks. They contributed in various ways to the research described in this thesis and in many ways; this thesis is a testament to their help in support. Finally, I would like to acknowledge my family and friends for their support and encouragement throughout my study.

Table of Contents

List of Figures

Chapter 1

Chapter 2

Chapter 3

List of Tables

Chapter 1

Chapter 2

Chapter 3

List of Equations

Abbreviations

ARSL	Applied Remote Sensing Laboratory at McGill University
ASD	Analytical Spectral Devices, Inc.
CASI	Compact Airborne Spectrographic Imager
CDI	Cadaver Decomposition Island
CHL	Chlorophyll
CPRC	Canadian Police Research Centre
DRDC	Defense Research and Development Canada
FLAASH	Fast Line-of-sight Atmospheric Analysis of Spectral Hypercubes
FRL	Flight Research Laboratory
FWHM	Full Width at Half Maximum
GPS	Global Positioning System
HSI	Hyperspectral Imaging
NM	Nanometer (wavelength)
NRC	National Research Council
NSERC	Natural Sciences and Engineering Research Council of Canada
PMI	Postmortem interval
ROI	Region of Interest
RCMP	Royal Canadian Mounted Police
SASI	Shortwave IR Airborne Spectrographic Imager
SPVM	Service de police de la Ville de Montréal
SQ	Sûreté du Québec
SSHRC	Social Sciences and Humanities Research Council of Canada
SWIR	Short-Wave Infrared
VNIR	Visible Near Infrared
YOW	Ottawa MacDonald-Cartier International Airport

I. Chapter 1 - Introduction and Background

1.1. Introduction

Barring an individual unexpected stumbling upon a body in passing, most unknown buried bodies would remain undetected for long periods without the help of an informant who leads law enforcement to the site. Unfortunately, the informant's directions might be vague, misleading, or just wrong (Thomas, 2005). Traditional police methods of finding graves often involve large-scale gridded areas with personnel conducting 'finger-tip/line searches' and 'trial-and-error' excavations (Harrison & Donnelly, 2009). Ground penetrating radar (Schultz, Collins, & Falsetti, 2006), resistivity and magnetometry (Hunter & Cox, 2005), as well as Cadaver dogs have all been utilized as forms of gravesite detection. Each have their own associated strengths and limitations.

The detection of clandestine and previously unknown burial sites is of interest to police and first responder agencies (M. Aruda (SPVM), Pers. Communication 2011), as a large number of missing persons cases go unsolved each year, with an estimated 250 new cases added across Canada per year (M. Aruda (SPVM) Pers. Communication). Cases of missing persons arise both from victims of crime as well as situations where no foul play is suspected such as missing hunters and hikers (A. Croteau and C. Silva, Sûreté du Québec, Pers. Communication 2011). Being able to effectively investigate a large area and discover burial sites/remains is highly relevant with respect to First Responders such as Search and Rescue and Police, to whom this task falls.

A burial is an interference with a given environment; an inhumation of an external object into a pre-existing environment (either natural or developed), thereby disrupting and altering that ecosystem in content and form (Thomas, 2005). Being able to detect these interferences in the environment may make it possible to utilize them as a means to detect clandestine and previously unknown gravesites and bodies.

There are many ways to dispose of a body, but in cases of foul play, most perpetrators chose the most expedient manner. Wrapping a body in a garbage bag or in cloth such as a carpet or tarp, and then tossing the body in a ravine, deep bushes, or even a ditch are the most commonly encountered scenarios (S. Pharand, SPVM, Pers. Communication 2011). When burial is utilized, the perpetrator(s), often in a hurry to conceal the crime, usually digs the smallest hole possible, just deep enough to hide the body, and then makes it level with the ground so it does not attract immediate attention (Thomas, 2005). Drawing on these characterizations, taken from the literature, and from law enforcement, graves sites are considered as the burial of single individuals in soil or left on the surface of the ground for the purpose of this thesis.

Against this scenario, and its challenges and limitations the use of hyperspectral remote sensing detection of clandestine mass graves is emerging as a potential alternative tool in forensic investigations and studies (Kalacska, Bell, Sanchez-Azofeifa, & Caelli, 2009). However, the basis of detection is based on commonly held, but mostly unverified anecdotes of the duration of body decomposition and its effects on the surrounding environment that may manifest on the soil surface. Essentially the body is treated as being a form of environmental contamination. The simple question of how much body mass is necessary in order to produce a detectable change in the environment surrounding the body is currently unknown.

It is known that a decomposing body alters the surrounding soil environment and that the changes in the soil matrix alter plant chemistry (Forbes, 2008). Plants undergo a stress response due to chemical changes in the soil, which, in turn, change the levels of plant pigments. The subsequent changes in plant pigments are detectable by a hyperspectral sensor (Liu & Mason, 2009) (Figure 1).

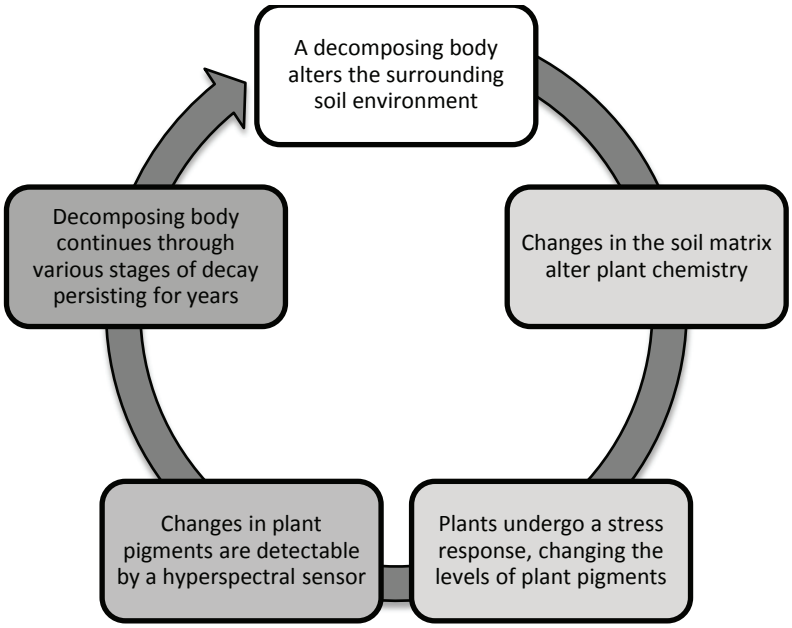

Figure 1. Proposed cycle of environmental effects following body decomposition

This thesis investigates the use of hyperspectral remote sensing as a technique for the detection of single body gravesites. The aim is to demonstrate how the presence of a decomposing body affects its surrounding environment, through detecting these effects with a hyperspectral sensor, monitoring how these effects change over the course of a year, and identifying the key chemicals released from bodies that are responsible for the detectable changes in spectral signatures.

Detection of gravesites through hyperspectral remote sensing is a multidisciplinary approach encompassing tools from a variety of disciplines such as physical anthropology, geology, plant physiology, and remote sensing. A brief review is necessary in order to illustrate how tools from the various disciplines contribute to this stud

1.2. Literature Review

The first section of this chapter presents a review of the current state of knowledge through outlining the literature on the decomposition process, release of decompositions products, absorption of these products by the soil and vegetation, and in turn, the effect these products have on spectral signatures **(Table 1).**

The following electronic databases were used:

1. Google Scholar (http://scholar.google.com)
2. Academic Search Complete (EBSCO) (http://web.ebscohost.com)
3. Proquest Research Library (Proquest) (http://proquest.com)
4. SCOPUS (http://www.scopus.com)
5. Web of Science (http://apps.isiknowledge.com

Table 1. Keywords used in Systematic Literature Review, " " indicate search phrases

Section	Keyword
cadaver decomposition	cadaver decomposition , "cadaver decomposition"
decomposition stages	cadaver, decomposition stages, terrestrial cadaver decomposition stages ,VOC
cadaver decomposition island	"cadaver decomposition island"
soil	"soil contamination, "remote sensing AND soil", decomposition fertilizer
plants	"nutrient uptake", "plant stress", "remote sensing plants"
remote sensing	"Cadaver decomposition", remote sensing, "grave detection", "remote sensing", fertilizer, spectral signatures

To develop as broad a sense of the state of knowledge as possible I decided to use the terms "cadaver" AND "decomposition" as the search terms within the different electronic databases mentioned previously (**Table 2**). This resulted in 5,290 hits solely within the Google scholar database.

Table 2. Search Results using separate cadaver and decomposition words as search terms

Keywords	Database	Results
cadaver decomposition	Google Scholar (http://scholar.google.com)	5290
	Academic Search Complete (EBSCO) (http://web.ebscohost.com)	80
	Proquest Research Library (Proquest) (http://proquest.com)	1435
	SCOPUS (http://www.scopus.com)	299
	Web of Science (http://apps.isiknowledge.com)	118

This scale of returns was too broad and wide reaching to be useful for this literature review. The search terms were therefore refined by searching for "cadaver decomposition" as an entire expression. By searching for "cadaver decomposition" as an expression, the numbers of returns were dramatically reduced (Table 3). This permitted me to focus on the 187 results of Google scholar and of the other databases. It is important to note that the results obtained between databases often overlapped; however, Google scholar seemed to pick up more 'grey' literature and book sections than the other databases.

Table 3. Using the phrase "cadaver decomposition" as query, and its impact on search results

Keywords	Database	Results
"cadaver decomposition"	Google Scholar (http://scholar.google.com)	187
	Academic Search Complete (EBSCO) (http://web.ebscohost.com)	9
	Proquest Research Library (Proquest) (http://proquest.com)	30
	SCOPUS (http://www.scopus.com)	33
	Web of Science (http://apps.isiknowledge.com)	15

This type of online search may leave out some key sources from the results. Some important sources may be in printed form only and neither available nor searchable online therefore, library catalogues search was conducted as well in order to ensure that relevant literature was represented.

Table 4. Cadaver Decomposition Island as query

Keywords	Database	Results
"cadaver decomposition island"	Google Scholar (http://scholar.google.com)	21
	Academic Search Complete (EB SCO) (http://web.ebscohost.com)	0
	Proquest Research Library (Proquest) (http://proquest.com)	0
	SCOPUS (http://www.scopus.com)	2
	Web of Science (http://apps.isiknowledge.com)	1

Table 5. Final query looking with various search terms

Keywords	Database	Results
soil chemistry, "remote sensing", decomposition	Google Scholar (http://scholar.google.com)	1480
	Academic Search Complete (EBSCO) (http://web.ebscohost.com)	61
	Proquest Research Library (Proquest) (http://proquest.com)	74
	SCOPUS (http://www.scopus.com)	1
	Web of Science (http://apps.isiknowledge.com)	1

Google scholar, in comparison to the other search engines used for this literature review often returned more results. However, it includes more 'grey' literature within, such as novels, newsletters, and commercial product manuals. This being said, SCOPUS and Proquest, seem to be a valid alternative to search for peer review articles, nonetheless books and theses are often left out from these searches.

Due to the multidisciplinary and rather unique subject nature of this thesis, I broke my literature review into four independent and more manageable categories of: taphonomy, soil chemistry, plant chemistry, and remote sensing in order to address all the necessary background **(Figure 2).**

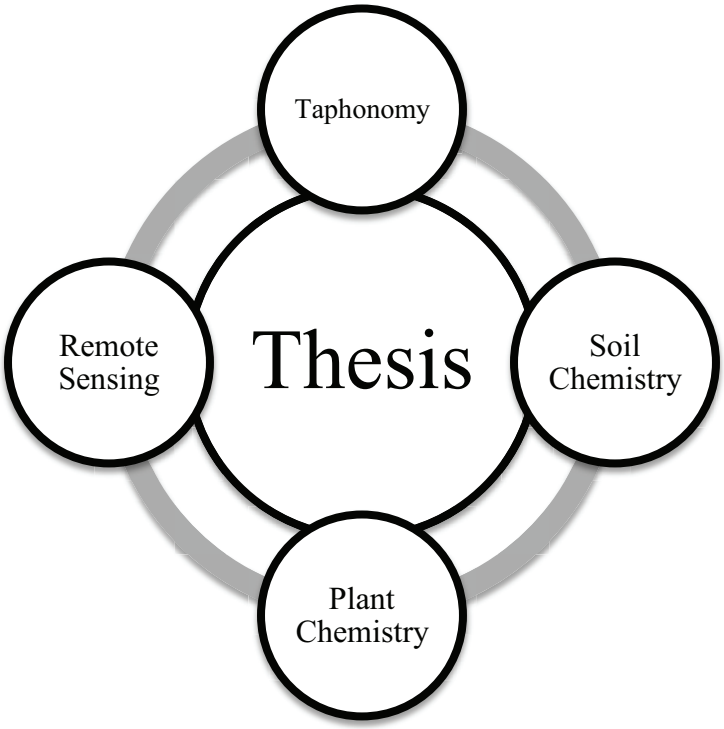

Figure 2. Discipline topics covered in literature review

2. Taphonomy

2.1. Decomposition stages

The term *taphonomy* was first introduced by the Russian geologist Efremov to encompass studies in what he referred to as the "transition of animal remains from the biosphere into the lithosphere" (Bristow, Simms, & Randolph-Quinney, 2011). The definition has since been refined to "Taphonomy concerns the comprehension of multiple factors which play a role in the disintegration and scatter of a body and its accouterments until they have been environmentally recycled and incorporated into the earth, its waters, its air, and its inhabitants" (Davis, 1997 in (Haglund & Sorg, 1997).

Decomposition can be described as the process by which the body breaks down and decays, finally resulting in skeletonization (Bristow et al., 2011). The brain is first to degrade while the bones and teeth are last (Klepinger, 2006).

Decay of a dead body is a continuum that is often difficult to divide into discrete defining categories; however, for the purposes of classification, post-mortem changes can be subdivided into several categories (Bristow et al., 2011, Goff, 2009). These categories include early post-mortem changes, decomposition, and skeletonization. Each has characteristics that can overlap with advancing time and vary depending on environmental conditions and the physiologic state of the body at the time of death (Catanese, Levy, & Catanese, 2010). At room temperature (21 degrees Celsius), decompositional changes usually become evident after about 24 hours, with a definite odour that represents a hallmark of decomposition (Prahlow, 2010). Decomposition is the aggregate of three processes: autolysis, putrefaction, and, environmental factors (Prahlow, 2010). As time advances, decomposition gradually increases (Tibbett & Carter, 2009).

2.2. Autolysis and Putrefaction

The decomposition of a cadaver results in the release of the chemical components of the body through autolysis and putrefaction (Stokes, Forbes, Benninger, Carter, & Tibbett, 2009). Autolysis refers to the post-mortem disintegration of the cells and tissues through the action of digestive enzymes (Larizza, 2010). Putrefaction is the result of microbiological activity usually initiated by autolytic processes, and is generally observed later in the post-mortem period. It may vary considerably depending on the surrounding environmental conditions (Wilson et al., 2007). The process does not occur at a uniform rate, and, consequently, decomposition may take place much earlier in some tissues than in others. As decomposition proceeds, and microorganisms continue to 'feed' on the corpse; gases, and fluids are produced and become evident within various parts of the body. As these processes are occurring, the entire body tends to become bloated (because of the gas production), and decomposition fluids are expelled, or purged, from the mouth, nose and other orifices (**Table 6)**. This red-brown fluid referred to as "purge fluid", adds organic matter as well as inorganic compounds such as, ammonium, calcium, potassium, magnesium, sodium, sulfur

and manganese to the soil matrix (Forbes, 2008; Harrison & Donnelly, 2009). During decomposition, materials from a cadaver will enter associated soil (grave soil) providing a localized pulse of nutrients and contaminants which eventually results in the formation of a concentrated island of fertility after a period of curtailment, also known as a cadaver decomposition island (CDI)(Carter, Yellowlees, & Tibbett, 2007). The initial release of cadaveric fluids on aboveground bodies can occur as early as 48 hours after death during warm summer months (Tibbett & Carter, 2009). There are environmental factors that affect the decomposition process and it is necessary to note these since they can influence the presence and extent of a CDI (Carter et al., 2007).

Table 6. Comparison of the stages of decomposition in above and below ground cadavers

Above Ground	Below Ground
Fresh	Fresh
Bloat	Inflated
Active Decay	Deflation and Decomposition
Advanced Decay	Disintegration
Dry and Remains	Skeletonization

(Tibbett & Carter, 2009)

In above-ground bodies, the *Advanced Decay* stage is the stage which evidences the greatest amount of nutrient release, whereas in below-ground bodies, the peak of nutrient release occurs in the *Deflation* and *Decomposition* stage (**Table 6**) (Tibbett & Carter, 2009).

2.3. Environmental factors

All aspects of the nature and rate of decomposition are dependent upon the immediate environment (Klepinger, 2006). There are several key environmental factors that play important roles in the decomposition process (**Table 7**) (Wilson et al., 2007).

Table 7. Summary of Factors Affecting the Rate of Decomposition

Factors that Accelerate Decomposition	Factors that Decelerate Decomposition
Small body size	Large body size
Open wounds	Uninjured body
Exposed flesh	Clothing or wrapping
Warm, humid climate	Container
Moist or acidic soil	Burial
Scavenging animals	Cold climate
Insect activity	Alkaline soil
Exposure to air	Submergence in water

(Modified after (Goff, 2009)

Variability in temperature is the most important factor influencing the rate of decomposition of a corpse (Swann, Forbes, & Lewis, 2010). Heat greatly increases the decomposition process, while cold impedes it (Carter, Yellowlees, & Tibbett, 2008). Currently the lowest temperature at which mammalian tissue has been shown to decompose is two degrees Celsius (Carter et al., 2008).

Bodies buried in soil typically decompose at a slower rate compared to those left open to air (Swann et al., 2010). An old '*rule*' that some forensic pathologists utilize is the following: one week in on surface exposed to air equals eight weeks buried in soil in terms of progress of decomposition (Prahlow, 2010). Though no experimental evidence verifies and supports this estimation (Tibbett & Carter, 2009).

Animal scavengers, such as rodents, larger carnivores, or insects, are

another environmental factor that can significantly contribute to the decomposition process (Prahlow, 2010). If insects and other animals are present, the decomposition process is significantly accelerated both in surface and below-ground burials. Small and large animals will feed on the body, and can "deflesh" a body very quickly (Prahlow, 2010). Mice, fox, dogs, and even deer will pick up old bones and carry them off, scattering a skeleton over a wide area. Cadavers that are not readily consumed by vertebrate scavengers are subject to microbial and invertebrate decomposition (Carter et al., 2007). The overwhelming majority of soft tissue destruction during decomposition is due to feeding by insects (Swann et al., 2010). The liquid 'soup' in which the maggot mass develops also envelops surrounding leaf litter, vegetation and topsoil (Hanson et al., 2009) increasing the area over which nutrients are deposited. If insects are absent from the corpse, decomposition will proceed at a significantly slower rate (Swann et al., 2010)

Through a combination of autolysis, putrefaction, and environmental, animal, and insect factors, a dead body will ultimately be stripped of most or all of its soft tissues and be left only as skeletal remains (Prahlow, 2010). Portions of the skeleton exposed to direct sunlight dry out more quickly, bleach, and may eventually exfoliate on the exposed surface. The drying and bleaching can happen in a matter of a few months, even in temperate latitudes (Klepinger, 2006). The process of decomposition may require days, months, or even years to be completed depending on the surrounding environment (Swann et al., 2010). The skeletal remains will also continue to alter the surrounding soil environment adding minerals to the soil (Tibbett & Carter, 2009).

2.4. Cadaver Decomposition Island (CDI)

The increased recognition of the soil-cadaver interface in the last decade has led to research on soil analysis in a taphonomic context gaining significant momentum (Hanson et al., 2009). This marks a shift from traditional studies of the body itself and the aboveground activity of insects and scavengers to the grave soils immediately surrounding it (Tibbett & Carter, 2009). The formation and

ecology of grave soil represent a dynamic medium of complex interactions with the capability to rapidly respond to ground disturbances resulting from the input of a cadaver; a nutrient-rich habitat with a heavy, indigenous microbial flora (Hanson et al., 2009). Decomposition of a cadaver in soil provides a localized pulse of nutrients, the compounds and materials produced throughout the various stages of decomposition produce a concentrated island of fertility surrounding the cadaver (***Figure 3***), known as the cadaver decomposition island (CDI). Changes in the vertical and lateral extent of the CDI are also known to occur over time (Carter & Tibbett, 2008).

Figure 3. Pig Carcass demonstrating CDI effect on vegetation (Photo by author)

3. Soil Structure and Chemistry

How cadaver decomposition is affected by and in turn affects soil composition relates to the basic characteristic of the soil. Soil is a mixture of four components: mineral particles, organic matter, water, and air in varying proportions microorganisms (Ruffel & McKinley, 2008). Soil is a natural body, having both mineral and organic components in addition to physical, chemical, and biological properties. Most soil types are dynamic and change over time depending on moisture, temperature and the way it is utilized (Hall, 2007). For example releases of such elements as nitrogen, phosphorus, and sulphur from organic matter through mineralization are slowed when temperatures are low (Jones, 2003).

The particle size of the soil will be a factor in determining its water and nutrient holding capacity and its pH (Foth, 1990). Soil pH affects the mobility of nutrients in the soil, which in turn affects the ease with which the vegetation surrounding graves can absorb them (Haslam & Tibbett, 2009; Kabata-Pendias, 2011).

Soil organic matter is a mixture that includes leaves, twigs, plant and animal parts in various stages of decomposition, and microorganisms (Ruffel & McKinley, 2008). The decayed remains of plant and animal materials, partially transformed by bacterial action, are collectively called humus (Gabler, 2009). Humus is an important catalyst in chemical reactions in the soil that help plants to extract nutrients (Haider & Schäffer, 2009). Humus also supplies nutrients and minerals to the soil (Gabler, 2009). Nutrients in a normal soil matrix are rarely, if ever, uniformly distributed in soils (Gregory, 2006).

Quantitatively, trace elements are negligible chemical constituents of soils, but are critical to plant growth and a deficiency or excess of a particular nutrient can drastically reduce growth rates or even kill plants (Hall, 2007; Kabata-Pendias, 2011). Although trace elements are mainly inherited from the parent material, their distribution within the soil profiles and their partitioning between

the soil components reflect various pedogenic processes as well as the impact of external, especially anthropogenic factors such as excavating a cavity then backfilling will alter distribution of the trace elements (Kabata-Pendias, 2011).

Knowledge of the total composition of the soil solution or any nutrient solution is essential for predicting plant uptake of nutrients or plant growth (Kabata-Pendias, 2011). Factors such as rainfall, evaporation, and plant transpiration can change trace element concentrations in soil solutions by more than tenfold, whereas the observed variations for major nutrients (Ca, Mg, K, Na, NO_3^-, and P) are much less (Kabata-Pendias, 2011).

In terms of burials and cadaver decomposition, the type of soil matters in terms of how rapidly a cadaver decomposes. The soil type of grave sites is likely to vary based with local environmental factors such as vegetation and its associated soil microbiology, climate, geology, topography or aspect and age (Aitkenhead-Peterson, Owings, Alexander, Larison, & Bytheway, 2012). Nevertheless, the release of chemicals from the body, the rapidity and how far chemicals from the body spread around the body will be influenced by the amount of soil organic matter, the pH, moisture, and temperature (Larizza, 2010). In soils with high clay moisture content, the decomposition of the cadaver will be hindered (Larizza, 2010). Soil chemistry has been used to estimate post mortem interval (PMI), especially under decomposing or dry remains of pigs and humans, however it is still a new field of research and needs to be further developed (Larizza, 2010).

Decomposition is not just a breakdown of material; it is a creation of new substances (Haider & Schäffer, 2009). Cadaver decomposition can have a significant and persistent effect on grave soil chemistry (Aitkenhead-Peterson et al., 2012). New compounds are produced when a body's chemicals, which normally do not associate with each other, mix together due to the breakdown of the body (Goff, 2009). For example, if the soil pH is low, ammonia (NH_3) from the decomposition of body protein may be converted to ammonium (NH_4^+) when then can be utilized by surrounding plants (Swann et al., 2010).

The decomposition of a cadaver releases nutrients which results in the formation of an enriched environment for vegetative growth (Benninger, Carter, & Forbes, 2008).Various studies involving human cadavers and pig cadaver proxies have found that the grave soil levels of calcium, potassium, sodium, dissolved organic nitrogen, phosphorus were an 'order of magnitude higher within the grave soils than is normally observed in natural environments' (Aitkenhead-Peterson et al., 2012). It is currently understood that nutrient concentrations remain elevated in the soil even after the body has skeletonized, but it is not known how long this effect can persist (Kabata-Pendias, 2011).

The soil is a complex, ever-changing matrix supporting a complex living ecosystem (Hall, 2007). The most visible aspect of the ecosystem is vegetation, which in turn supports, and depends on, a range of larger organisms such as insects, mites, spiders, earthworms and ants as well as small organisms including bacteria, fungi and actinomycetes (Swann et al., 2010). These organisms are active in converting soil nutrients into plant available forms (Swann et al., 2010).

3.1. Plant-Grave Soil Relationships

Plants and soil form an integrated system, vegetation influences soil processes and vegetation processes are influenced by the soil matrix (Prasad, Sajwan, & Naidu, 2006). At present, there are 15-22 trace elements which are considered to be essential for all plants (**Table 8**) (Sharma, 2006, Kabata-Pendias, 2011). Although essential for growth, at higher concentrations some also can also have toxic effects on cells. This is worth bearing in mind when considering that cadaver decomposition acts like an application of fertilizer on localized area and may create similar 'fertilizer burn' toxic effect if any nutrient level gets too high (Kabata-Pendias, 2011). In general, under cooler conditions, plant growth is slower and means slower uptake of a number of nutrients including N, P, K, S, Mg, B, and Zn (Jones, 2003).

A body decomposing on the surface or in the soil matrix is essentially a source of nutrients and trace elements for the vegetation to utilize. Some elements are more susceptible to phytoavailability than others. The ability of different plants to absorb trace elements varies greatly, however, their accumulating ability illustrates some general trends such as a linear absorption response to some elements such as cadmium (Cd), boron (B), bromine (Br), cesium (Cs), and rubidium (Rb) are exceptionally easily taken up by vascular plants such as Grasses, while barium (Ba), titanium (Ti), zirconium (Zr), scandium (Sc), bismuth (Bi), gallium (Ga) and, to an extent, iron (Fe) and selenium (Se), are but slightly available to the vegetation (Kabata-Pendias, 2011)

Table 8. Soil nutrients deemed essential for plant growth

Nutrient	**Element**
Primary	Nitrogen (N)
	Phosphorus (P)
	Potassium (K)
Secondary	Calcium (Ca)
	Magnesium (Mg)
	Sulfur (S)
Micronutrients	Boron (B)
	Chlorine (Cl)
	Copper (Cu)
	Iron (Fe)
	Manganese (Mn)
	Molybdenum (Mo)
	Sodium (Na)
	Vanadium (V)
	Zinc (Zn)

(Kabata-Pendias, 2011)

The absorption of trace elements by roots can be both passive (non-metabolic) and active (metabolic), but there are disagreements concerning which

type is critical to certain elements (Kabata-Pendias, 2011). Mechanisms of uptake differ depending on the given element. Lead (Pb) and nickel (Ni) are preferably absorbed passively, while copper (Cu), molybdenum (Mo), and zinc (Zn) are preferably absorbed actively (Kabata-Pendias, 2011).

When biological and structural properties of root cells are altered such as those that occur when the plant is stressed, all elements are taken up passively (Kabata-Pendias, 2011). This is also the case when concentrations of elements pass over a threshold value for a physiological barrier (Kabata-Pendias, 2011).The distribution and accumulation patterns of trace elements vary for each element, species of plant, and growth season (Kabata-Pendias, 2011).What is known is that the rate of element uptake will positively correlate with its available pool at the root surface (Kabata-Pendias, 2011). Although plants adapt to chemical stress, they may also be very sensitive to an excess of a particular trace element but toxic concentrations of these trace elements in plant tissues can be challenging to establish (Catanese et al. 2010).

The nutrients – nitrogen (N), phosphorus (P), potassium (K), calcium (Ca), and magnesium (Mg) – are required in larger amounts than other plant nutrients, hence termed "macronutrients" (Hall, 2007). Levels of potassium and nitrogen are closely related in most plants (Jones, 2003). Magnesium plays an important part in photosynthesis, being part of the chlorophyll molecule (Jones, 2003).

4. Plant physiology

Plant roots, can be extremely destructive of bone. Although seemingly delicate, roots and shoots can exert enormous pressures that are sufficient to force apart the sutures of the skull and various other bones (Gunn, 2008), these fine roots can travel through the medullary cavity (White & Folkens, 2005) and split long bones lengthwise enabling more rapid demineralization and release of bone minerals into the soil matrix (Dix & Graham, 2000).

In order to be considered useful vegetation for detecting grave sites plant

species must meet certain requirements: suitable accumulation rate of pertinent elements that alter the vegetation pigments responsible for the changes in spectral signatures, be present in large amounts in the ecosystem under investigation, and be easy to identify and sample (Dix & Graham, 2000). An ideal plant would have a prominent and long term presence, and have a strong correlation between its accumulation of nutrients and the nutrient levels in the soil matrix (Dix & Graham, 2000).

Plant succession is the process of one plant community replacing another, and begins after a disturbance to the ecosystem such as the placement of a body on the surface or burial in the soil (Gregory, 2006; Gunn, 2008). Plant succession will be affected by the nature of the soil, exposure to sunlight, the surrounding vegetation and the time of year at which burial takes place (Gunn, 2008). Assuming that the grave surface was left bare after body disposal, one can expect to observe that the plant composition is initially dominated by species that specialize in colonizing disturbed ground/bare soil (Gunn, 2008). A typical succession pattern would be grasses and herbaceous plants, followed by shrubs and then trees. However, this does not mean that tree species would be absent until long after a grave was dug, if present in the seed bank, tree seeds will germinate and their seedlings grow as soon as the conditions are suitable (McCook, 1994)

Chloroplasts in the leaves of most plants contain two major kinds of chlorophyll (Stern, Bidlack, & Jansky, 2008). Chlorophylls are the main photosynthetic pigment and control the amount of solar radiation that a leaf absorbs (Blackburn, 2007) Chlorophyll a is blue-green in color and chlorophyll b is yellow-green in color (Gabler 2009). Other such pigments include carotenoids (yellowish to orange pigments) and anthocyanins which are water-soluble flavonoids (Blackburn, 2007). Chlorophyll concentration (Chl) in higher plant leaves changes throughout different stages of plant development and is affected when terrestrial vegetation is exposed to various kinds of natural and anthropogenic stresses (Carter & Tibbett, 2008). Remote determination of Chl

concentration from near and far distance by non-invasive methods is therefore a good means to detect physiological states and stress conditions in plants (Gitelson & Merzlyak, 1998).

5. Remote Sensing

5.1. Basic Principles

Remote sensing is the acquisition of information about an object without physically touching it (Konecny, 2002). This is accomplished through the use of instruments to measure the interaction of electromagnetic energy from a source such as the sun, with a physical object **(Figure 4**). This energy is reflected, transmitted, and/or absorbed (Palmer & Grant, 2010).

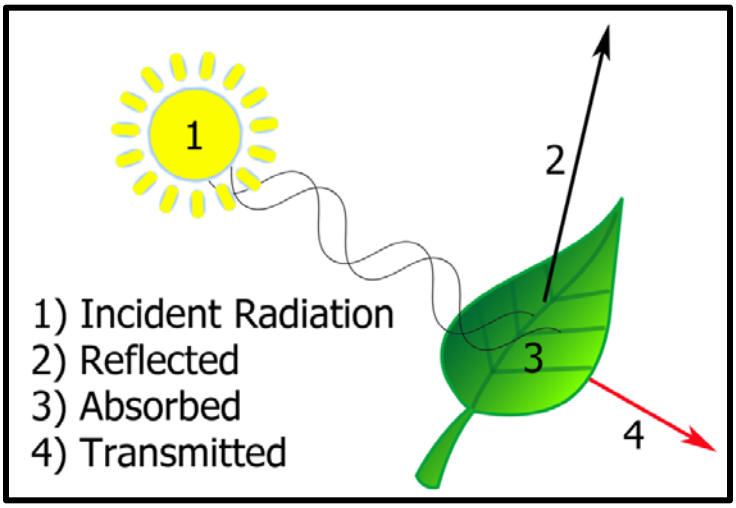

Figure 4. Interaction of electromagnetic energy from a source with a physical object

The reflectance and absorption of electromagnetic energy at various wavelengths by an object is of crucial importance for remote sensing and varies for different spectral ranges for a particular object (Konecny, 2002). The spectral reflectance of almost all different materials can be measured in the laboratory or in the field. Because objects have unique spectral features they can, in theory, be

identified from remote sensing imagery according to their unique spectral characteristics (Xie, Sha, & Yu, 2008).

Reflectance is the ratio of the amount of light leaving a target to the amount of light striking the target (Palmer & Grant, 2010). The reflection can be specular (in the mirror direction), diffuse (scattered into the entire hemisphere), or a combination of both. Most objects are a mixture of both.

5.2. Hyperspectral Remote Sensing

The spectral resolution of a remote sensing system can be described as its ability to distinguish different parts of the range of measured wavelengths (Smith, 2012). An "image" produced by a sensor system can consist of one very broad wavelength band, a few broad bands, or many narrow wavelength (Figure 5). The names usually used for these three image categories are panchromatic, multispectral, and hyperspectral, respectively (Konecny, 2002).

In hyperspectral imagery, the data source includes ten or more, and usually hundreds of bands of data (S. Prasad, Bruce, & Chanussot, 2011). The bandwidth of the data typically ranges from 1 to 15 nanometers (Palmer & Grant, 2010). These bands provide a wealth of information regarding the physical and chemical nature of different objects in the scene imaged by the sensors.

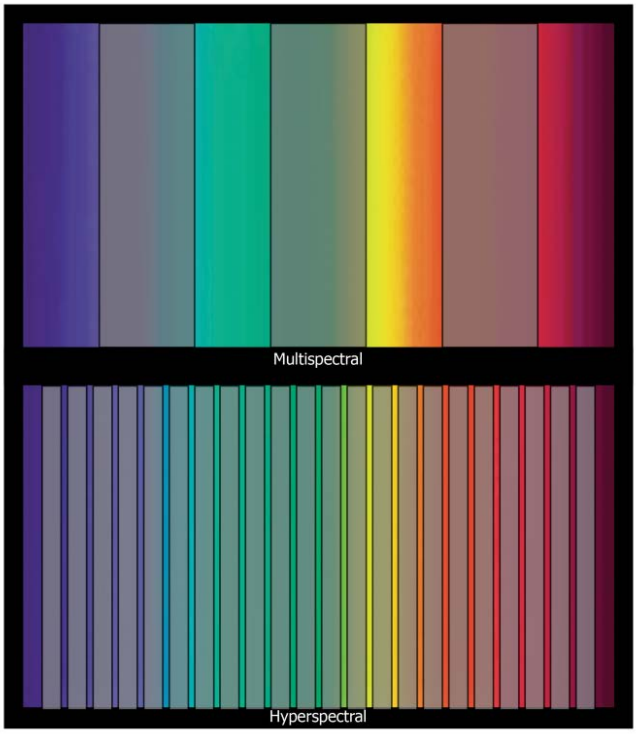

Figure 5. The grey bars represent spectral bands with the number and width of multispectral bands (top row) compared to the number and width of hyper- spectral bands (bottom row) in the same area demonstrating the greater amount of detail available in hyperspectral data.

5.3. Spectral Signature of Soil

Soil, like any other Earth surface cover, is a mixture of constituents, and this creates variations. These variations are information-bearing, not noise (Landgrebe, 2003). The manner in which the small subtle differences in the mixture reflect the illuminating light results in the differences in the data (Landgrebe, 2003).

Soil spectra vary with the mineralogical properties of the soil and also its moisture status. The latter varies temporally and spatially (Mather & Koch, 2011). Soil has been traditionally analyzed using chemical and physical analytic techniques, however, it is possible to utilize hyperspectral remote sensing in both lab and field conditions to assess soil (Rossel, Walvoort, McBratney, Janik, &

Skjemstad, 2006). Using reflectance, several direct and indirect soil properties, as well as soil contamination characteristics, can be extracted. The reflectance however represents only the surface and cannot provide information on the soil profile (Schwartz, Eshel, & Ben-Dor, 2011).

5.4. Vegetation Spectra

The concept of using plants as indicators for soil contamination has been around for many years (Schwartz et al., 2011). There are three main reasons for this: 1) inorganics in general do not exhibit characteristic absorption features in the VNIR-SWIR wavelength region; 2) the plant's root system extracts and transports contaminants to the aboveground plant parts, and 3) soil is rarely bare; it is often covered with vegetation (Schwartz et al., 2011).

While the reflection on smooth object surfaces is simple, the interaction of energy in plants is more complicated (Konecny, 2002). Green vegetation has a distinctive spectrum (Gates, Keegan, Schleter, & Weidner, 1965). Reflectance is relatively low in the visible range, but is higher for green light than for red or blue, producing the characteristic 'green peak' in reflectance responsible for our perception of vegetation being green (**Figure 6**) (Gitelson, Gritz, & Merzlyak, 2003).

Photosynthetic pigments are intimately associated to the biochemical reactions of photosynthesis. They also govern light transfer in the leaf and thus drive leaf optical properties such as reflectance or transmittance (Peñuelas, Gamon, Fredeen, Merino, & Field, 1994). This offers the opportunity of using measurements of reflected radiation as a non-destructive method for quantifying pigments (Blackburn, 2007).

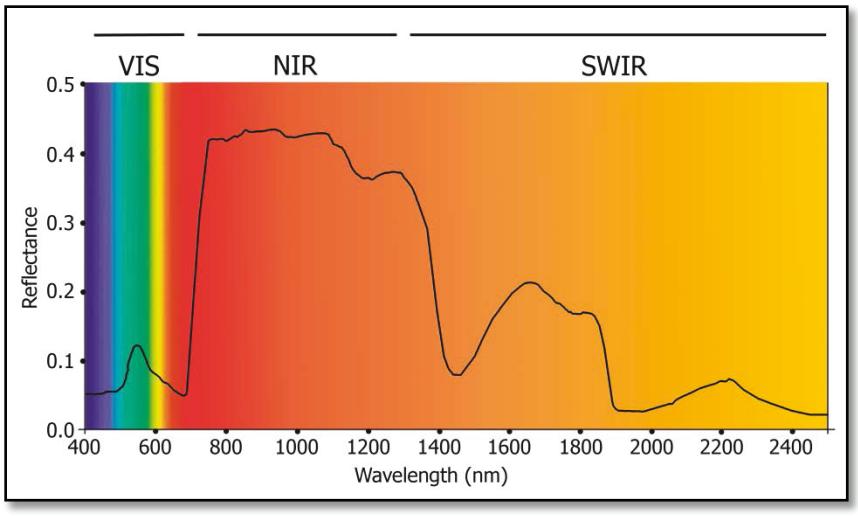

Figure 6. Typical reflectance curve of a healthy green leaf. VIS, NIR and SWIR refer to the visible (400–700 nm), near-infrared (700–1300 nm) and shortwave-infrared (1300–2500 nm) spectral region.

One of the most noticeable features of the vegetation spectrum (**Figure 6**) is the dramatic rise in reflectance characterised by an abrupt change in canopy reflectance between the red (670 nm) and near infrared (NIR) (800 nm), caused by the combined effects of strong chlorophyll absorption in the red wavelengths and high leaf structure-influenced reflectance in the NIR (Blackburn, 2007; Gitelson & Merzlyak, 1998). The shape and position of the red-edge are influenced by variations of chlorophyll content and leaf structure (Peñuelas et al., 1994). The reflectance near 700 nm and in the range from 530 to 630 nm is particularly sensitive to chlorophyll concentration (Gitelson et al., 2003; Koger, Bruce, Shaw, & Reddy, 2003). However the reflectance spectra of vegetation change continuously throughout the growing season (Hoffbeck & Landgrebe, 1996). Stress to the vegetation can interfere with photosynthesis and the physical structure of the plant, and in turn affect absorption of light energy and thus alter the reflectance spectrum of plants. Fortunately, studies have shown good relationships between spectral reflectance and the chlorophyll content in green vegetation (Carter, 1994). As well multiple studies have looked at the effects of soil minerals on vegetation, with areas of vegetation that show adverse effects

due to the presence (or absence) of certain minerals in the soil called *geobotanical anomalies* (Mather & Koch, 2011).

Using functions calculated from the reflectance spectra, called spectral vegetation indices (SVIs), the various vegetation pigment levels can be calculated to infer vegetation characteristics such as plant stress, which may be an useful indicator of burial sites (Kalacska et al., 2009). This will be further discussed with relevant details in the methods chapter.

There are three key types of optical sensing modalities: 1) handheld, 2) airborne (aerial), and, 3) space borne (on board a satellite) (Liu & Mason, 2009). Field and laboratory spectrometers are commonly used to attain 'pure' spectral signatures from known objects in order to build spectral libraries. Using airborne and space borne sensors to acquire information relates with the synoptic view from altitude (Landgrebe, 2003). The higher one goes, the more one can see, and that potentially leads to a more economical way to gather the data (Landgrebe, 2003). Higher altitudes also means greater quantities of data must be dealt with, thus it is important to find ways of analyzing the data to extract the desired information (Landgrebe, 2003).

6. Spectral Analysis

Analysis of soil and vegetation spectra can be segregated into three distinct categories: 1) Indices, 2) Spectral shape and amplitude metrics and 3) Image Classification

6.1. Indices

Indices are functions of surface reflectance at two or more wavelengths designed to highlight a particular property of the spectra, in this case soil and vegetation. More than 150 indices have been published in scientific literature,

however only some are of use to these particular data. In this thesis, the focus is only on the most common vegetation indices. Measurement of spectral reflectance provides a fast, non-destructive method for pigment estimation (Sims & Gamon, 2002). As a group, leaf pigments are mainly analyzed in the visible portion of the spectrum (400 nm to 700 nm) despite some unique traits in the SWIR (Peñuelas & Filella, 1998). The last seven vegetation indices described are more appropriate to airborne acquired data.

The Normalized Difference Vegetation Index (NDVI) is based on the reflectance contrast between the red and the NIR (Tucker, 1979). Two version were utilized (Equation 1, Equation 2), where ρ refers to the reflectance at a particular wavelength. The value of this index ranges from -1 to 1. A zero means bare rock/soil a value that is not seen with vegetation and large values close to one indicates the highest possible density of green vegetation.

Equation 1

$$NDVI = \frac{(\rho 800 - \rho 680)}{(\rho 800 + \rho 680)}$$

Equation 2

$$NDVI = \frac{(\rho 774 - \rho 677)}{(\rho 774 + \rho 677)}$$

The Simple Ratio (SR) is the ratio of the highest reflectance to the absorption bands of chlorophyll (Sellers, 1985). The value of this index ranges from 0 to more than 30. The reason there are two indices presented is the values are sensor dependent and these two are the most commonly utilized ones (Equation 3, Equation 4).

Equation 3

$$SR = \frac{\rho 750}{\rho 705}$$

Equation 4

$$SR = \frac{\rho 774}{\rho 677}$$

The Vogelmann Red Edge Indices (VOG1, VOG2, and VOG3) are narrowband reflectance measurements (Equation 5, Equation 6, Equation 7) that are sensitive to the combined effects of foliage chlorophyll concentration, canopy leaf area, and water content (Vogelmann, Rock, & Moss, 1993).

Equation 5

$$VOG1 = \frac{\rho 740}{\rho 720}$$

Equation 6

$$VOG2 = \frac{(\rho 734 - \rho 747)}{(\rho 715 + \rho 726)}$$

Equation 7

$$VOG3 = \frac{(\rho 734 - \rho 747)}{(\rho 715 + \rho 720)}$$

The Photochemical Reflectance Index (PRI) is a reflectance measurement sensitive to changes in carotenoid pigments (particularly xanthophyll) in live foliage (Equation 8). Carotenoid pigments are indicative of photosynthetic light use efficiency. As such, it is used in studies of vegetation productivity and stress (Sims & Gamon, 2002). The value of this index ranges from -1 to 1. The common range for green vegetation is -0.2 to 0.2.

Equation 8

$$PRI = \frac{(\rho 531 - \rho 570)}{(\rho 531 + \rho 570)}$$

The Structure Insensitive Pigment Index (SIPI) is a reflectance measurement designed to maximize the sensitivity of the index to the ratio of carotenoids to chlorophyll (Equation 9). Increases in SIPI are thought to indicate increased canopy stress (Sims & Gamon, 2002). The value of this index ranges from 0 to 2. The common range for green vegetation is 0.8 to 1.8.

Equation 9

$$SIPI = \frac{(\rho 800 - \rho 445)}{(\rho 800 - \rho 680)}$$

The Plant Senescence Reflectance Index (PSRI) is designed to maximize the sensitivity of the index to the ratio of bulk carotenoids (for example, alpha-carotene and beta-carotene) to chlorophyll (Equation 10). An increase in PSRI indicates increased canopy stress (Sims & Gamon, 2002). The value of this index ranges from -1 to 1. The common range for green vegetation is -0.1 to 0.2.

Equation 10

$$PSRI = \frac{(\rho 680 - \rho 500)}{\rho 750}$$

The Modified Red Edge Normalized Difference Vegetation Index ($mNDVI_{705}$) is a modification of the Red Edge NDVI (Sims & Gamon, 2002). The $mNDVI_{705}$ capitalizes on the sensitivity of the vegetation red edge to small changes in the physical structures of the vegetation (Carter & Knapp, 2001). It differs from the Red Edge NDVI by incorporating a correction for leaf specular reflection (Equation 11) (Sims & Gamon, 2002). The value of this index ranges from -1 to 1. The common range for green vegetation is 0.2 to 0.7.

Equation 11

$$mNDVI \frac{\rho 750 - \rho 705}{\rho 750 + \rho 705 - 2(\rho 445)}$$

The Simple Ratio Pigment Index (SRPI) is based on the ratio of Carotenoids and Chlorophyll a (Equation 12), commonly used to asses plant stress (Penuelas et al., 1995).

Equation 12

$$SRPI = \frac{\rho 430}{\rho 680}$$

The Normalized Phaeophytinization Index (NPQI) or Normalized difference pigment index NDPI, is based on the ratio of carotenoids and chlorophyll a (Equation 13), and commonly used to asses plant stress (Peñuelas & Filella, 1998).

Equation 13

$$NPQI = \frac{(\rho 415 - \rho 435)}{(\rho 435 + \rho 415)}$$

The Normalized Pigment Chlorophyll Index (NPCI) is commonly used to assess plant stress by evaluating the proportion of total photosynthetic pigments to chlorophyll (Equation 14) (Peñuelas, Gamon, Fredeen, Merino, & Field, 1994)**.**

Equation 14

$$NPCI = \frac{(\rho 680 - \rho 430)}{(\rho 680 + \rho 430)}$$

The Lichtenthaler or PI4 is a chlorophyll-based index (Equation 15) for plant stress detection (Lichtenthaler, 1996; Röder & Hill, 2009)

Equation 15

$$Lichtenthaler = \frac{\rho 440}{\rho 690}$$

The Carter indices are specialized narrowband indices (Equation 16,) for the monitoring of plant stress (Carter, 1994).

Equation 16

$$Carter\ \left(Red\right)=\frac{\rho 695}{\rho 760}$$

The Enhanced Vegetation Index (EVI) optimizes vegetation analysis from space borne platforms (Equation 17) and complements NDVI results (Huete, Liu, Batchily, & van Leeuwen, 1997). NIR/Red/Blue are atmospherically-corrected surface reflectance, L is the canopy background adjustment, and C1, C2 are the coefficients of the aerosol resistance.

Equation 17

$$EVI=2.5\frac{\rho NIR-\rho \mathrm{Re}\, d}{\rho NIR+C_1\rho \mathrm{Re}\, d-C_2 pBlue+L}$$

The Atmospherically Resistant Vegetation Index (ARVI) is another enhancement to the NDVI, is it relatively resistant to atmospheric factors through using the reflectance in blue to correct the red reflectance (Equation 18) for atmospheric scattering (Gitelson, Merzlyak, & Gritz, 1996).

Equation 18

$$ARVI=\frac{\rho NIR-\rho RB}{\rho NIR+\rho RB}$$

The Carotenoid Reflectance Index 1 and 2(CRI1 and CRI2) are indices that measure carotenoid content relative to chlorophyll (Equation 19). CRI2 is used when there is high carotenoid concentration (

Equation 20) (Gitelson et al., 2002).

Equation 19

$$CRI1 = \frac{1}{\rho 510} - \frac{1}{p550}$$

Equation 20

$$CRI2 = \frac{1}{\rho 510} - \frac{1}{p700}$$

The Anthocyanin Reflectance Indices (ARI1 and ARI2) are sensitive to anthocyanin pigments (Equation 21) (Anatoly A. Gitelson, Merzlyak, & Chivkunova, 2001). ARI2 is used for high concentrations of anthocyanins (Equation 22).

Equation 21

$$ARI1 = \frac{1}{\rho 550} - \frac{1}{p700}$$

Equation 22

$$ARI2 = \rho 800\left[\frac{1}{\rho 550} - \frac{1}{p700}\right]$$

The Red Edge Position (REP) Index is sensitive to changes in chlorophyll concentration; an increased chlorophyll concentration moves the red edge to longer wavelengths (Equation 23). It is useful for vegetation stress detection (Curran, Windham, & Gholz, 1995).

Equation 23

$$REP = \frac{\rho 670 + \rho 780}{2}$$

The Sum Green (SG) index is the mean of reflectance across the 500 - 600 nm portion of the spectrum used for detecting changes in vegetation greenness (Lobell & Asner, 2003). It is mostly used to detect changes in forest canopy cover rather than monitoring vegetation health. The mean value is then normalized by the number of bands to convert it back to units of reflectance (Lobell & Asner, 2003).

The Red Green Ratio (RG) can be used as an indicator of plant stress based on the ratio of anthocyanins to chlorophylls (Gamon & Surfus, 1999). It is calculated by the mean of all bands in the red range divided by the mean of all bands in the green range.

6.2. Spectral amplitude (delta) and shape (theta)

Delta – RMS difference (or root-mean-square error) is a frequently used measure of the differences between values, and is one measure used to assess accuracy. In this case delta (Equation 24) is used to determine how similar a spectral signature is in amplitude to a reference one (Price, 1994). *D* is root-mean-square difference between two spectra, S_1 (reference) and S_2 (comparison), averaged over the spectral interval of observation λa to λb, the λ is the wavelength compared (Price, 1994).

Equation 24

$$D = \left[\frac{1}{\lambda_b - \lambda_a} \int_{\lambda a}^{\lambda b} \left[S_1(\lambda) - S_2(\lambda) \right]^2 d\lambda \right]^{1/2}$$

Theta – Shape Difference (**Equation 25**), quantifying the theta value differences between spectral signatures, the greater the difference the more dissimilar the spectral signatures (Price, 1994). , S_1 (reference) and S_2 (comparison) spectra at each wavelength λ.

Equation 25

$$\theta = \cos^{-1}\left[\frac{\int S_1(\lambda)S_2(\lambda)d\lambda}{\left[\int S_1(\lambda)^2 d\lambda\right]^{1/2}\left[\int S_2(\lambda)^2 d\lambda\right]^{1/2}}\right]$$

7. Image Processing and Analysis

General steps involved in extracting remote sensing information from data include image preprocessing and image classification. Preprocessing generally precedes data analysis or information extraction. Its goal is the reduction of distortion or the enhancement of some aspect of the data (Landgrebe 2003). Spectral preprocessing techniques are used to remove any irrelevant information which cannot be handled properly in the later steps (Schwartz et al., 2011). This is especially true when a time series of imagery is used or when an area is imaged by multiple sensors, since it is essential to make these images compatible spatially and spectrally (Xie et al., 2008). Preprocessing generally comprises of three categories, radiometric correction, geometric correction and atmospheric correction.

7.1. Radiometric Correction

Radiometric correction (or radiometric calibration) of remote sensing data normally involves the process of correcting radiometric errors or distortions of digital images through correcting the data for sensor irregularities and sensor

noise, and converting the data so they accurately represent the radiance measured by the sensor (Landgrebe, 2003). Relative radiometric correction normalizes multiple scenes to each other to a selected reference data (Prasad et al. 2011)).

7.2. Geometric Correction

Geometric correction is used to avoid geometric distortions in an image and is achieved by establishing the relationship between the image coordinate system and the geographic coordinate system using the calibration data of the sensor, the measured data of position and altitude and the ground control points (Xie et al., 2008). In airborne imagers, geometric correction corrects the variations in aircraft/platform altitude, velocity and attitude.

When an image is geometrically corrected so as to have the coordinate and scale properties of a map, it is said to be *georeferenced* (Mather & Koch, 2011).Some sensors can be integrated with the aircraft's GPS/INS system and produce data cubes that can be georeferenced; thus each pixel in the image corresponds to a single unit area on the ground and is represented by a spectrum (Schwartz et al., 2011). The advantage of geometrically correcting an image prior to further analysis and interpretation is that it then allows proper measurements of distances and areas to be made from features in the image; this is a feature critical for real world applications of small target in vast landscapes (one or two pixels in an image of millions).

7.3. Vicarious Calibration

'Vicarious calibration' also known as *ground truthing* refers to the process by which a calibration is established using a method independent of that which was used for the primary calibration of the sensor. Reflectance-based vicarious calibration (RBVC) is the most common method utilized for the kind of sensors used this study (Secker, Staenz, Gauthier, & Budkewitsch, 2001). The airborne

data is calibrated by comparison against a target located within the flight area, with simultaneous acquisition of the ground-based reflectance data obtained using a field spectrometer (Secker et al., 2001). Markelin *et al* (2012) argue that the vicarious radiometric calibration of the sensor in operational conditions is crucial for accurate results, and by using ground truthing it is possible to have a reflectance accuracy of level 5 % in operational conditions.

7.4. Image Enhancement

Sometimes the images will be more distinguishable for interpretation if image enhancement is performed, which emphasizes and sharpens particular image features to alter the impact of the image on the viewer. Some image enhancements used include gray scale conversion, histogram conversion, color composition, color conversion between red-green-blue (RGB), and hue–saturation–intensity transform (HSI) (Xie et al., 2008).

8. References:

Aitkenhead-Peterson, J. A., Owings, C. G., Alexander, M. B., Larison, N., & Bytheway, J. A. (2012). Mapping the lateral extent of human cadaver decomposition with soil chemistry. *Forensic Science International, 216* (1-3), 127-134.

Benninger, L. A., Carter, D. O., & Forbes, S. L. (2008). The biochemical alteration of soil beneath a decomposing carcass. *Forensic Science International, 180*, 70-75.

Blackburn, G. A.(2007). Hyperspectral remote sensing of plant pigments. *Journal of Experimental Botany, 58*(4), 855-867.

Bristow, J., Simms, Z., & Randolph-Quinney, P. (2011). Taphonomy. In S. M. Black & E. Ferguson (Eds.), *Forensic anthropology: 2000 to 2010* (pp. xviii, 409 p.). Boca Raton: CRC Press.

Carter, D. O., & Tibbett, M. (2008). Cadaver Decomposition and Soil. In M. Tibbett & Carter (Eds.), *Soil Analysis in Forensic Taphonomy: chemical and biological effects of buried human remains* Boca Raton: CRC Press.

Carter, D. O., Yellowlees, D., & Tibbett, M. (2008). Temperature affects microbial decomposition of cadavers (Rattus rattus) in contrasting soils. *Applied Soil Ecology, 40*(1), 129-137.

Carter, D. O., Yellowlees, D., & Tibbett, M. (2007). Cadaver decomposition in terrestrial ecosystems. *Naturwissenschaften, 94*(1), 12-24.

Carter, G. A. (1994). Ratios of leaf reflectances in narrow wavebands as indicators of plant stress. *International Journal of Remote Sensing, 15*(3), 697-703.

Carter, G. A., & Knapp, A. K. (2001). Leaf optical properties in higher plants: linking spectral characteristics to stress and chlorophyll concentration. *American Journal of Botany, 88*(4), 677-684.

Catanese, C. A. , Levy, B., & Catanese, G. (2010). Postmortem Change and Time of Death. In C. A. Catanese (Ed.), *Color Atlas of Forensic Medicine and Pathology* (pp. 111-146). Boca Raton: Taylor and Francis Group, LLC.

Curran, P. J., Windham, W. R., & Gholz, H. L. (1995). Exploring the relationship between reflectance red edge and chlorophyll concentration in slash pine leaves. *Tree Physiol, 15*(3), 203-206.

Dix, J., & Graham, M. (2000). *Time of death, decomposition and identification: an atlas*. Boca Raton: CRC Press.

Forbes, S. L. (2008). Decomposition Chemistry in a Burial Environment. In M. Tibbett & D. O. Carter (Eds.), *Soil analysis in forensic taphonomy: chemical and biological effects of buried human remains.* Boca Raton: CRC Press.

Foth, H. D. (1990). *Fundamentals of soil science* (8th ed.). New York: Wiley.

Gabler, R. E. (2009). *Physical geography* (9th ed.). Belmont, CA: Brooks/Cole, Cengage Learning.

Gamon, J. A., & Surfus, J. S. (1999). Assessing leaf pigment content and activity with a reflectometer. *New Phytologist, 143*(1), 105-117.

Gates, D. M., Keegan, H. J., Schleter, J. C., & Weidner, V. R. (1965). Spectral Properties of Plants. *Applied Optics, 4*(1), 11

Gitelson, A. A., Gritz, Y., & Merzlyak, M. N. (2003). Relationships between leaf chlorophyll content and spectral reflectance and algorithms for non-destructive chlorophyll assessment in higher plant leaves. *Journal of Plant Physiology 160*, 271-282.

Gitelson, A. A., & Merzlyak, M. N. (1998). Remote sensing of chlorophyll concentration in higher plant leaves *Adv Space Res 22*(5), 689-692.

Gitelson, A. A., Zur, Y., Chivkunova, O. B., & Merzlyak, M. N. (2002). Assessing Carotenoid Content in Plant Leaves with Reflectance Spectroscopy. *Photochemistry and Photobiology, 75*(3), 272-281.

Goff, M. L. (2009). Early post-mortem changes and stages of decomposition in exposed cadavers. *Exp Appl Acarol, 49*, 21-36.

Gregory, P. J. (2006). *Plant roots : growth, activity, and interaction with soils*. Oxford ; Ames, Iowa: Blackwell Pub.

Gunn, A. (2008). *Essential forensic biology* (2nd ed.). Chichester, West Sussex ; Hoboken, NJ: J. Wiley.

Haglund, W. D., & Sorg, M. H. (1997). *Forensic taphonomy : the postmortem fate of human remains*. Boca Raton: CRC Press.

Haider, K., & Schäffer, A. (2009). *Soil biochemistry*. Enfield, NH: Science Publishers.

Hall, R. E. (2007). *Soil essentials : managing your farm's primary asset*. Collingwood, Vic.: CSIRO Publishing.

Hanson, I. , Djohari, J., Orr, J., Furphy, P., Hodgson, C., Cox, G., & Broadbridge, G. (2009). New Observations on the Interactions Between Evidence and the Upper Horizons of the Soil In K. Rittz, L. Dawson & D. Miller (Eds.), *Criminal and Enviromental Soil Forensics* (pp. 529). Aberdeen: Springer Science + Business Media.

Harrison, M. , & Donnelly, L. J. (2009). Locating Concealed Homicide Victims: Developing the Role of Geoforensics. *Criminal and Enviromental Soil Forensics* 529.

Haslam, T. C. F., & Tibbett, M. (2009). Soils of Contrasting pH Affect the Decomposition of Buried Mammalian (Ovis aries) Skeletal Muscle Tissue. *Journal of Forensic Sciences, 54*(4), 900-904.

Hoffbeck, J. P., & Landgrebe, D. A. (1996). Classification of remote sensing images having high spectral resolution. *Remote Sensing of Environment, 57*(3), 119-126.

Huete, A. R., Liu, H. Q., Batchily, K., & van Leeuwen, W. (1997). A comparison of vegetation indices over a global set of TM images for EOS-MODIS. *Remote Sensing of Environment, 59*(3), 440-451.

Hunter, J., & Cox, M. (2005). *Forensic archaeology : advances in theory and practice*. London ; New York: Routledge.

Joesten, M. D., Wood, J. L., & Castellion, M. E. (2007). *The world of chemistry : essentials* (4th ed.). Belmont, CA: Thomson Brooks/Cole.

Jones, J. B. (2003). *Agronomic handbook : management of crops, soils, and their fertility*. Boca Raton, Fla.: CRC Press.

Kabata-Pendias, A. (2011). *Trace elements in soils and plants* (4th ed.). Boca Raton: CRC Press.

Kalacska, M. E., Bell, L. S., Sanchez-Azofeifa, G., & Caelli, T. (2009). The Application of Remote Sensing for Detecting Mass Graves: An Experimental Animal Case Study from Costa Rica. *Journal of Forensic Sciences, 54*(1), 159-166.

Klepinger, L. L. (2006). *Fundamentals of forensic anthropology*. Hoboken, N.J.: Wiley-Liss.

Koger, C. H., Bruce, L. M., Shaw, D. R., & Reddy, K. N. (2003). Wavelet analysis of hyperspectral reflectance data for detecting pitted morningglory (Ipomoea lacunosa) in soybean (Glycine max). *Remote Sensing of Environment, 86*(1), 108-119

Konecny, G. (2002). *Geoinformation : remote sensing, photogrammetry and geographical information systems*. London: Taylor & Francis.

Landgrebe, D. A. (2003). *Signal theory methods in multispectral remote sensing*. Hoboken, N.J.: Wiley.

Larizza, M. (2010). *Physical and Chemical Analysis of Pig Carcass Decomposition in a Fine Sand.* (Masters of Applied Bioscience), University of Ontario Institute of Technology.

Liu, J., & Mason, P. J. (2009). *Essential image processing and GIS for remote sensing*. Chichester, West Sussex, UK ; Hoboken, NJ: Wiley-Blackwell.

Lobell, D. B., & Asner, G. P. (2003). Comparison of Earth Observing-1 ALI and Landsat ETM+ for crop identification and yield prediction in Mexico. *Geoscience and Remote Sensing, IEEE Transactions on, 41*(6), 1277-1282.

Markelin, L., Honkavaara, E., Takala, T., Schläpfer, D., Suomalainen, J., & Pellikka, P. (2012). *Novel Approach for the Radiometric Correction of Airborne Hyperspectral Image Data*. Paper presented at the ISPRS Commission VII/3 Melbourne.

Mather, P. M., & Koch, M. (2011). Preprocessing of Remotely-Sensed Data *Computer Processing of Remotely-Sensed Images* (pp. 87-124): John Wiley & Sons, Ltd.

Palmer, J. M., & Grant, B. G. (2010). *The art of radiometry*. Bellingham, Wash.: SPIE Press.

Peñuelas, J., & Filella, I. (1998). Visible and near-infrared reflectance techniques for diagnosing plant physiological status. *Trends in Plant Science, 3*(4), 151-156.

Peñuelas, J., Filella, I., Lloret, P., Munoz, F., & Vilajeliu, M. (1995). Reflectance assessment of mite effects on apple trees. *International Journal of Remote Sensing, 16*(14), 2727-2733.

Peñuelas, J., Gamon, J. A., Fredeen, A. L., Merino, J., & Field, C. B. (1994). Reflectance indices associated with physiological changes in nitrogen- and water-limited sunflower leaves. *Remote Sensing of Environment, 48*(2), 135-146.

Prahlow, J. (2010). *Forensic Pathology for Police, Death Investigators, Attorneys, and Forensic Scientists*. New York: Springer Science+Business Media, LLC.

Prasad, M. N. V., Sajwan, Kenneth S., & Naidu, R. (2006). *Trace elements in the environment : biogeochemistry, biotechnology, and bioremediation*. Boca Raton: CRC/Taylor and Francis.

Prasad, S., Bruce, L. M., & Chanussot, J. (2011). *Optical remote sensing advances in signal processing and exploitation techniques*. Berlin ; Heidelberg: Springer.

Richter, R. (1990), A fast atmospheric correction algorithm applied to Landsat TM images. Int. J. Remote Sens. 11:159-166.

Röder, A., & Hill, J. (2009). *Recent advances in remote sensing and geoinformation processing for land degradation assessment*. Boca Raton Fla. ; London: CRC Press.

Rossel, R. A. V., Walvoort, D. J. J., McBratney, A. B., Janik, L. J., & Skjemstad, J. O. (2006). Visible, near infrared, mid infrared or combined diffuse reflectance spectroscopy for simultaneous assessment of various soil properties. *Geoderma, 131*(1-2), 59-75.

Schultz, J. J., Collins, M. E., & Falsetti, A. B. (2006). Sequential monitoring of burials containing large pig cadavers using ground-penetrating radar. *Journal of Forensic Sciences, 51*(3), 607-616.

Schwartz, G. , Eshel, G., & Ben-Dor, E. (2011). *Reflectance Spectroscopy as a Tool for Monitoring Contaminated Soils*. Soil Contamination, MSc Simone Pascucci (Ed.), ISBN: 978-953-307-647-8, InTech.

Secker, J., Staenz, K., Gauthier, R. P., & Budkewitsch, Paul. (2001). Vicarious calibration of airborne hyperspectral sensors in operational environments. *Remote Sensing of Environment, 76*(1), 81-92.

Sellers, P. J. (1985). Canopy reflectance, photosynthesis and transpiration. *International Journal of Remote Sensing, 6*(8), 1335-1372.

Sharma, C. P. (2006). *Plant micronutrients*. Enfield, NH: Science Publishers

Sims, D. A., & Gamon, J. A. (2002). Relationships between leaf pigment content and spectral reflectance across a wide range of species, leaf structures and developmental stages. *Remote Sensing of Environment, 81*(2–3), 337-354.

Smith, Randall B. . (2012). *Remote Sensing of Enviroment (RSE)* Lincoln NE MicroImages Inc

Stern, K. R., Bidlack, J. E., & Jansky, S. (2008). *Introductory plant biology* (11th ed.). Boston: McGraw-Hill Higher Education.

Stokes, K. L. , Forbes, S. L. , Benninger, L. A. , Carter, D. O., & Tibbett, M. (2009). Decomposition Studies Using Animal Models in Contrasting Environments: Evidence from Temporal Changes in Soil Chemistry and Microbial Activity. In K. Rittz, L. Dawson & D. Miller (Eds.), *Criminal and Enviromental Soil Forensics* (pp. 529). Aberdeen: Springer Science + Business Media.

Swann, L. M., Forbes, S. L., & Lewis, S. W. (2010). Observations of the temporal variation in chemical content of decomposition fluid: A preliminary study using pigs as a model system. *Australian Journal of Forensic Sciences 42*(3), 199-210.

Thomas, P. (2005). *Forensic Anthropology : The Growing Science of Talking Bones*. New York Facts On File, Inc.

Tibbett, M., & Carter, D. O. (2009). Research in Forensic Taphonomy: A Soil-Based Perspective. In K. Rittz, L. Dawson & D. Miller (Eds.), *Criminal and Enviromental Soil Forensics* (pp. 529). Aberdeen: Springer Science + Business Media.

Vogelmann, J. E., Rock, B. N., & Moss, D. M. (1993). Red edge spectral measurements from sugar maple leaves. *International Journal of Remote Sensing, 14*(8), 1563-1575.

White, T. D., & Folkens, P. A. (2005). *The human bone manual*. Amsterdam ; Boston: Elsevier Academic.

Wilson, A. S. , Janaway, R. C. , Holland, A. D., Dodson, H. I. , Baran, E., Pollard, M., & Tobin, D. J. (2007). Modelling the buried human body environment in upland climes using three contrasting field sites. *Forensic Science International 169*, 6-18.

Xie, Y., Sha, Z., & Yu, M. (2008). Remote sensing imagery in vegetation mapping: a review. *Journal of Plant Ecology, 1*(1), 9-23.

II. Chapter 2 - Materials and Methods

1. Study Area

1.1. Site Location

The field site chosen for this study is a level field adjacent to Ottawa Macdonald-Cartier International Airport, 45°19’34” N, 75°40’04” W, (Figure 1). The field site is on Crown land managed by the National Research Council of Canada’s Flight Research Laboratory (FRL). The field is fenced in by a six-foot wire (1.83m) mesh fence on three sides which prevents public access and minimizes scavenger activity (Figure 2). This site was chosen due to the proximity of the FRL hangar, whose research flight operations enabled more frequent data collection.

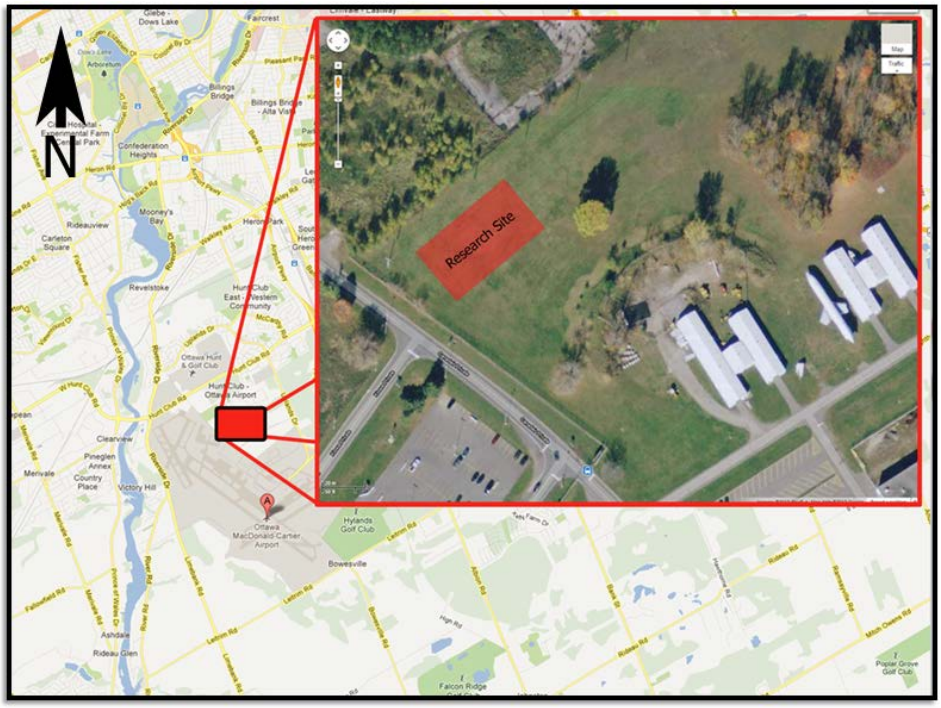

Figure 1. Location of research site on NRC property adjacent to the to Ottawa Macdonald-Cartier International Airport

1.2. Climate

The humid continental climate of this site (Environment Canada, 2011) is typified by large seasonal temperature differences, with warm to hot (and often humid) summers, and cold winters (Figure 3). The air temperature, humidity and precipitation are monitored and are freely available from Environment Canada with the weather monitoring station less than 100 meters from the site, therefore onsite monitoring was not required.

Figure 2. Panorama of site before set up

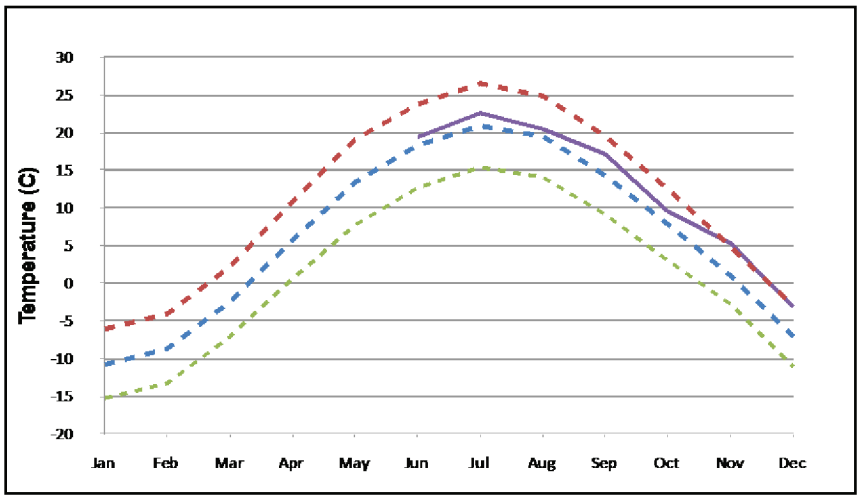

Figure 3. Annual monthly temperatures for 2000-2010 with average(blue), high (red) and low(green) daytime temperature, and monthly average temperatures, or June-December 2011 (purple line) illustrating the warmer than average weather (Environment Canada, 2012)

1.3. Soil Type and Vegetation

The soil composition of the site is varied due to the construction of the adjacent airfield, first in 1927 and later with major construction in the 1950's (Thie, 2006). The soils at the site are mostly of well-drained, sandy loam (M. Dalva, Pers. Communication). The parent material of the site is shale at a depth of 1 to 2 m with fragments of granite, gneiss, limestone and dolomite (Schut & Wilson, 1987). The pH of the soils at the site ranges from 5.5 to 8.1 (M. Dalva, Pers. Communication). At the beginning of the study vegetation consisted of grasses and forbs. There was no bare soil or woody vegetation on the site.

2. Carcasses

Pigs (*Sus scrofa domesticus)* were used as animal proxies for the experiment, a common practice in physical anthropology and forensic studies to simulate human studies (Chavez, Marino, & Schowengerdt, 1994; Kamusoko, Mundia, & Murayama, 2010). The pigs were purchased from a commercial meat processing facility, Desormeaux Meats in Crysler, Ontario (Figure 4). Based on McGill University's Research Board of Ethics and the National Research standards (McGill University, 2011), animal carcasses from commercial meat processing facilities do not require animal ethics permits because the specimens are not alive. They are also not a biohazard because they are not laboratory specimens (they are human consumption grade meat carcasses).

Figure 4. Pig carcasses being transported from delivery truck to burial site

Inspected pig carcasses from commercial abattoirs are not considered deadstock as defined by the Ontario Provincial Food Safety and Quality Act, 2001 S.O. 2001, Chapter 20 Part 1 Section 2; *"deadstock" means an animal that is specified in the regulations and that has died from a cause, other than slaughter; ("animaux morts").* Once an animal is inspected and slaughtered at a commercial meat processing facility it is no longer considered deadstock and the Food Safety and Quality Act, 2001 no longer applies to its disposal (McGill, 2010). There currently are no regulations forbidding the use and burial of inspected pig carcasses from a commercial abattoir in Ontario (T. Norry, Pers. Communication), but precautionary measures to prevent any possible contamination of the environment were taken. These measures were based on the guidelines in the Environmental Protection Act R.S.O. 1990 as well as the Ontario Disposal of Dead Farm Animals regulations and include the burials being set back at least 50 m from a well or water source, not placed in an area subjected to flooding, not within 200 meters of a residential area or near any livestock or crop fields, and the burial pits be at least 0.9 m above bedrock or an aquifer and not contain more than 2,500 kg of animal carcasses.

3. Experimental Design

The pig carcasses were of similar weights (85 ±10 kg). The carcasses were buried at two depths, at 60 and 120 cm with 30 and 90 cm of soil cover, respectively. The graves were dug with a mechanical backhoe provided by FRL. One additional set of carcasses was left on the surface, a common occurrence with bodies discovered by police agencies in Canada (SPVM, Pers. Communication). Some of the pig carcasses, half at each burial depth, were wrapped in black garbage bags because this was an element identified by the police agencies as occurring frequently in crime scenarios (Alberta RCMP, Pers Communication). The surface burial carcasses were covered in an extruded plastic mesh to limit animal scavenging activity during the first 3 weeks (Figure 5).

Figure 5. Protective plastic mesh cage constructed around surface remains

Two sets of reference sites were dug to the same depths as the burials but

without bodies, making a total of six reference sites. The burial sites were spaced eight m apart from the centroid of the neighbouring graves to avoid any cross contamination between sites (Figure 6). The site treatments were assigned randomly.

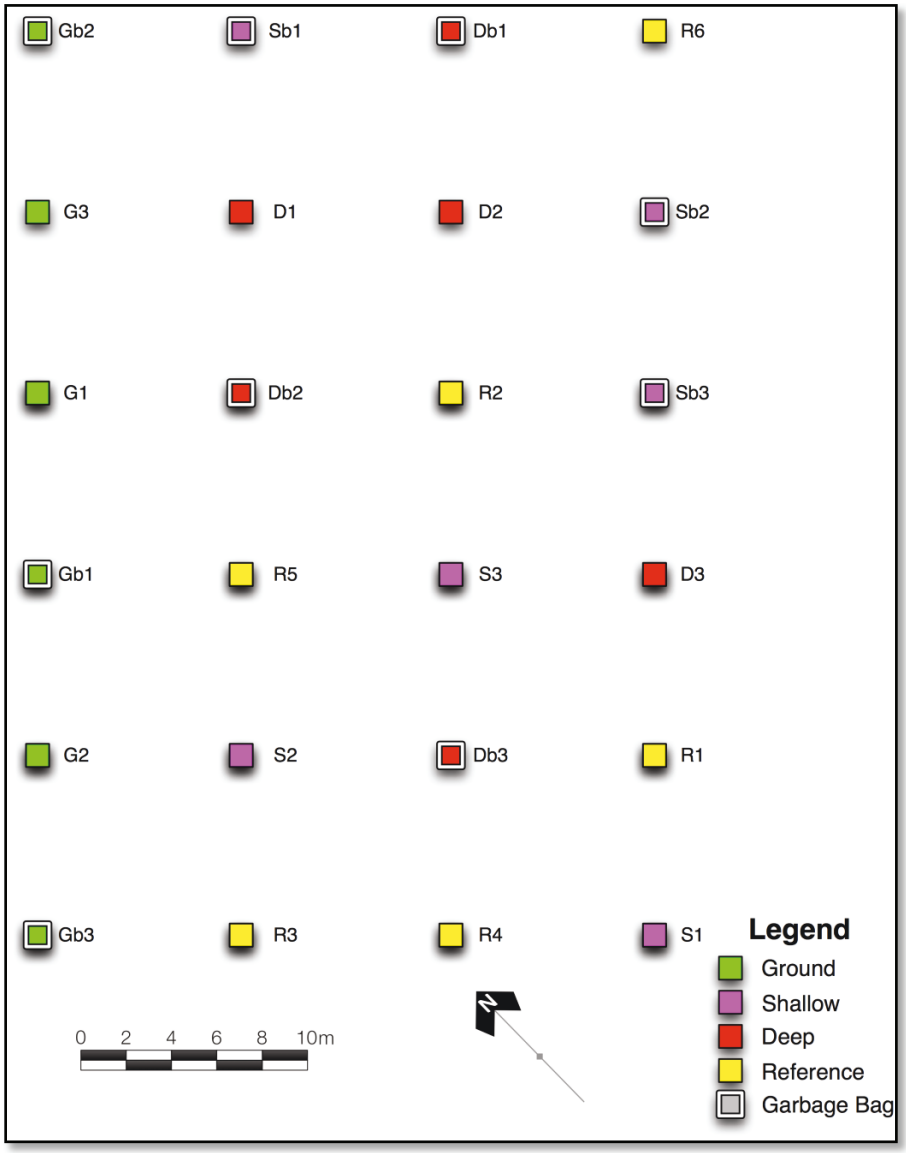

Figure 6. Site layout to scale, lowercase 'b' indicates carcass is wrapped in a plastic garbage bag

The entire experiment is contained in an area of approximately 1,500 m^2 to

minimize the impact on the surrounding land maintained by the FRL (Figure 7). For the duration of the study the site was undisturbed; there was neither grass mowing nor application of herbicides or pesticides.

Figure 7. Study site immediately after set up, facing north-east.

4. Data Collection

Data collection commenced from the site set up stage with soil collection and airborne sensor fly-overs one day (July 19, 2011) before the carcasses were put in place. The end of the ground experimental data collection was November 15, 2011. Data collection consisted of aerial hyperspectral imagery, laboratory soil and vegetation spectra, as well as soil and plant samples, which were analyzed in the lab for elemental concentrations and pigments, respectively.

4.1. Labeling Scheme

The labeling scheme consisted of a standardized format for all data collections (i.e. photos and spectra) and samples of soils and vegetation. The format is based on a modified format used in the Applied Remote Sensing Laboratory and FRL. The example format is as follows: **YYMMDD_Code_Grave#.** For example,

110601_G_3 would correspond to a sample point taken June 1, 2011 of 'Surface exposed grave' number 3 (Table 1).

Table 1. Letter codes for burial types used in labeling of collected soil and vegetation samples

Code	Burial Type
G	Surface exposed
S	Shallow 30 cm burial
D	Deep 90 cm burial
Gb	Surface exposed w/ garbage bag
Sb	Shallow 30 cm burial w/ garbage bag
Db	Deep 90 cm burial w/ garbage bag
R	Reference

4.2. Soil Collection and Analyses

Soil samples were collected from each grave site a trowel and placed in plastic Ziploc bags. The sampling point was the south east corner of each site. The surface sample of the soil was collected from same location on each gravesite each time. Vegetation and roots were not a concern on the disturbed soil sites since regrowth had not yet occurred. For the Surface bodies' samples, the initial collection removed vegetation and roots, and those had not returned when sampling for the season ended. The soil samples were collected whenever possible to be coincident with fly-over times (Table 2). These samples were used for the analysis of the evolution of the spectral signatures. The samples were placed in paper or plastic bags for storage and transported to McGill University. Soils were then oven-dried at 60 °C for 24-48 hours (until constant weight was

achieved), coarse sieved with a 100 mesh and then fine sieved with a 230 mesh. These sieved samples were then placed in plastic 50 ml vials.

Table 2. Collection dates for soil samples and airborne images

	Airborne Image	Soil Collection
Time 0	July 19	June 23
Time 1	July 27	July 28
Time 2	Aug 05	Aug 08
Time 3	Aug 12/Sept 9	Aug 22
Time 4	Nov15	Nov 15

4.3. Soil Chemical Composition

For each collection date and gravesite, 1.5 grams of the dried sieved soil was sent to ACME Laboratory (Vancouver, BC) for Aqua Regia Digestion for a 32-element analysis of the soil via inductively coupled plasma mass spectroscopy. The results were received in Microsoft Excel format, which was convenient for further organization into time series and grave types for later analysis.

4.4. Soil Spectral Analysis

A FieldSpec® 3 Portable Spectroradiometer (Analytical Spectral Devices Inc., Boulder, Colorado) was used to collect soil spectra in the lab. This spectrometer measures reflectance from 350 to 2500 nm. The FWHM is 3 nm at 700 nm, 10 nm at 1400 nm and 12 nm at 2100 nm (Analytical Spectral Devices Inc, 2012). The spectrometer was fitted with a contact probe (with an internal halogen light source) to ensure a constant lighting and viewing geometry for the soil samples. The laboratory walls are painted matte black with all surfaces designed to minimize light reflection. All light sources within the laboratory except for the laptop screen and the outside hall lights were turned off, and dark matte full sleeve clothing was worn during sampling times. The workbench was cleaned

with canned air and Lysol wipes before every sampling session to prevent contamination from other projects.

A Spectralon white reference was used to optimize the instrument before each session since optimization is required before any data is acquired. Optimizing the spectrometer results in automatic setting of gains and offsets for the two SWIR detectors, automatic setting of the integration time for the VNIR detector, and a measure of the dark current. The integration time is the time the detectors in the spectrometer can capture light reflected from samples. This time was adjusted automatically to maximize the signal without saturating the detector. The instrument was re-optimized after any change in temperature, and since the laboratory is an enclosed, poorly ventilated room, I chose 30-min intervals. The dark current is the small electronic noise present in all photosensitive devices; by doing a dark current calibration this background noise is subtracted from the final data. A white reference calibration was run with the 99% reflective Spectralon white reference to use in the ratio calculations of reflectance. There was no adjustment for the calibration of the reference panel in neither this study nor the 8°-hemispherical versus 0°-45° optical properties of Spectralon.

The sampling of spectra average was set to 30 scans. The data were collected in units of reflectance (i.e. simple ratio between the Spectralon panel and the sample). Three spectra were collected for each sample, moving the black cardstock holding plates between each collection. To prevent contamination through the contact probe, spectra were collected at a distance of 3 – 4 mm from the soil samples. The probe was cleaned with canned air and kimwipes after each soil sample. A white reference was taken after each sample. Spectral data were imported and organized in MS Excel using the pre-existing Applied Remote Sensing Lab template (Appendix A).

5. Vegetation

Once plants had regrown and the leaf blades were large enough for analysis, (five months after site set up), leaf samples were gathered on November 15, 2011. Ten leaf blade samples were collected from each gravesite that had sufficient vegetation regrowth, for 220 usable samples. The sample bags were placed in a cooler with ice packs to limit degradation as per Foley et al. (2006), and brought to the McGill Applied Remote Sensing Laboratory.

The spectra of vegetation were collected using an ASD Handheld spectrometer in the 325nm -1075nm wavelength range. The collection utilized the leaf clip attachment that holds the leaf samples in place (without damaging the leaf tissue), excludes ambient light, and has an embedded 99% reflective white panel. Following the collection of the spectra, the leaf blades were wrapped in aluminum foil and placed in bags, then placed in the freezer for the chlorophyll and carotenoid extraction at a later date (Ben-Dor & Banin, 1995; Carter, 1994; Foley et al., 2006).From the original 220 vegetation samples, 184 samples underwent chlorophyll and carotenoid extraction utilizing dimethyl sulfoxide (DMSO) as described by Hiscox & Israelstam (1979). The remaining samples were too desiccated to use and discarded. A standard size was attained by using a 28 mm^2 hole punch to cut a piece from each leaf. Each sample was placed into a 15 ml centrifuge tube with 10 ml of DMSO. Tubes were then placed in a 65°C water bath for 30 min. When cooled, 3 ml of the resulting liquid was transferred to a disposable 1 cm path length cuvette using a disposable plastic pipette. Cuvettes were then placed into Thermo Scientific GENESYS 10S UV-Vis spectrophotometer to record the absorbance values at 470 nm (carotenoid), 650 nm (chlorophyll a) and 666 nm (chlorophyll b). Pigment concentrations were calculated using Arnon's (1949) equations (Appendix B) for chlorophyll a and b as well as carotenoids (Hiscox & Israelstam, 1979).

6. Analysis and Analytical Tools

The analysis of the first four data series followed the same general pattern. The data was first tested for normality with the Shapiro-Wilk test, then, a one-way analysis of variance (ANOVA) was carried out to determine if there was any differences between the means of the data groups within each dataset. To narrow down where and between which means the differences lay a Students t test was used.

Additionally the vegetation pigments and the vegetation and soil spectra data underwent a different type of analysis using statistical pattern recognition classifiers. The MATLAB PRTools Toolbox was used to add the necessary statistical pattern recognition functions to enable classification analysis of the soil chemical data. The PRTools Toolbox 4.1 is an open source toolbox that adds over 200 pattern recognition routines and an additional 200 support routines (http://prtools.org/files/). The classifiers used in MATLAB are summarized below in Table 3. Each classifier attempts to separate the datasets according to different criteria hence the need to try several to find optimum ones.

Table 3. PRTools Toolbox Classifiers used in MATLAB analysis

Classifiers	Classifier Description
knnc	k-nearest neighbor classifier
lcd	Normal densities based linear classifier
qdc	Normal densities based quadratic classifier
bpxnc	Train neural network classifier by back-propagation
klldc	Linear classifier by KL expansion of common covariance
quadrc	Quadratic classifier
parzenc	Parzen classifier
nmc	Nearest mean classifier

6.1. Soil Chemistry

Results reported from ACME laboratories were organized in MS Excel for analysis. The detection limits for each element as well as the accuracy of the instrument were included with the results (Appendix C). Out of the 32 elements reported by ACME, aluminum (Al), calcium (Ca), iron (Fe), magnesium (Mg), manganese (Mn), sodium (Na), phosphorus (P), sulphur (S), potassium (K) and zinc (Zn) are of interest. Any values below detection threshold were set to 0. Data were then imported into SAS JMP 10 where the Shapiro-Wilk test was used to test for normality. After confirming a normal distribution, a one-way analysis of variance (ANOVA) was performed with a Students t test to determine if the soil chemistry of the gravesites was significantly different.

6.2. Vegetation Pigments

The classification analysis in MATLAB version 2011b as used to determine whether it was possible to classify the sites according to type of burial. The first question was whether the background vegetation is separable from disturbed grave site vegetation, and whether it was then possible to separate the disturbed/grave sites into distinct categories based on total chlorophyll and carotenoids as well as chlorophyll a and b. Ten question scenarios (Table 4) and eight different classifiers were applied. Questions 4, 5, 7, and 10 address whether the background vegetation differs from the selected grave type vegetation, Questions 1,2, and 3 address the ability to separate background vegetation and different grave types with Question 3 being the most critical (Table 4). Question 8 addresses the classifiability between the references and sites with bodies- the surface, shallow and deep gravesites.

Table 4. Research Questions and Components for Vegetation Pigments. Background vegetation (B), Reference (R), Surface bodies (S), and the shallow and deep graves combined into one category (G).

Question	Components
Q1	B vs. G vs. R
Q2	B vs. G+S vs. R
Q3	B vs. G vs. S vs. R
Q4	B vs. G+S
Q5	B vs. R
Q6	G vs. S
Q7	B vs. G
Q8	R vs. G+S
Q9	R vs. G
Q10	B vs. S

Additionally the data were imported into JMP 10 and a One Way ANOVA was applied to each pigment category to determine if there was a difference in the means of the grave site categories. Basic analysis was performed using a Students t test to determine if the vegetation pigment categories where these means were significantly different, whether it was possible to separate the disturbed/grave sites into distinct categories based on total chlorophyll, chlorophyll a, chlorophyll b, and carotenoid levels.

Canonical Discriminant Analysis was used to distinguish among the vegetation samples and classify them into groups. The key assumption of canonical discriminant analysis is that all individuals can be assigned to one and only one group in advance (Sall, Creighton, & Lehman, 2007). The goals are to 1) find the axis that best separates the groups, 2) test whether the means of those groups along that axis are significantly different, and 3) attempt to assign individual test sites to groups. The discrimination is most effective when there are

large differences among the mean values of the different groups such as the background vegetation from the disturbed (Sall et al., 2007).

7. Vegetation and Soil Spectra

7.1. Soil Spectra

For the classification analysis a third party toolbox - PRTools v 4.1- was used in MATLAB 2011b. The soil spectra were converted and imported into MS Excel from the proprietary ASD format, and cropped to the 450-2,300 nm range to remove the majority of the signal noise. The data were then imported and organized in MATLAB. The soil spectra data were separated into four categories: surface bodies (G), shallow(S), deep (D), and reference (R) reflecting the original soil collection categories. Using these organized data, I employed a forward feature selection for classification using the 'featself' function to find the optimal number of bands in the 11 research questions (Table 5) of the various combinations between the four categories of interest. The reduced band data was organized to use half the data as a training set and the other half as a testing sets upon which the eight classifiers in Table 3 were applied to determine which classifier produced the lowest error.

Table 5. Soil Spectral Analysis Separability Questions. Deep Burial (D), Shallow Burial (S), Reference (R), Surface bodies (G), and category (X) combined the shallow and deep graves.

Question	Components
Q1	R vs. D
Q2	R vs. S
Q3	R vs. G
Q4	R vs. X
Q5	R vs. X + G

Q6	R vs. X vs. G
Q7	R vs. S vs. G vs. D
Q8	D vs. S
Q9	D vs. G
Q10	G vs. S
Q11	X vs. G

The two main themes of this analysis are: do the reference graves differ from grave types that contain bodies, and do the surface body sites different from shallow, deep and reference sites? Questions 1 - 7 seek to address the first question; while questions 9- 11 seek to determine if burial depth matters. With Question 8 used determine if shallow graves and deep graves are distinct.

To analyze the two themes mentioned above, the spectral amplitude (delta) and shape (theta) of the soil data were imported and sorted into JMP 10. The reference signature used in the comparisons was the same site utilized in the vegetation analysis, Reference 1 (R1). A One Way ANOVA was applied to assess if there was a difference in each gravesite category means. Afterwards the Student's T test was used on the organized delta and theta data, to determine if the soil categories were significantly different, and whether it was possible to classify the gravesites into distinct categories based on delta and theta values.

7.2. Vegetation Spectra

Water, pigment, and nutrient content of vegetation are reflected in the 400 - 2500 nm range in reflectance spectra, with overlapping, but spectrally distinct features making vegetation separable from other natural materials, such as soils and water bodies. Certain Spectral Vegetation Indices have been derived to provide a measure of stress-related pigments present in vegetation. The null hypothesis in the analysis was that there are no differences in the spectral vegetation indices amongst the various grave types from the November 15, 2011

collection. From field observations, it expected to be able to differentiate between the index values of the vegetation growing around the surface bodies, background vegetation, and disturbed soil (shallow, deep and reference).

The results of the vegetation indices were imported into JMP and sorted by gravesite class. A Shapiro-Wilk W Test assessed distribution of the indices; half the indices had normal distributions based on test results, however visual assessment of the histograms showed a bell curve distribution in each one and fortunately, an ANOVA is not very sensitive to moderate deviations from normality. One Way ANOVA was applied to each Vegetation Index values to asses if there were differences in each gravesite category mean. On the Vegetation indices that showed that at least one mean value is statistically different from the rest of the grave types, a Students t test was performed on the results to test for pairwise differences.

Analysis of the spectral amplitude (delta) and shape (theta) of the vegetation spectra was done within each grave type first to assess the variation among the samples in one treatment; the reference sample was chosen based on which spectrum was closest to the mean at 535 nm. In addition to this, I then determined the amount of variation within the entire sample set in comparison to the Reference grave (R1) across all the spectra.

For the classification analysis the goal was to determine if it was possible to separate the four classes of plant spectra: Background (B), Grave (G), Surface (S), and Reference (R), and to determine which classifier produced the lowest error. Using these organized data, I employed a feature reduction using the 'featself' function to find the optimal number of bands for each of the ten research questions (**Table 6**). The resulting datasets were then equally subdivided into testing and training datasets, with every second data point relegated into the testing dataset. The classifiers used were the same as those for the soil spectra (Table 3).

Table 6. Research Questions and Components for Vegetation with four assessment categories; Surface Bodies (S), Background vegetation (B), Reference Graves (R), and Shallow and Deep Graves (G)

Question	Components
Q1	B vs. G vs. R
Q2	B vs. G+S vs. R
Q3	B vs. G vs. S vs. R
Q4	B vs. G+S
Q5	B vs. R
Q6	G vs. S
Q7	B vs. G
Q8	R vs. G+S
Q9	R vs. G
Q10	B vs. S

8. Airborne Analysis

8.1. Image Acquisition

The images were acquired by the National Research Council using CASI/SASI HSI mounted onboard a Twin Otter aircraft (Figure 8). The CASI/SASI are airborne hyperspectral sensors used coincidentally to cover the 450- 2450 nm range of the electromagnetic spectrum (ITRES, 2010). The CASI-500 (Compact Airborne Spectrographic Imager) focuses on the Visible and Near Infrared (VNIR) range, whereas the SASI-600 (Shortwave IR Airborne Spectrographic Imager) focuses on Short-Wavelength Infrared (SWIR) (Figure 9).

Figure 8. NRC Twin Otter carrying the Airborne Sensors

The CASI has a unique feature in that it is a programmable sensor so that the number of bands, location of bands and width of bands are all user selectable. In this study, the CASI sensor collected 48 bands and the SASI sensor collected 180, for a total of 228 bands. The locations of the geographic centroids of each burial site were collected via GPS on August 28, 2011 to precisely locate the graves on the airborne imagery.

Figure 9. The CASI and SASI set up inside the NRC Twin Otter, meant to demonstrate the size of the sensors and future challenges of integrating them into smaller airborne vehicles

8.2. Image Preprocessing

The images were converted from raw sensor format into a .pix file format, a form that is usable by an end user. These conversions were done at the NRC's Flight Research Laboratory.

8.3. Radiometric Calibration and Atmospheric Correction

The spectroradiometric calibration of the SASI and CASI data was performed by two different processes. The CASI imagery was calibrated by York University, in Toronto, Canada, using in-house software developed from ITRES library functions by York University. The SASI imagery was calibrated to radiance at the NRC's FRL, using utilities and calibration files provided by ITRES. Both CASI and SASI images were atmospherically corrected to reflectance at the ARSL at McGill. The image files were converted from the .pix

files into ENVI standard BIL format file, since the input image for atmospheric correction must be either band-interleaved-by-line (BIL) or band-interleaved-by-pixel (BIP) format. For atmospheric correction, the FLAASH module was run using a Mid-Latitude Summer Atmospheric Model with a Rural Atmospheric Model using the 1135 nm water absorption feature for the water vapour estimation for the SASI images, and 820 nm water absorption for the CASI (full settings in Appendix D) to remove the influence of the atmosphere.

8.4. Geometric Correction

The spectral analysis of both the SASI and CASI images was performed on the non-geocorrected data as the geocorrection process often "warps" the pixel spectral information (R. Soffer, Pers Communication 2011). For the determination of ground locations for the pixels of interest, geocorrection will eventually be done.

9. Image Processing

After importing the CASI and SASI images into ENVI 4.8, the study site area was subset from the rest of the flight line. This was accomplished through creating a rectangular ROI (Region of Interest) of the study site then utilizing the ‘Subset via ROIs ‘function in ENVI.

9.1. Vegetation Indices

I attempted to explore the small-scale vegetation anomalies caused by soil disturbance and cadaver decomposition using vegetation indices available with ENVI that were described in the literature review in chapter 1.

9.2. RX Anomaly Detection

The images were opened in ENVI where the RX Anomaly Detection tool was used to detect differences between disturbed soil sites, surface bodies and the background ground cover. The flight line was subset to the study site area to focus only on the area of interest in order to limit the anomaly detection. Spectral subsetting was done on the CASI to limit to channels 5-45 (455.34-898.80 nm) to eliminate the bad bands, and the SASI images limited to channels 8-141(958-2389 nm). Two algorithms were used, the basic RXD algorithm and the hybrid RXD-UTD algorithm which subtracts the UTD (Uniform Target Detector) from the RXD to suppress the background and enhance the anomalies.

9.3. Hydroxyl (OH^-) ions

Using the SASI images, this analysis examines the reflectance data for the 2200 nm region. A relative enhancement of the 2203.5 nm data was used to highlight disturbed soils. There are five enhancements that can be used, these are; 1) Linear-a min/max linear contrast stretch , 2) Linear 2% - linear stretch using 96 percent of the pixel values, similar to a 2 standard deviation stretch, 3) Gaussian-creates a bell shaped output (normal distribution), 4) Equalization - scales the data to equalize the number of digital numbers in each histogram bin, and 5) Square Root-Takes the square root of pixel values and then applies a linear stretch. This methodology was especially useful for the latter part of the sampling season with the SASI only airborne collections.

10. References

Arnon, D. I. (1949). Copper Enzymes in Isolated Chloroplasts. Polyphenoloxidase in Beta Vulgaris. *Plant Physiol, 24*(1), 1-15.

Ben-Dor, E., & Banin, A. (1995). Near-Infrared Analysis as a Rapid Method to Simultaneously Evaluate Several Soil Properties. *Soil Sci. Soc. Am. J., 59*(2), 364-372.

Carter, G. A. (1994). Ratios of leaf reflectances in narrow wavebands as indicators of plant stress. *International Journal of Remote Sensing, 15*(3), 697-703.

Carter, G. A., & Knapp, A. K. (2001). Leaf optical properties in higher plants: linking spectral characteristics to stress and chlorophyll concentration. *American Journal of Botany, 88*(4), 677-684.

Chavez, P. S., Marino, C. M., & Schowengerdt, Robert A. (1994). *Recent advances in remote sensing and hyperspectral remote sensing : 27-29 September 1994, Rome, Italy*. Bellingham, Wash., USA: SPIE.

Curran, P. J., Windham, W. R., & Gholz, H. L. (1995). Exploring the relationship between reflectance red edge and chlorophyll concentration in slash pine leaves. *Tree Physiol, 15*(3), 203-206.

Foley, S. , Rivard, B., Sanchez-Azofeifa, G. A., & Calvo, J. (2006). Foliar spectral properties following leaf clipping and implications for handling techniques. *Remote Sensing of Environment, 103*(3), 265-275

Gamon, J. A., & Surfus, J. S. (1999). Assessing leaf pigment content and activity with a reflectometer. *New Phytologist, 143*(1), 105-117. doi: 10.1046/j.1469-8137.1999.00424.x

Gitelson, A. A., Merzlyak, M. N., & Gritz, Yuri. (1996). Novel Algorithms for Remote Sensing of Chlorophyll Content in Higher Plant Leaves. *Papers in Natural Resources*, 4. Retrieved from http://digitalcommons.unl.edu/natrespapers/238/ website:

Gitelson, A. A., Merzlyak, M. N., & Chivkunova, O. B. (2001). Optical Properties and Nondestructive Estimation of Anthocyanin Content in Plant Leaves¶. *Photochemistry and Photobiology, 74*(1), 38-45.

Gitelson, A. A., Zur, Y., Chivkunova, O. B., & Merzlyak, M. N. (2002). Assessing Carotenoid Content in Plant Leaves with Reflectance Spectroscopy. *Photochemistry and Photobiology, 75*(3), 272-281.

Hiscox, J. D., & Israelstam, G. F. (1979). A method for the extraction of chlorophyll from leaf tissue without maceration. *Canadian Journal of Botany, 57*(12), 1332-1334.

Huete, A. R., Liu, H. Q., Batchily, K., & van Leeuwen, W. (1997). A comparison of vegetation indices over a global set of TM images for EOS-MODIS. *Remote Sensing of Environment, 59*(3), 440-451.

ITRES. (2010). SASI 600. *ITRES Research Limited*. Calgary, Alberta, Canada: ITRES Research Limited.

Kamusoko, M., Charles, N., & Murayama, Y. (2010). *Recent advances in remote sensing and GIS in Sub-Sahara Africa*. Hauppauge, NY: Nova Science Publishers.

Lichtenthaler, H. K. (1996). Vegetation Stress: an Introduction to the Stress Concept in Plants. *Journal of Plant Physiology, 148*(1–2), 4-14

Lobell, D.B. & G.P. Asner, 2003. Hyperion studies of crop stress in Mexico. Proceedings of the 12th Annual JPL Airborne Earth Science Workshop. Pasadena, CA. (ftp://popo.jpl.nasa.gov/pub/docs/workshops/aviris.proceedings.html).

McGill University. (2011). Research Board of Ethics 2011, from www.mcgill.ca/animal/research

Penuelas, J., Filella, I., Lloret, P., Munoz, F., & Vilajeliu, M. (1995). Reflectance assessment of mite effects on apple trees. *International Journal of Remote Sensing, 16*(14), 2727-2733.

Peñuelas, J., Gamon, J. A., Fredeen, A. L., Merino, J., & Field, C. B. (1994). Reflectance indices associated with physiological changes in nitrogen- and water-limited sunflower leaves. *Remote Sensing of Environment, 48*(2), 135-146.

Peñuelas, J., & Filella, I. (1998). Visible and near-infrared reflectance techniques for diagnosing plant physiological status. *Trends in Plant Science, 3*(4), 151-156.

Price, J. C. (1994). How unique are spectral signatures? *Remote Sensing of Environment, 49*(3), 181-186.

Röder, A., & Hill, J. (2009). *Recent advances in remote sensing and geoinformation processing for land degradation assessment*. Boca Raton Fla. ; London: CRC Press.

Sall, J., Creighton, L., & Lehman, A. (2007). *JMP start statistics : a guide to statistics and data analysis using JMP* (4th ed.). Cary, NC: SAS Pub.

Schut, L. W. , & Wilson, E. A. . (1987). *The soils of the Regional Municipality of Ottawa-Carleton (excluding the Ottawa urban fringe)*. [Toronto]; [Ottawa]: Ministry of Agriculture and Food ; Agriculture Canada, Research Branch.

Sellers, P. J. (1985). Canopy reflectance, photosynthesis and transpiration. *International Journal of Remote Sensing, 6*(8), 1335-1372.

Sims, D. A., & Gamon, J. A. (2002). Relationships between leaf pigment content and spectral reflectance across a wide range of species, leaf structures and developmental stages. *Remote Sensing of Environment, 81*(2–3), 337-354.

Thie, J. (2006). The Canada Land Inventory (CLI) Ottawa-Gatineau Area., 2012

Tucker, C. J. (1979). Red and photographic infrared linear combinations for monitoring vegetation. *Remote Sensing of Environment, 8*(2), 127-150.

Vogelmann, J. E., Rock, B. N., & Moss, D. M. (1993). Red edge spectral measurements from sugar maple leaves. *International Journal of Remote Sensing, 14*(8), 1563-1575.

III. Chapter 3 - Results and Discussion

1. Site Condition

All aspects of decomposition are dependent upon the immediate environment in which the body is in. Of the several environmental factors that play important roles in the decomposition process, temperature is the key factor. The higher the temperature the faster the rate of decomposition (Carter et al., 2008). Once the temperature reaches four degrees Celsius or less the decomposition rate is essentially zero (Carter et al., 2008). Due to this and possibility of snow cover blocking the gravesites, the last sample collection for the research season was November 15 2011. This collection was only possible due to the unusually warmer weather in October and November (5 and 7 degrees Celsius warmer than the season average (Chapter 2 Figure 3). This seasonally unusual warmth extended the growing season well past the time when it has usually senesced. As a corollary, the unseasonal warmth also continued the decomposition process and accelerated the projected timeline for regrowth and state of decay. At the August 08, 2011 collection time the bodies were past the 'bloat stage' and well into the 'active decay' stage. For the surface bodies by the August 22, 2011 collection time they were past the' active decay' stage in an 'advanced decay' state moving towards the 'dry and remains' stage, with the bodies reduced to bones and some pieces of dehydrated skin. By November 15, 2011 the surface bodies were in 'advanced decay' stage again with the rehydrated skin (due to rainfall) undergoing decomposition. The condition of the buried bodies was unknown since we chose to not interfere with the burials based on suggestions from other research into taphonomy (Larizza, 2010). Using the 'rule of thumb' eightfold rule, it was assumed that the active decay stage, at a minimum had been reached. However evidence from the data seemed to indicate that it was not the case. This was later confirmed (March 2012 - 230+days post burial) by observation of one of the sites,

which had undergone scavenging activities by coyotes, the shallow burial body was mostly intact, and just reaching the active decay stage.

2. Soil Chemistry

Of the 32 elements analyzed by ACME, only calcium (Ca), iron (Fe), magnesium (Mg), manganese (Mn), sodium (Na), phosphorus (P), sulphur (S), and potassium (K) are of interest because of their relationship between cadaver decomposition chemicals and vegetation pigment effect. A One Way ANOVA was applied to each element to asses if there were differences in each grave site category mean (Table 1).

Table 1. Results of ANOVA on elements through the four sampling periods. Bold numbers indicate results that show that at least one value is statistically different from the rest of the grave type element mean in that time period. Italics indicate values that while not statistical significant at the 95% confidence interval, produce operationally acceptable 80% confidence interval values.

Jul-28	F	df	p	Aug-22	F	df	p
Mn	2.12	3,20	0.13	**Mn**	2.28	3,19	*0.11*
Fe	2.6	3,20	*0.08*	**Fe**	2.82	3,19	*0.07*
Ca	1.54	3,20	0.23	**Ca**	3.2	3,19	**0.046**
P	2.4	3,20	*0.09*	**P**	14.2	3,19	**0.0001**
Na	0.16		0.92	**Na**	4.1	3,19	**0.02**
Mg	1.57	3,20	0.22	**Mg**	2.69	3,19	*0.07*
K	1.18	3,20	0.34	**K**	10	3,19	**0.0003**
S	0	3,20	0	**S**	1	3,19	0.41
Aug-08	**F**	**df**	**p**	**Nov-15**	**F**	**df**	**p**
Mn	2.29	3,20	*0.11*	**Mn**	0.16	3,20	0.92
Fe	2.82	3,20	*0.07*	**Fe**	2.01	3,20	*0.15*
Ca	3.2	3,20	**0.046**	**Ca**	0.43	3,20	0.74
P	14.2	3,20	**0.001**	**P**	1.01	3,20	0.41
Mg	2.6	3,20	*0.07*	**Na**	2.52	3,20	*0.09*
Na	4.09	3,20	**0.02**	**Mg**	0.47	3,20	0.71
K	10	3,20	**0.0003**	**K**	6.64	3,20	**0.003**
S	1	3,20	0.41	**S**	230.5	3,20	**0.0001**

Soil manganese concentrations ranged from 206 to 3905 ppm over the four time periods across the different grave types (Table 18). With the exception of the increase in concentration over time there is no clear pattern of mean concentrations by grave type over time observed. Manganese is released in cadaver decomposition initially from the liver and kidneys, and later from the bone. Based on previous taphonomic studies, Mn reaches its peak around 23 days post mortem in surface bodies (Carter et al., 2007). The findings in the literature used for the background review seem to correlate with the timing mean concentration of Mn in the soil associated with surface bodies reaching significantly higher that the reference soil on August 08 approximately 20 days post mortem.

Table 2. Mean Mn concentrations and standard deviation (ppm) over time for each grave type. The bold font highlights the peak in surface bodies on August 08

	July 28		**August 08**		**August 22**		**November 15**	
	Mean	**Std Dev**	**Mean**	**Std Dev**	**Mean**	**Std Dev**	**Mean**	**Std Dev**
Deep	1315	235	977	443	1024	534	2907	1034
Shallow	766	370	577	446	493	437	2126	877
Surface	1186	349	**1210**	306	1099	265	2385	629
Reference	775	314	436	340	482	699	2385	1003

Concentrations of soil Fe ranged from 0.05 to 3.94% through the four time periods across the different grave types. Average concentrations in Reference grave soils were lower than those associated with Surface bodies especially in the first three sampling periods, by about 70% (Table 19). The surface bodies had the greatest concentration of iron in the soil of the grave types in each sampling time period with values ranging 1.31-1.5% versus 0.91-1.4% in soils of the other grave types (Table 3). The average concentration in soils of surface burials also

increased from 1.11% in the initial collection period to 3.11% in the last. Considering that pigs and humans are composed of ~40-70 ppm iron (the typical adult human body contains about 2200-4000 mg of iron), it forms a sizable amount of iron to be released during early decomposition (Carter, Yellowlees, & Tibbett, 2007). Iron is released during early decomposition from the blood, liver and other soft organs.

Table 3. Mean Fe concentrations (%) in soil over time for each grave type

	July 28		**August 08**		**August 22**		**November 15**	
	Mean	**Std Dev**	**Mean**	**Std Dev**	**Mean**	**Std Dev**	**Mean**	**Std Dev**
Deep	1.27	0.38	1.28	0.22	1.38	0.38	3.11	0.26
Shallow	1.27	0.32	0.91	0.38	1.01	0.28	3.19	0.43
Surface	1.31	0.28	1.50	0.31	1.43	0.22	2.86	0.35
Reference	0.91	0.19	0.98	0.24	1.08	0.70	2.99	0.58

The Ca concentration varied considerably across the collection time and grave types, ranging from 0.09% to 7.03%. It is further interesting to note that soils at surface burials generally had had the least amount of Ca ranging from 0.2-2.89% with median of 0.35% over the four collection periods. The variability in Ca concentration of surface burial soils was low, the standard deviation was 0.55 versus 1.5-2.5 for other grave types (Table 4). Calcium is likewise essential for many plant functions, mainly for the role it plays in relation to magnesium uptake. Calcium is also a vital part of mammalian bodies. Calcium enters the soil in advanced decomposition stages around the same time as manganese (Carter et al., 2007).

Table 4. Average Ca concentration (%) in soil over time for each grave type

	July 28		August 08		August 22		November 15	
	Mean	**Std Dev**	**Mean**	**Std Dev**	**Mean**	**Std Dev**	**Mean**	**Std Dev**
Deep	0.25	0.17	1.06	0.82	0.61	0.69	1.76	1.43
Shallow	0.18	0.10	0.17	0.90	0.18	0.07	0.81	0.99
Surface	0.29	0.28	0.32	0.25	0.31	0.27	0.6	0.94
Reference	0.21	0.19	0.27	0.71	0.34	0.99	1.21	2.57

The P levels measured over the sampling period increased over time, from an overall mean of 0.067% to 0.168%. The difference in P concentrations soils associated with surface bodies versus the reference sites were 28-58%, indicating the difference between the surface bodies and the rest of the sites. Phosphorus and Ca form non-soluble compounds (up to 90% of the total P in some soils) that cannot be utilized by plants, leading to possible phosphorus deficiency even if soil tests indicate high levels of phosphorus (Jones, 2003). Phosphorus persists in the soil matrix for a fairly long time and according to Towne's (2000) findings the phosphorus levels in surface bodies should remain at above basal levels at least three years postmortem.

Table 5. Average soil P (%) concentration over time for each grave type

	July 28		August 08		August 22		November 15	
	Mean	**Std Dev**	**Mean**	**Std Dev**	**Mean**	**Std Dev**	**Mean**	**Std Dev**
Deep	0.066	0.01	0.091	0.02	0.08	0.02	0.155	0.04
Shallow	0.068	0.02	0.053	0.01	0.06	0.01	0.165	0.03
Surface	0.074	0.01	0.096	0.01	0.11	0.02	0.233	0.07
Reference	0.058	0.01	0.061	0.01	0.07	0.02	0.165	0.02

Sodium is sometimes not considered essential in plants, however it is taken up readily from soil (Subbarao, Ito, Berry, & Wheeler, 2003). The sodium level in the soils of surface burials was higher than other grave types in the fourth collection period, 0.018% versus 0.012% (Table 6). The ANOVA results for sodium indicated at least one means was statistically different and from looking at the values it was the surface bodies' sites.

Table 6. Average soil Na concentrations (%) over time for each grave type

	July 28		**August 08**		**August 22**		**November 15**	
	Mean	**Std Dev**	**Mean**	**Std Dev**	**Mean**	**Std Dev**	**Mean**	**Std Dev**
Deep	0.006	0.01	0.010	0.01	0.008	0.01	0.010	0.01
Shallow	0.007	0.01	0.000	0.00	0.000	0.00	0.012	0.02
Surface	0.005	0.01	0.010	0.01	0.020	0.01	0.018	0.01
Reference	0.003	0.01	0.003	0.01	0.003	0.01	0.012	0.02

Concentrations of Mg were significantly lower in soils of the surface grave sites than the other grave types especially in the fourth collection time when soils associated with the surface bodies had the 0.68% Mg versus the 1.21-1.41% of the disturbed grave sites (Table 7). Cadaver decomposition studies have shown an increase in the concentration of Mg and peak deposition of Mg into the soil matrix in surface cadavers generally occurs at the same time as Mn and Ca (~23 days) (Carter et al., 2007). However in the data from my research site, the peak in Mg was not present on the grave surface soils at the time the peak was present for Mn and Ca.

Table 7. Average soil Mg concentrations (%) over time for each grave type

	July 28		August 08		August 22		November 15	
	Mean	**Std Dev**	**Mean**	**Std Dev**	**Mean**	**Std Dev**	**Mean**	**Std Dev**
Deep	0.22	0.08	0.52	0.30	0.46	0.34	1.21	0.85
Shallow	0.17	0.08	0.17	0.07	0.18	0.06	1.22	1.36
Surface	0.22	0.19	0.28	0.18	0.28	0.01	0.68	0.57
Reference	0.16	0.04	0.30	0.24	0.41	0.38	1.41	1.48

The soil associated with surface cadavers had roughly two times more K than the other grave types (Table 8) and concentrations increased from 0.06% to 0.18% as decomposition continued over time. Carter et al (2007) found that decomposition results in an increase in the concentration of K in the soil surrounding the cadaver. This increase in K should persist from early decomposition through to advanced and 'dry' stages, at trend that appears in the surface K values (Vass, Bass, Wolt, Foss, & Ammons, 1992).

Table 8. Average soil K concentrations (%) over time for each grave type, bold font highlights the high values for the surface bodies at each collection time

	July 28		August 08		August 22		November 15	
	Mean	**Std Dev**	**Mean**	**Std Dev**	**Mean**	**Std Dev**	**Mean**	**Std Dev**
Deep	0.06	0.02	0.07	0.02	0.07	0.03	0.11	0.03
Shallow	0.05	0.02	0.05	0.01	0.05	0.01	0.13	0.02
Surface	**0.09**	**0.06**	**0.11**	**0.04**	**0.14**	**0.05**	**0.18**	**0.04**
Reference	0.05	0.01	0.05	0.01	0.06	0.02	0.11	0.03

Sulfur was only measurable in the soil of surface sites which had cadaver decomposition (Table 1). This is reasonable as others have suggested that elevated sulfur levels are indicators of body decomposition (Hopkins, Wiltshire, & Turner, 2000).

Table 9. Average soil S concentration (%) of over time for each grave type, highlighting the only detectable values for the surface bodies at each collection time

	July 28		**August 08**		**August 22**		**November 15**	
	Mean	**Std Dev**	**Mean**	**Std Dev**	**Mean**	**Std Dev**	**Mean**	**Std Dev**
Deep	0	0	0	0	0	0	0	0
Shallow	0	0	0	0	0	0	0	0
Surface	**0**	**0**	**0.01**	**0.02**	**0.02**	**0.03**	**0.07**	**0**
Reference	0	0	0	0	0	0	0	0

Examination of the soil chemistry results suggests that some of changes are caused by disturbance of the soil, rather than any chemicals released from the decomposing bodies, such as seen in the Mg, Ca and Fe levels, especially in the fourth collection period. However, it is also clear that the cadaver decomposition played a role in the levels of S, K, and P since they are greatly elevated in the decomposed surface bodies.

3. Vegetation Pigments – Chlorophyll and Carotenoids

Vegetation pigments were only sampled on November 15, 2011 (118 days post mortem). Four categories of vegetation pigments were analyzed chlorophyll a, chlorophyll b, total chlorophyll, and carotenoids.

Table 10. Maximum, Minimum and Mean values (mg/cm^2) for All Vegetation Pigments across All Sites

	Chl a	Chl b	Chl Total	Car
Max	0.07	0.03	0.08	5.24
Min	0.03	0.00	0.01	0.45
Mean (arithmetic)	0.03± 0.010	0.01 ± 0.003	0.045±0.013	2.29±0.75

A One Way ANOVA was applied to each pigment category to asses if there was a difference between grave site means (Table 10). The p-values, indicate that at least one mean value was statistically different for each pigment type (Table 11).

Table 11. Oneway ANOVA results for each pigment category

	F	Df	P value
Chl a	16.9	2,198	<.0001
Chl b	38.5	2,198	<.0001
Total Chl	23.4	2,198	<.0001
Carotenoids	4.97	2,198	0.006

However, the ANOVA did not indicate where the difference lies. For this another test was performed. Basic analysis was performed using a Students t test to determine if the vegetation categories were significantly different and whether there was significant difference in the means in order to separate background vegetation from disturbed/grave site vegetation, and whether it was further

possible to separate the disturbed/grave sites into distinct categories based on total chlorophyll, chlorophyll a, chlorophyll b, and carotenoid levels.

Chlorophyll a

Concentrations of chlorophyll a differentiated between background vegetation, surface grave vegetation, and disturbed/shallow/deep grave sites. The chlorophyll a concentration in background vegetation is clearly separable from other vegetation groups ($p < 0.0005$). The concentrations in vegetation associated with surface bodies were also distinct from the remaining three vegetation groups with probabilities of 0.01 for shallow, 0.04 for reference and 0.13 for deep graves. The median chlorophyll a concentration in the vegetation growing around the surface bodies was higher than the median background, shallow graves and reference sites (Table 12). The chlorophyll a values from the deep graves, the reference sites and the shallow graves are not significantly different (p-values 0.41-0.79), indicating an overall disturbance effect rather than a direct effect on the vegetation from the decomposition chemical from buried remains.

Table 12. Minimum, Median and Maximum Chlorophyll a concentrations (mg/cm^2) for each grave type

Level	Minimum	Median	Maximum
Background	0.00	0.02	0.04
Deep	0.01	0.03	0.06
Graves (surface body)	0.01	0.03	0.07
Reference	0.02	0.03	0.06
Shallow	0.02	0.03	0.05

Chlorophyll b

It was possible to differentiate between background vegetation, surface grave vegetation, and disturbed/shallow/deep grave sites using chlorophyll b.

These results mirror the chlorophyll a results. Background vegetation is clearly separable from other vegetation groups with a p-value of <.0001. The chlorophyll b concentrations in the vegetation growing around the surface bodies are not significantly higher than the background, shallow graves or reference sites (Table 13) with p-values of 0.003 for shallow, 0.021 for reference, and 0.107 for deep grave sites. The chlorophyll b values from the deep graves, the reference sites and the shallow graves are not significantly different (p-values 0.268-0.612), indicating an overall disturbance effect rather than a direct effect on the vegetation from the decomposition chemical from buried remains.

Table 13. Minimum, Median and Maximum Chlorophyll b values (mg/cm^2) for each grave type

Level	Minimum	Median	Maximum
Background	0.00	0.01	0.02
Deep	0.01	0.01	0.02
Grave (surface body)	0.01	0.01	0.03
Reference	0.01	0.01	0.02
Shallow	0.01	0.01	0.02

Total Chlorophyll

Total Chlorophyll is a sum of both chlorophyll a and b, and it is unsurprising that the results of the analysis reflect similar to the results in chlorophyll a and chlorophyll b. The differences between background and the grave sites are even more distinct in the medians of this dataset (p-value <0.0001) with almost double the total chlorophyll level in the disturbed soils versus the undisturbed background (Table 14).

Table 14. Minimum, Median and Maximum Chlorophyll Total values (mg/cm^2) for each grave type, bold indicated highest value of mean.

Level	Minimum	Median	Maximum
Background	0.01	0.03	0.05
Deep	0.02	0.04	0.08
Grave (surface body)	0.02	**0.05**	0.08
Reference	0.03	0.04	0.08
Shallow	0.03	0.04	0.07

Carotenoids

While still maintaining some separability between the background, and surface bodies from the rest of the categories, there is less separability using carotenoids than the chlorophyll results (Table 15). Background vegetation has a significantly lower median concentration (1.6 mg cm^{-2}) of carotenoids than disturbed soil vegetation (2.3 mg/cm^2). Background vegetation is clearly separable from other vegetation groups based on carotenoids with a p-value of 0.0014-0.0018. Surface bodies were not as distinct from the other vegetation groups, shallow was the only site type with a significant level of probability(0.0407), the reference p-value of 0.798 and the deep p-value of 0.74 indicate that carotenoids do not seem to be a viable method for separating the disturbed vegetation categories.

Table 15. Minimum, Median and Maximum Carotenoid concentrations (mg/cm^2) for each grave type

Level	Minimum	Median	Maximum
Background	0.45	1.59	3.43
Deep	1.09	**2.27**	4.62
Grave (surfaces body)	1.11	**2.27**	4.33
Reference	1.06	**2.23**	5.24
Shallow	1.06	**2.13**	3.35

Using Canonical Discriminant Analysis to distinguish among the vegetation samples and classify them into groups (Figure 1). The key assumption of canonical discriminant analysis is that all individuals can be assigned to one and only one group in advance (Sall, Creighton, & Lehman, 2007).

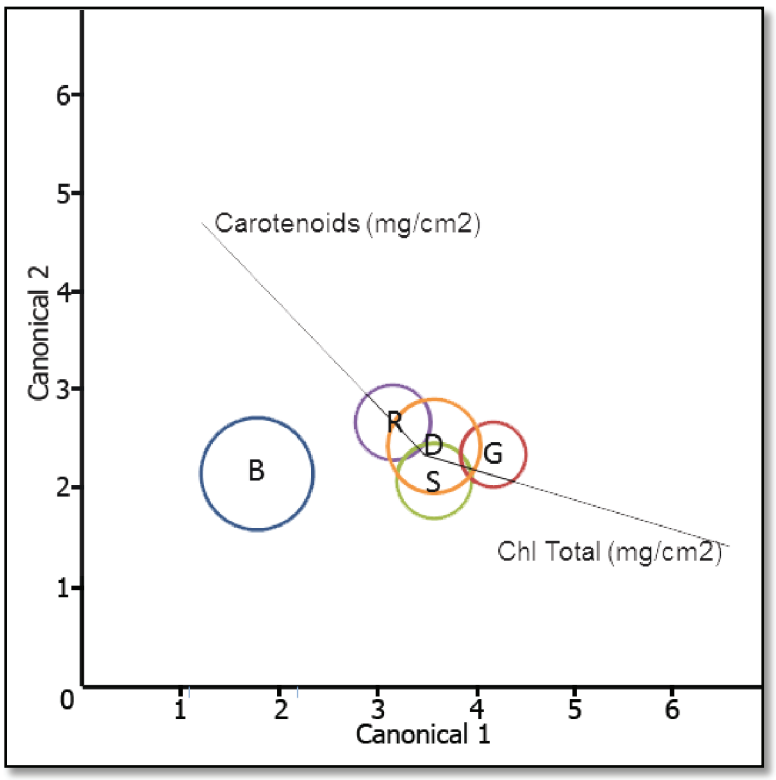

Figure 1. Canonical Discriminant Analysis based on Total Chlorophyll and Carotenoids in showing Background (B) vegetation distinct from the disturbed grave site vegetation, Reference grave (R) are more influenced by carotenoids whereas Surface bodies (G) are more classified by Chlorophyll. Shallow and Deep graves are neither direction and not well classified into each group.

In summary, the vegetation pigments indicate that there is something occurring on the disturbed sites to affect the chlorophyll and carotenoid levels, some of these changes are caused by disturbance of the soil which explains the separability of the background vegetation from the disturbed sites. However, it is

also clear that the cadaver decomposition has a role to play in enabling separability between the surface bodies and the rest of the vegetation, and the products released from the decomposition are likely the cause of the differences in chlorophyll and carotenoid levels. A future potential contribution to our understanding of these processes will be to track how the decomposition of the shallow and deep burials will affect the vegetation pigments.

I used the PRTools Classifiers In MATLAB to determine whether it was possible to classify background vegetation into a group distinct from disturbed/grave site vegetation, and whether it was then possible to classify the disturbed/grave sites into distinct groups based first on chlorophyll a and chlorophyll b and then on total chlorophyll and carotenoids The vegetation pigment data was separated into four categories with the shallow and deep graves were clumped into one class. Based on these categories 10 questions were asked in terms of classifiability. I chose to accept 80% accuracy (error < 0.20) based on what operational parameters would be in real scenarios. Questions 5, 7 and 10 address whether the background vegetation differs from the selected grave/disturbance type vegetation. Questions 1 through 4 attempt to classify the vegetation types into different combination of classes. Questions 6, 8 and 9 address the separability between the disturbed soil classes.

Question 1, which is intended to separate the dataset into three categories of background, graves, and reference vegetation; question 2 which attempts to classify the data into three categories of background, reference and gravesites with bodies and question 3 addressing the separability of the four grave types into background, reference, graves, and surfaces bodies were shown to be unfeasible using these classifiers on total chlorophyll and carotenoids levels with results from testing indicating there was not possible to classify between the classes in both testing and training with any accuracy, with the error values ranging from 21.8-67.6% error in training (Table 16) and 27-78% error in testing (Table 17) .

Classifying the background vegetation from the all body containing sites using total chlorophyll and carotenoids (Q4) training results of 0.064-0.423 (6.4-

42.3%) and testing results of 0.065-0.45 (6.5-45%) across all however there were six classifiers (ldc, qdc, bpxnc, klldc, quadrc, and parzenc) which performed better with values of 0.064-0.231(6.4-23.1%) in training and 0.065-0.156 (6.5-15.6%) in testing (Figure 2) .

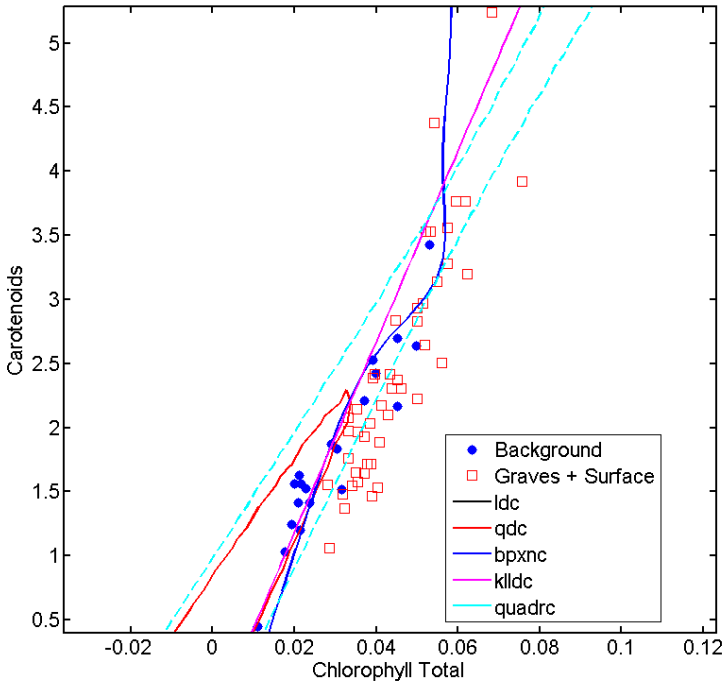

Figure 2. Classification of the background vegetation versus the all body containing sites (Q4) using total chlorophyll and carotenoids showing selected classifiers with <0.20 or better results.

A critical question in classifying background vegetation from the reference graves (Q5) using total chlorophyll and carotenoids yielded values from 0.091-0.458 (9.1-45.8% error). The ldc, qdc, bpxnc, klldc, and quadrc classifiers had acceptable classification error rates of 9.1-18.2% in testing but 18.2-30.3% in testing (Figure 3). Successful classification of background vegetation from reference grave sites using total chlorophylls and carotenoids indicates that some of the detectable effects on vegetation are due to soil disturbance rather than cadaveric decomposition chemicals.

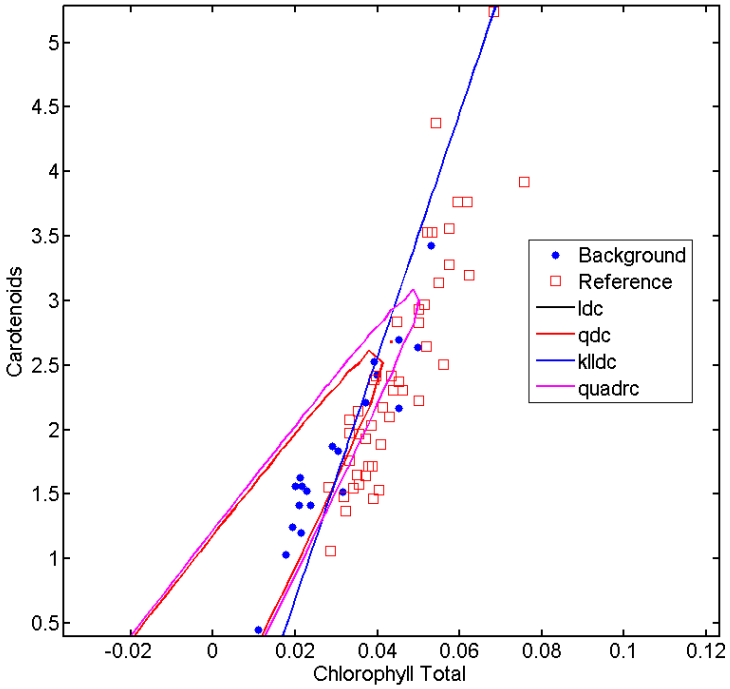

Figure 3. Question 5 Classifying background vegetation from the reference graves (Q5) using total chlorophyll and carotenoids showing selected classifiers with <0.20 or better results.

Classifying surface bodies from shallow and deep burial (Q6) indicated that classification into those classes was not very accurate with 23.4-44.1% error rates in training and 34.3-56.7% error rates in testing. Use of total chlorophyll and carotenoids to separate background vegetation into a class distinct from the shallow and deep burial gravesites (Q7) yielded errors of 12.5-45.8% in training and 10.1-404% in testing. Six of the classifiers (knnc, ldc, qdc, bpxnc, klldc, quadrc, and parzenc) had errors under 20% in training but only four (ldc, qdc, bpxnc, klldc) in testing (Figure 4).

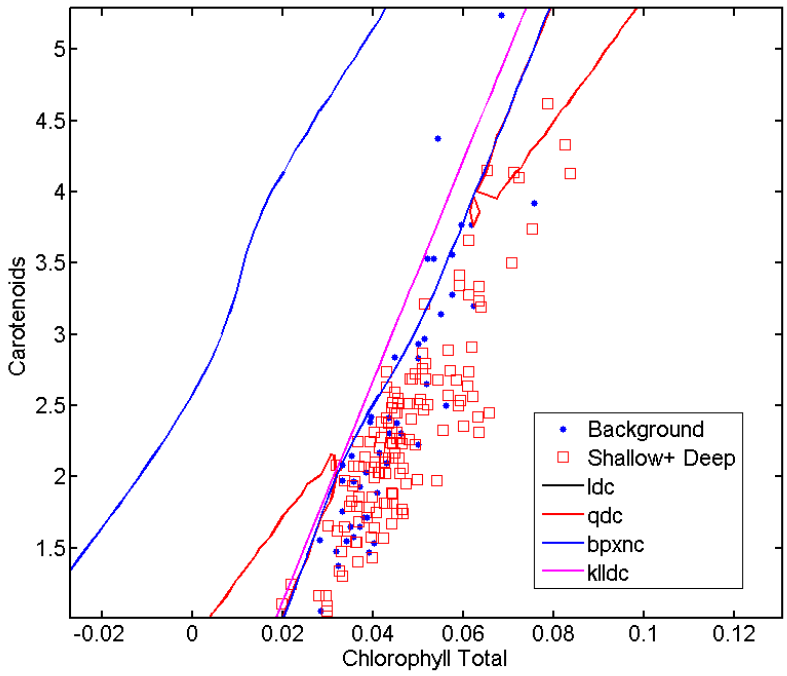

Figure 4. Question 7 Classifying background vegetation from the shallow and deep graves using total chlorophyll and carotenoids showing selected classifiers with <0.20 or better results.

Questions 8 and 9 address similar points of classifying the reference graves from the shallow and deep grave sites (Q8) and reference from all sites containing bodies (Q9). With errors of 24.2-45.9% in training and 23.3-44.4% in testing indicates inability to classify them accurately. This further indicates that some of the detectable effects on vegetation are due to soil disturbance rather than cadaveric decomposition chemicals.

Classification of background vegetation vs. the surface bodies had errors of 2.5-50% in training and testing. Six of the eight classifiers had errors below 20% with four of them (ldc, qdc, bpxnc, klldc) at 2.5% error. This level of classification into the two categories indicates that the cadaveric decomposition chemical in the surface graves play a significant role in the differences in total chlorophyll and carotenoid pigments.

Table 16. Total Chlorophyll and Carotenoid Training results of all classifiers across the ten questions. Background (B), reference (R), Surface bodies (S), and Graves containing shallow and deep burials (G)

Train	knnc	ldc	qdc	bpxnc	Klldc	quadrc	parzenc	nmc
Q1 B vs. G vs. R	0.37	0.38	0.35	0.31	0.38	0.48	0.44	0.68
Q2 B vs. G+S vs. R	0.33	0.27	0.26	0.22	0.27	0.40	0.33	0.60
Q3 B vs. G vs. S vs. R	0.61	0.48	0.44	0.42	0.48	0.55	0.60	0.67
Q4 B vs. G+S	0.13	0.09	0.10	0.06	0.09	0.23	0.13	0.42
Q5 B vs. R	0.30	0.18	0.15	0.09	0.18	0.12	0.30	0.40
Q6 G vs. S	0.23	0.35	0.31	0.28	0.35	0.37	0.32	0.44
Q7 B vs. G	0.21	0.13	0.15	0.13	0.13	0.25	0.21	0.46
Q8 R vs. G+S	0.25	0.24	0.25	0.20	0.24	0.39	0.24	0.45
Q9 R vs. G	0.28	0.36	0.34	0.33	0.36	0.41	0.36	0.46
Q10 B vs. S	0.20	0.03	0.03	0.03	0.03	0.08	0.25	0.50

Table 17. Total Chlorophyll and Carotenoid Testing results of all classifiers across the 10 questions. Background (B), reference (R), Surface bodies (S), and Graves containing shallow and deep burials (G)

Test	knnc	ldc	qdc	bpxnc	klldc	quadrc	parzenc	nmc
Q1 B vs. G vs. R	0.44	0.36	0.39	0.37	0.36	0.46	0.43	0.66
Q2 B vs. G+S vs. R	0.33	0.27	0.27	0.28	0.27	0.41	0.33	0.66
Q3 B vs. G vs. S vs. R	0.60	0.47	0.53	0.55	0.47	0.64	0.61	0.78
Q4 B vs. G+S	0.13	0.08	0.07	0.09	0.08	0.16	0.13	0.46
Q5 B vs. R	0.30	0.21	0.18	0.18	0.21	0.30	0.30	0.33
Q6 G vs. S	0.57	0.37	0.34	0.37	0.37	0.34	0.46	0.45
Q7 B vs. G	0.21	0.11	0.11	0.09	0.11	0.23	0.21	0.40
Q8 R vs. G+S	0.26	0.24	0.23	0.29	0.24	0.29	0.26	0.44
Q9 R vs. G	0.42	0.33	0.35	0.35	0.33	0.35	0.38	0.43
Q10 B vs. S	0.20	0.03	0.03	0.03	0.03	0.08	0.25	0.50

Using chlorophyll a and b the same research questions yielded a similar pattern of results. Question 1, which attempts to distinguish among background, graves, and reference vegetation, question 2 which attempts to distinguish among background, reference and gravesites with bodies and question 3 which attempts to classify the four grave types into background, reference, graves, and surfaces bodies were shown to be unfeasible in testing using these classifiers on chlorophyll a and b with errors of 28-70% (Table 19) despite the low error rate in knnc in training (Table 18).

Classifying the background vegetation from the all body containing sites using chlorophyll a and b (Q4) training results of 0.065- 0.221 (6.5-22.1%) and testing results of 0.051-0.321 (5.1-32%) across all however there were seven of the eight classifiers (knnc, ldc, qdc, bpxnc, klldc, quadrc, and parzenc) which performed better with values of 0.064-0.13 (6.4-13%) in training and 0.051-0.09 (5.1-9.%) in testing.

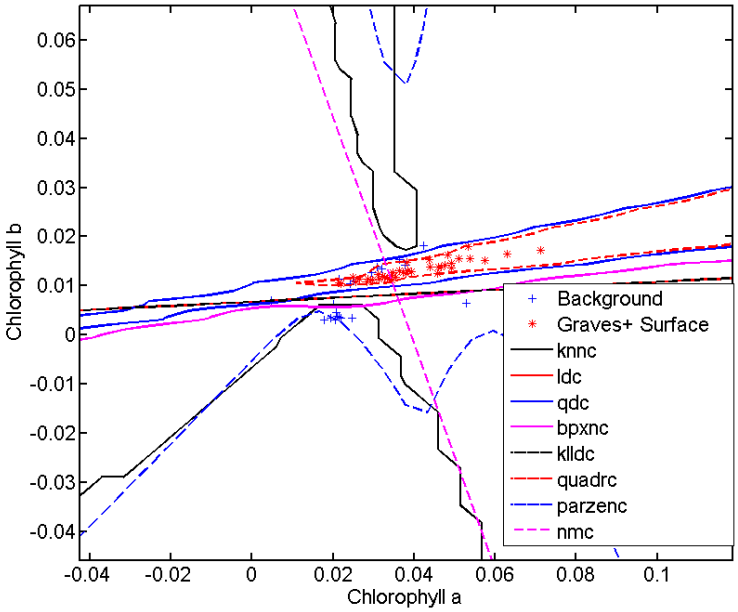

Figure 5. Classifying the background vegetation from the all body containing sites (Q4) using total chlorophyll a and b showing selected classifiers with error <0.20 or better results.

In classifying background vegetation from the reference graves (Q5) using chlorophyll a and b yielded values from 0.121-0.303 (12.1-30.3% error) in training and 0-39.4% error in testing (Figure 6). The knnc, ldc, qdc, bpxnc, klldc, and quadrc classifiers had acceptable classification error rates of 12.5-21.2% in testing but 0-15.2% in testing. Being able to classify background vegetation from reference grave sites using total chlorophylls and carotenoids indicates that some of the detectable effects on vegetation are due to soil disturbance rather than cadaveric decomposition chemicals.

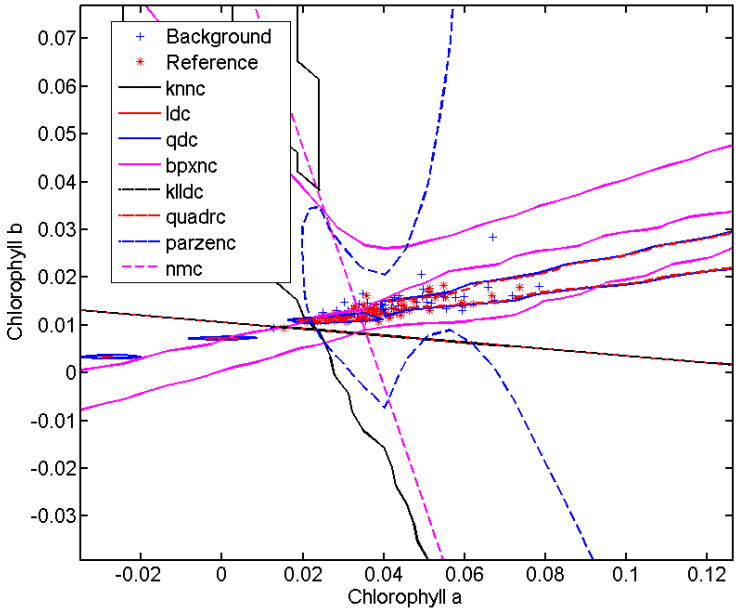

Figure 6. Question 5 Classifying background vegetation from the reference graves (Q5) using chlorophyll a and b

Classifying surface bodies from shallow and deep burial (Q6) indicated that classification into those classes was not very accurate with 34.3-47.8% error in training and 32.4-41.2% in testing across all the classifiers.

For classifying background vegetation from the shallow and deep burial gravesites (Q7) using chlorophyll a and b was shown to be doable with a low error

rate of 8.5-19.2% in training and a range of 4.2-35.4 % in testing with seven of the eight classifiers having error rates of 4.2-14.6%. .

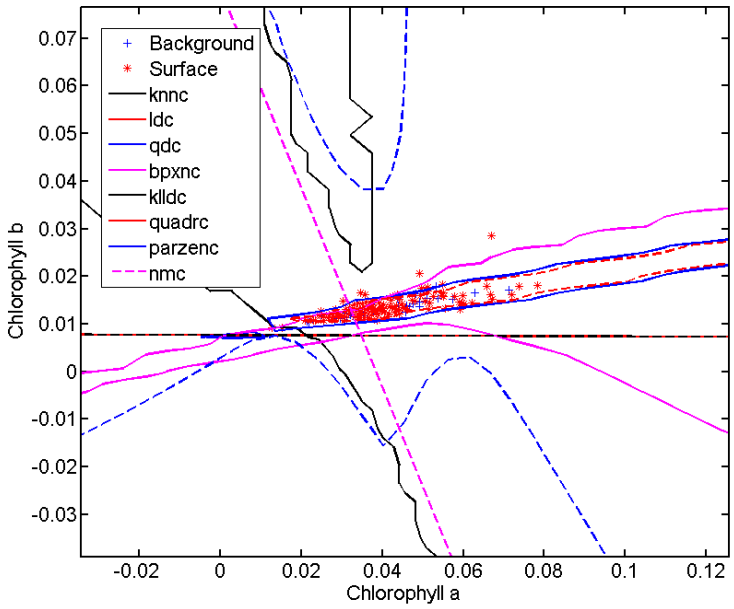

Figure 7. Classifying background vegetation from the shallow and deep graves using chlorophyll a and b showing all classifiers

Questions 8 and 9 classifying the reference graves from the shallow and deep grave sites (Q8) and reference from all sites containing bodies (Q9) had error values between 25.3-52.8% in training and testing.

The last question of classifying background vegetation from surface graves presented 7.5-27.5% error rates in training and testing. Seven of the eight classifiers (knnc, ldc, qdc, bpxnc, klldc, quadrc, and parzenc) had error rates under 20% (7.5-15%).

Table 18. Chlorophyll a and b Training results of all classifiers across the ten questions. Background (B), reference (R), Surface bodies (S), and Graves containing shallow and deep burials (G).

Chl a and b Train	knnc	Ldc	qdc	bpxnc	klldc	Quadrc	parzenc	nmc
Q1 B vs. G vs. R	0.03	0.39	0.38	0.39	0.39	0.41	0.47	0.66
Q2 B vs. G+S vs. R	0.03	0.27	0.29	0.27	0.27	0.30	0.27	0.52
Q3 B vs. G vs. S vs. R	0.09	0.51	0.52	0.48	0.51	0.55	0.56	0.60
Q4 B vs. G+S	0.07	0.07	0.09	0.07	0.07	0.10	0.13	0.22
Q5 B vs. R	0.18	0.12	0.15	0.21	0.12	0.15	0.18	0.30
Q6 G vs. S	0.48	0.37	0.40	0.45	0.37	0.40	0.46	0.34
Q7 B vs. G	0.09	0.09	0.13	0.09	0.09	0.11	0.13	0.19
Q8 R vs. G+S	0.25	0.25	0.25	0.22	0.25	0.53	0.25	0.52
Q9 R vs. G	0.45	0.42	0.38	0.37	0.42	0.33	0.40	0.43
Q10 B vs. S	0.10	0.15	0.13	0.08	0.15	0.15	0.13	0.28

Table 19. Chlorophyll a and b Testing results of all classifiers across the ten questions. Background (B), reference (R), Surface bodies (S), and Graves containing shallow and deep burials (G).

Chl a and b Test	knnc	ldc	qdc	bpxnc	klldc	quadrc	parzenc	Nmc
Q1 B vs. G vs. R	0.53	0.39	0.43	0.40	0.39	0.39	0.47	0.56
Q2 B vs. G+S vs. R	0.38	0.28	0.29	0.29	0.28	0.31	0.29	0.56
Q3 B vs. G vs. S vs. R	0.70	0.52	0.52	0.56	0.52	0.58	0.55	0.65
Q4 B vs. G+S	0.08	0.06	0.06	0.05	0.06	0.08	0.09	0.32
Q5 B vs. R	0.15	0.15	0.09	0	0.15	0.09	0.12	0.39
Q6 G vs. S	0.35	0.34	0.35	0.37	0.34	0.32	0.35	0.41
Q7 B vs. G	0.15	0.10	0.08	0.04	0.10	0.13	0.15	0.35
Q8 R vs. G+S	0.28	0.26	0.26	0.27	0.26	0.41	0.25	0.44
Q9 R vs. G	0.30	0.38	0.36	0.25	0.38	0.49	0.36	0.46
Q10 B vs. S	0.10	0.15	0.13	0.08	0.15	0.15	0.13	0.28

In summary while it is possible to classify the background vegetation from all of the other graves types, classification amongst the four disturbed grave sites is not accurate. These results seem to show that the disturbance of the soil has a greater effect on the vegetation pigments than the cadaver decomposition chemicals. However at the time in which the vegetation samples were collected it appeared that insufficient decomposition had occurred in the shallow and deep burials to affect the soil chemistry. So as time progresses there may be a shift in the effect of the cadaver soil chemical on the vegetation pigments in those sites. The reference site may become classifiable from the body containing sites with a much higher level of accuracy than the current 25.5%.

Some of the classifiers performed better than others for the task of classifying the vegetation pigments into classes. The nmc (nearest mean classifier) had consistently poor performance with the highest error rates in each question with 45-65% error rates in the total chlorophyll and carotenoids data set. The error rates were lower for the chlorophyll a and b dataset but still > 25%. The knnc (*k*-nearest neighbor algorithm) and parzenc (parzen) classifiers were the next most poorly performing ones overall, though had some good low error rates in some questions namely the ones classifying background from disturbed soil sites. The next three, bpxnc (Back-propagation trained feed-forward neural net), klldc (KL expansion of the common covariance matrix) and quadrc (Quadratic Discriminant Classifier) have shown to be good choices for classifiers in this type of analysis, they had consistent results with error rate frequently under 20%. The remaining two classifiers ldc and qdc had consistently lowest error rates across both datasets. Any future analysis of the vegetation pigments will focus on the last five classifiers, since they had consistently lowest errors.

4. Soil and Vegetation Spectra

A soil reflectance spectral signature is affected by the mineral composition, the soil moisture and soil particle size (Wetterlind, Stenberg, & Rossel, 2013). Due to the sample preparation, the soil moisture and particle size across the samples have been standardized making it possible to compare just the optical properties of the chemical/mineral composition of the soil.

The first way of comparing the soil spectra involved examining the spectral amplitude (delta) and shape (theta) values. A One Way ANOVA was applied to determine if there was a difference between each grave site category means. ANOVA for the amplitude (delta) and the shape (delta) p-values in July 27, August 08 and November 15 indicated that the means were not significantly different, however the August 22 measurements had a probability of <0.0001 indicating that at least one of the means was different (Table 20).

Table 20. ANOVA results for delta and theta of soil spectra. Bold highlights results with statistically significant at 95% confidence interval, italic highlight results statistically significant at 80%

Delta			
	F	Df	p-value
Jul-28	*1.96*	*3,73*	*0.13*
Aug-08	0.31	3,69	0.82
Aug-22	**19.3**	**3,67**	**0.001**
Nov-15	1.44	3,68	0.24
Theta			
Jul-28	1.27	*3,73*	0.29
Aug-08	0.70	3,69	0.56
Aug-22	**17.7**	**3,67**	**0.001**
Nov-15	*1.77*	3,68	*0.16*

Despite the mixed ANOVA results, I chose to proceed to assess separability between the four soil categories, the values of the amplitude (delta) and the shape (delta) of the soil spectra were compared using a Students t test.

From the samples collected in July, amplitude (delta) means are only statistically different when comparing Reference graves to Surface bodies with a p= 0.034. Shallow and Deep graves versus reference had p= 0.08 and 0.05 which makes them statically significant in an 80% confidence interval. Comparing the other graves types to each other indicated no statistical difference (probabilities ranged from 0.7-0.92). There was no statistical difference in amplitude (delta) means at the 95% confidence interval with values ranging from 0.08-0.91, however reference graves versus surface, shallow and deep had p-values of 0.08-0.17 which makes them statically significant in a 80% confidence interval. For July the reference grave samples can be separated to a degree from the other grave types if looking at the delta values, no separation is evident if looking at the theta values. It is not possible to separate surface, shallow and deep graves.

As expected, there were no significant differences in the August 9 measurements using either delta or theta (p-values of 0.035-0.92 for delta and 0.18-0.71 for theta). It is interesting to note that there is more similarity between shallow and deep graves to the reference signature then there is by reference graves. To me this indicates there is more variation within the sample categories than that is within the whole data set.

Based on the ANOVA, the August 22 results seem the most promising. The surface bodies are clearly separable from the other sites using either delta or theta ($p < 0.0001$). At that time it had been 63 days post mortem and the surface bodies were well decomposed so the surface bodies should have affected the soil chemistry enough to be detectable. Reference sites were not significantly different from shallow and deep sites combined (probabilities ranged from 0.25-0.27) using the delta however the differences between surface and all other sites were significant (p=0.001), and for deep versus shallow p= 0.003. The results indicate that the deep and surface graves are significantly different from the other sites and

from each other enabling grouping of soil spectra into three categories of surface, deep, and shallow and reference sites.

The November 15 **r**esults indicate that is it possible to separate surface bodies from the reference graves using the theta (p-values of 0.038) but there was no statistical difference between any of the grave sites using the delta (p-values of 0.07-0.77).

The main purpose of undertaking a statistical analysis in MATLAB using PRTools 4 was to determine if it was possible to classify the four types of soil spectra using the complete range of 1,901 bands from 450-2350 nm, and to determine which classifier produced the lowest error rate.

Before classification the number spectra bands was reduced through the forward feature selection (featself) in MATLAB. Each question at every collection time period forms its own dataset for a total of 44 datasets for the study period (11 questions times 4 collection times) that needed to be reduced to optimal bands. The result of 'featself' is the optimal minimal number of bands needed to classify the classes being questioned in the dataset. From these the number needed for classification was applied to each dataset and classification was attempted using these bands reduced datasets.

For the soil spectra, eleven research questions were asked testing various combinations. Two main themes are prevalent in the questions asked in the MATLAB analysis; 1) are the reference graves statistically different from the other grave types that contain bodies , 2) are the surface body sites statically different from shallow, deep and reference sites? Questions 1, 2, 3,4,5,6 and 7 seek to address the first theme while questions 9, 10 and 11 seek to answer the surface body theme. Question 8 assessed the statistical difference and ability to classify into two separate groups between shallow and deep gravesites. Selected results from the classifiers are presented here; the complete results are available in the appendix.

Table 21. Results of the 'featself' on each collection period and research question listing optimal number of bands and the value. R = reference sites, D = deep graves, S = shallow graves, G = surface bodies, X = subsurface bodies (deep and shallow combined) selected classifiers results.

'featself'	July 28		Aug 08		Aug 22		Nov 15	
Question	**bands**	**value**	**bands**	**value**	**bands**	**value**	**bands**	**value**
1: R vs. D	9	0.95	15	0.95	7	0.83	8	0.92
2: R vs. S	3	1.00	53	0.97	7	0.89	13	0.75
3: R vs. G	13	0.97	2	1.00	3	1.00	3	1.00
4: R vs. X	8	0.98	8	0.95	3	0.83	6	0.83
5: R vs. X + G	11	0.97	5	0.95	3	0.87	8	0.92
6: R vs. X vs. G	6	1.00	18	0.93	3	0.83	17	0.83
7: R vs. S vs. G vs. D	20	0.94	76	0.87	3	0.78	3	0.70
8: D vs. S	6	0.98	2	0.97	3	0.89	11	0.92
9: D vs. G	2	1.00	2	1.00	3	0.97	8	1.00
10: G vs. S	2	1.00	2	0.97	3	0.94	10	0.92
11: X vs. G	3	1.00	2	0.97	3	0.97	9	1.00

For the July data, distinguishing the reference sites from the gravesites (Questions 1-7) was possible with every classifier in training except the nmc, which had substantially higher errors of 44% - 77%. When it came to classifier performance in testing, the nmc fared a bit better but still had a 30%-76% error rate. The klldc classifier also fared worse in testing than with the training, with 21%-45% error. The bpxnc classifier performed well in most questions, with an acceptable 3%-15% error rate in 10 out of 11 questions. The quadrc classifier appears to have separated the spectra the best with a 0.00% error rate in all classifications but this may be an artefact of the large number of bands and low sample size (Table 22). Separation of surface bodies from the other three site types (Questions 9-11) was feasible using the bpxnc, klldc and quadrc classifiers with 0%-17% error rates, which are well within the acceptable operational limits. However with the nmc classifier, the error rate was unacceptably high, ranging from 29% to 56% (Table 22).

Table 22. Classification results from the July 28th sampling date. R = reference sites, D = deep graves, S = shallow graves, G = surface bodies, X = subsurface bodies (deep and shallow combined) selected classifiers results.

July 28	Training Error				Testing Error			
Question	bpxnc	klldc	quadrc	nmc	bpxnc	klldc	quadrc	nmc
1: R vs. D	0.05	0.05	0.00	0.48	0.15	0.30	0.00	0.30
2: R vs. S	0.00	0.00	0.00	0.44	0.33	0.39	0.00	0.50
3: R vs. G	0.00	0.06	0.00	0.50	0.11	0.22	0.00	0.61
4: R vs. X	0.00	0.00	0.00	0.47	0.03	0.21	0.00	0.38
5: R vs. X + G	0.00	0.03	0.00	0.51	0.08	0.26	0.00	0.42
6: R vs. X vs. G	0.00	0.00	0.00	0.77	0.03	0.34	0.00	0.76
7: R vs. S vs. G vs. D	0.00	0.05	0.00	0.77	0.11	0.45	0.00	0.76
8: D vs. S	0.00	0.14	0.00	0.38	0.10	0.05	0.00	0.35
9: D vs. G	0.00	0.10	0.00	0.29	0.00	0.05	0.00	0.40
10: G vs. S	0.00	0.06	0.00	0.44	0.11	0.11	0.00	0.56
11: X vs. G	0.03	0.17	0.00	0.33	0.10	0.17	0.00	0.45

For the August 9 classifier data, separating the reference sites from the gravesites (Questions 1-7) was possible with every classifier in training except the nmc, which, depending on the question returned a high error of 22% - 77%. When it came to classifier performance in testing the nmc resulted in an equally high 22%-76% error rate. The klldc classifier also fared worse in the testing than it did with the training with 0%-28% error rate. The bpxnc classifier performed poorly in most questions with 6%-42% error rate. The quadrc classifier performed the best with a 0%-11% error rate in all classifications (Table 23), but similar to the July sampling date these results may be an artefact of the sample size in relation to the number of bands used. Trying to separate surface bodies from the other three site types (Questions 9-11) was feasible using the bpxnc, klldc and quadrc classifiers with 0%-6% error rates, well within the acceptable operational limits.

Table 23. Classification results from the August 09th sampling date. R = reference sites, D = deep graves, S = shallow graves, G = surface bodies, X = subsurface bodies (deep and shallow combined).

Aug 09	Training				Testing			
Question	bpxnc	klldc	quadrc	nmc	bpxnc	klldc	quadrc	nmc
1: R vs. D	0.00	0.00	0.00	0.28	0.06	0.28	0.11	0.44
2: R vs. S	0.17	0.00	0.00	0.56	0.33	0.06	0.00	0.39
3: R vs. G	0.00	0.00	0.00	0.22	0.00	0.00	0.00	0.22
4: R vs. X	0.04	0.00	0.00	0.41	0.19	0.07	0.04	0.56
5: R vs. X + G	0.19	0.00	0.00	0.44	0.28	0.08	0.03	0.36
6: R vs. X vs. G	0.00	0.00	0.00	0.75	0.11	0.08	0.03	0.75
7: R vs. S vs. G vs. D	0.25	0.00	0.00	0.75	0.42	0.11	0.11	0.75
8: D vs. S	0.00	0.00	0.00	0.22	0.17	0.17	0.06	0.56
9: D vs. G	0.00	0.00	0.00	0.17	0.00	0.00	0.00	0.22
10: G vs. S	0.00	0.00	0.00	0.28	0.06	0.00	0.00	0.33
11: X vs. G	0.00	0.00	0.00	0.26	0.00	0.00	0.00	0.26

Separating the reference sites from the gravesites (Questions 1-7) with the August 22 classifier data was possible with every classifier in training with the exception of Q7 for bpxnc and the nmc which had the high error rate of 22% - 77% depending on the question. . When it came to classifier performance in testing, the nmc returned a 22%-76% error rate. The klldc classifier also fared worse in the testing than it did with the training, with the exception of question 1 (28%), which had an acceptable 0%-11% error rate. The bpxnc classifier performed poorly in most questions with 0%-42% error rate. The quadrc classifier fared the best with a 0%-11% error rate in all classifications (Table 24). Separation of surface bodies from the other three site types (Questions 9-11) proved feasible using the bpxnc, klldc and quadrc classifiers with 0%-6% error rates, well within the acceptable operational limits. However with the nmc classifier the error rate was an unfeasible 22% to 33% (Table 24).

Table 24. Classification results from the August 22nd sampling date. R = reference sites, D = deep graves, S = shallow graves, G = surface bodies, X = subsurface bodies (deep and shallow combined).

Aug 22	Training				Testing			
Question	bpxnc	klldc	quadrc	nmc	bpxnc	klldc	quadrc	nmc
1: R vs. D	0.00	0.00	0.00	0.28	0.06	0.28	0.11	0.44
2: R vs. S	0.17	0.00	0.00	0.56	0.33	0.06	0.00	0.39
3: R vs. G	0.00	0.00	0.00	0.22	0.00	0.00	0.00	0.22
4: R vs. X	0.04	0.00	0.00	0.41	0.19	0.07	0.04	0.56
5: R vs. X + G	0.19	0.00	0.00	0.44	0.28	0.08	0.03	0.36
6: R vs. X vs. G	0.00	0.00	0.00	0.75	0.11	0.08	0.03	0.75
7: R vs. S vs. G vs. D	0.25	0.00	0.00	0.75	0.42	0.11	0.11	0.75
8: D vs. S	0.00	0.00	0.00	0.22	0.17	0.17	0.06	0.56
9: D vs. G	0.00	0.00	0.00	0.17	0.00	0.00	0.00	0.22
10: G vs. S	0.00	0.00	0.00	0.28	0.06	0.00	0.00	0.33
11: X vs. G	0.00	0.00	0.00	0.26	0.00	0.00	0.00	0.26

For the November classifier data separating the reference sites from the gravesites (Questions 1-7) was possible with every classifier in training with the exception of nmc, which had a high error rate of 17% - 77% depending on the question. When it came to classifier performance in testing, I reran the classifiers three times to make sure the values were correct. Every classifier performed poorly, returning 33%-100% error rates (Table 25).

Table 25. Classification results from the November 15th sampling date. R = reference sites, D = deep graves, S = shallow graves, G = surface bodies, X = subsurface bodies (deep and shallow combined).

Nov 15	Training				Testing			
Question	bpxnc	klldc	quadrc	nmc	bpxnc	klldc	quadrc	nmc
1: R vs. D	0.00	0.17	0.00	0.33	0.67	0.67	0.83	0.67
2: R vs. S	0.00	0.00	0.00	0.17	0.83	0.83	1.00	0.83
3: R vs. G	0.00	0.17	0.00	0.17	0.67	0.33	0.50	0.67
4: R vs. X	0.00	0.00	0.00	0.22	0.67	0.67	0.56	0.56
5: R vs. X + G	0.00	0.00	0.00	0.17	0.58	0.58	0.58	0.58
6: R vs. X vs. G	0.00	0.00	0.00	0.75	0.67	0.50	0.58	0.75
7: R vs. S vs. G vs. D	0.00	0.00	0.00	0.75	0.67	0.75	0.92	0.75
8: D vs. S	0.00	0.17	0.00	0.50	0.83	0.50	0.83	0.67
9: D vs. G	0.00	0.17	0.00	0.50	0.17	0.17	0.50	0.67
10: G vs. S	0.00	0.00	0.00	0.33	0.17	0.17	0.17	0.50
11: X vs. G	0.00	0.11	0.00	0.44	0.44	0.22	0.22	0.56

Trying to separate surface bodies from the other three site types (Questions 9-11) proved feasible using the bpxnc, klldc and quadrc classifiers with 0%-17% error rate in training, but proved to be unfeasible for most of questions in training. bpxnc and klldc had acceptable 17% error rates in questions 9 and 10 but an unacceptable 44% and 22% error rate in question 11. This is the first dataset in which the quadrc performed poorly in testing with only one question, question 10 having an acceptable error rate of 17%. The nmc classifier continued to perform poorly with 50%-67% error rate (Table 25). For the soil spectra classifiers, the general trend was better error rates in training than in testing results. Some classifiers were shown to perform poorly such as the nmc. Out of the three classifiers that performed well, the quadrc classifier provided consistently usable results and would be my first choice for analyzing spectra datasets in the future. The klldc classifier would be my second choice to use. The

bpxnc classifier, while not as consistent as the quadrc and klldc, was useful in some questions and would provide additional support in any analyses

1.1. Vegetation

A One Way ANOVA was applied to the spectral amplitude (delta) and shape (theta) values of the vegetation spectra to determine if there was a difference amongst grave site category means (Table 26). ANOVA for the amplitude (delta) showed the means were not significantly different (p= 0.4520),however the shape (theta) values has a p-value of <0.0001 indicating the at least one of the means was different but not which one.

Table 26. Maximum, Minimum and Mean with Standard Deviation for Vegetation Spectra Delta and Theta Values

	Delta	**Theta**
Max	0.14	0.17
Min	0.01	0.01
Mean	0.04±0.031	0.05 ±0.02

From spectral shape (theta) it is possible to differentiate between background vegetation and other vegetation groups (p-value <.0001). The surface bodies were not statistically different from the remaining three vegetation groups with p-values of 0.53 for surface, 0.91 for reference and 0.59 for deep graves. In spectral amplitude (delta) there was no statistical difference between the means with p-values ranging between 0.073-0.92.

Table 27. Vegetation Spectra Delta and Theta Mean Values for each grave type

	Delta Mean	Theta Mean
Background	0.05	**0.08**
Deep	0.05	0.05
Graves	0.05	0.05
Reference	0.04	0.05
Shallow	0.05	0.05

Unlike the soil spectra, which covered the VIS-SWIR range, the vegetation spectra only covered the 451 bands in the 450-950 nm range (VIS-NIR). The plant spectra data were organized into four categories of interest: Background, Graves (combining shallow and deep), Surface, and Reference. Two types of analysis of the vegetation spectra were performed in MATLAB using the PRTools toolbox. I first employed a feature reduction using the 'featself' function (forward feature selection) to find the optimal number of bands as well as determine which bands were most frequently chosen among the ten research questions of the various combinations between the four vegetation grave site categories.

Table 28. Results of Forward Feature Selection

Question	# of bands	Value
Q1	32	0.69
Q2	17	0.71
Q3	9	0.48
Q4	35	0.94
Q5	34	0.92
Q6	9	0.66
Q7	19	0.91
Q8	14	0.83
Q9	8	0.76
Q10	15	0.95

The 'featself' results for the nine questions enabled me to determine which areas of the spectrum are most critical for classification based on how often they show up in the various query combinations as well as reducing the number of bands used for the classification. Figure 8 illustrates the for bands chosen from the forward feature selection from all questions, whereas Figure 9 is the histogram including bands from all questions without question 5; background versus reference, as a way to highlight any differences between areas of interest (graves and surface bodies) versus the background and reference sites that did not contain any bodies. Figure 8 shows two clusters, around the 450-500nm and the 570-600 nm. The 450-500 nm range corresponds to one of the two areas of chlorophyll and b absorption, the 450 nm area also corresponds to maximum carotenoid absorption.

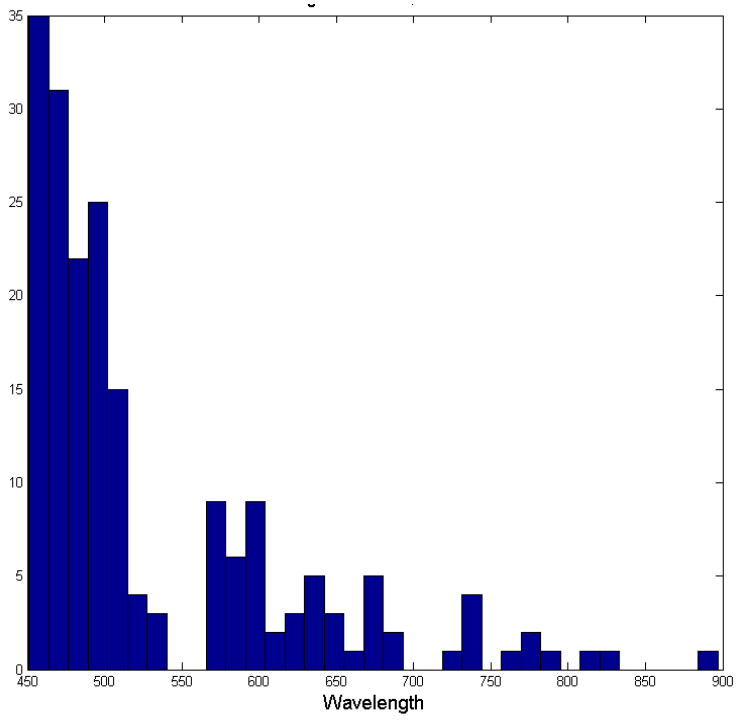

Figure 8. Histogram of Wavelength distribution from the forward features selection analysis of the vegetation spectra across all questions.

Figure 9 still shows a cluster in the 450-500 nm range but with slightly different distribution highlighting a possible area in the 500- 530nm range of

bands to use for separating the spectra of the vegetation from the graves versus the background.

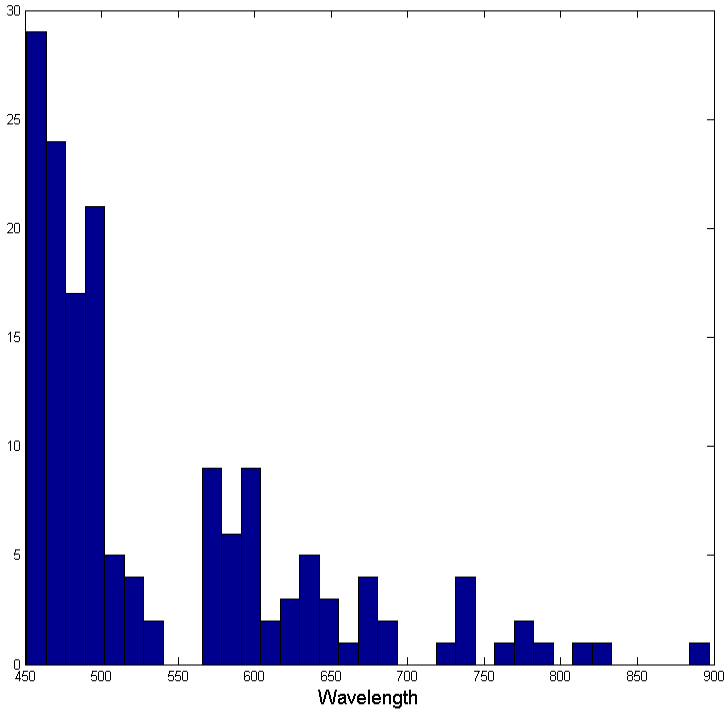

Figure 9. Histogram of Wavelength distribution across all questions except Q5.

The second research question was to see if it was possible to classify the four classes of plant spectra into correct classes, and to determine which classifier produced the lowest error rate. Similar to the previous soil spectral analysis two main themes are prevalent in the questions asked in the classification analysis; 1) are the spectra of the vegetation growing on the classifiable from those growing on the graves 2) are spectra of the vegetation growing around the surface body sites different from those of vegetation growing on the shallow and deep graves and reference sites. Questions, 1, 2, 3,4,5,7 and 10 seek to address the first theme, while questions 6, 8 and 9 seek to answer the surface body theme. Same as with the soil spectra, the analysis was performed on the 'featself' reduced spectra data sets not the full 451 bands.

For the vegetation spectra classifier data separating the background vegetation from the gravesites (Questions, 1, 2,3,4,5,7 and 10) were reasonable with quadrc and nmc in training with a 0-9% error rate however those same classifiers performer poorly in testing with a 24%-61% error rate. The parzenc which performed almost acceptable results in training with 0-27% error rate, had a very good result of 0% error rate in testing, likewise the bpxnc had 7%-56% error rates in training, performed adequately with 0-28% error rate in testing. The klldc fared poorly in both training and testing (Table 29).

Table 29. Selected Vegetation Classifier Results from the November 15th Vegetation. R = reference sites, B =Background, G= Grave (Shallow and Deep burials), and S = Surface burials.

	bpxnc		klldc		quadrc		parzenc		nmc	
Q1 B vs. G vs. R	0.39	0.15	0.38	0.43	0.04	0.45	0.22	0	0.09	0.57
Q2 B vs. G+S vs. R	0.30	0.21	0.28	0.36	0	0.48	0.17	0	0.06	0.39
Q3 B vs. G vs. S vs. R	0.56	0.28	0.62	0.56	0	0.61	0.27	0	0.06	0.61
Q4 B vs. G+S	0.11	0	0.10	0.09	0	0.30	0.01	0	0.03	0.47
Q5 B vs. R	0.07	0	0.24	0.14	0	0.24	0.07	0	0	0.33
Q6 G vs. S	0.34	0.10	0.41	0.40	0.08	0.49	0.16	0	0.04	0.51
Q7 B vs. G	0.11	0	0.11	0.18	0	0.34	0	0	0.05	0.49
Q8 R vs. G+S	0.20	0.19	0.22	0.30	0	0.49	0.19	0	0.05	0.37
Q9 R vs. G	0.30	0.22	0.36	0.40	0.03	0.46	0.27	0	0.08	0.39
Q10 B vs. S	0.05	0.10	0.02	0.05	0	0.02	0	0.21	0.47	0.29

Trying to classify the surface bodies from the other three site types (Questions 6,8 and 9) proved feasible using with quadrc and nmc in training with a 0-8% error rate however those same classifiers performer poorly in testing with a 37%-51% error rate. The parzenc which performed almost acceptable results in training with 16%-27% error rate, had a very good result of 0% error rate in testing, likewise the bpxnc had 20%-34% error rates in training, performed

adequately with 10-22% error rate in testing. The klldc fared poorly in both training and testing (Table 29).

The results of this analysis indicate that cadaver decomposition chemicals play a role in the ability to classify the surface sites from the other sites but that disturbance of the soil plays a greater role in being able to classify between the background vegetation and other sites. This is demonstrated in question five with trying to classify background and reference sites with error rates of 0-14% in four of the five classifiers indicating that they are different enough to classify separately and it must be the soil disturbance that is responsible for the difference.

For future analysis I would utilize the parzenc and klldc classifiers since both had consistently low error rates across all the question and datasets. The quadrc and bpxnc classifiers may prove to be useful later on. The nmc classifier consistently had low error rates in training but high rates in testing the datasets so will be avoided in the future.

The results of the vegetation indices on the vegetation spectra from the Spectral Reflectance Analyzer were imported into JMP v10 and sorted by gravesite class. Then a One Way ANOVA was applied to each Vegetation Index dataset to asses if there were differences in each gravesite category (Table 30). From the ANOVA results, the NPQI and Lichtenthaler indices were eliminated from further analysis. The remaining vegetation indices were subject to basic analysis using a Students t test to determine if the vegetation categories were significantly different and whether there was significant difference in the means in order to separate background vegetation from disturbed/grave site vegetation, and then whether it was possible to separate the disturbed/grave sites into distinct categories based on the index values.

Using the values from SRPI the deep sites were classifiable from all other grave types with p-values ranging 0.001-0.016 but p-values of 0.22-0.94 for all other sites indicate lack of classification between grave types using this index.

Table 30. Results of the One Way ANOVA applied to each Vegetation Index. The * indicates at least one class value is statistically different between gravesite types for each index.

Vegetation Index	ANOVA results
NDVI 1	F (4,214)= 3.4,p=0.0103*
NDVI 2	F (4,214)= 3.29, p=0.012*
SR 1	F (4,214)= 5.86, p= 0.0002*
SR2	F (4,214)= 9.11, p=<0001*
VOG1	F (4,214)= 7.75, p=0001*
VOG 2	F (4,214)= 7.53, p=0001*
VOG 3	F (4,214)= 7.51, p=0001*
PRI	F (4,214)= 4.44, p=0.0018*
SIPI	F (4,214)= 4.00, p=0.0038*
mNDVI	F (4,214)= 5.42, p=0.0004*
SRPI	F (4,214)= 3.06, p=0.0178*
NPQI	F (4,214)= 2.07, p=0.0859
NPCI	F (4,214)= 3.10, p=0.0165*
Lichtenthaler	F (4,214)= 0.38, p=0.8200
Carter VIS	F (4,214)= 3.30, p=0.0120*
Carter Red	F (4,214)= 5.57, p=0.0003*

The result for NPCI are similar with p-values of 0.0008- 0.014 for deep sites versus all other but p-values of 0.097- 0.96 for all other sites. This limits the usability of these indices for classification between grave types. There are no clear results for Carter VIS, some p-values are statistically significant such as between deep and shallow, and deep and surface but others range from 0.09- 0.96. This index is not useful for classifying between grave types.

PRI values classified the background vegetation from the remaining grave types with p-values of <.0001- 0.016. The surface bodies were distinct from the deep (p-value 0.017) and reference graves (p-value 0.033) however the shallow grave sites had a p-value of 0.60. The values between the deep, shallow and reference sites are not significantly different (p-value 0.08-0.91). These results are very similar to NDVI 1 and NDVI 2 with the background being distinct but not

between the disturbed soil sites (p-values 0.072-0.80). SR 1 and SR 2 also have this same pattern with p-values of 0.05-0.80 for the non-background sites. SIPI, Vogelman 1, Vogelman 2, Vogelman 3, Carter Red, and mNDVI all mirror this pattern of background being distinct but not being able to differentiate between the disturbed soil sites. These results limit the indexes to classifying background vegetation from disturbed vegetation.

5. Airborne Images

5.1. RX Anomaly detection

The August 05 2011 CASI flight line was subset to the study site area with spectral subsetting to 455.34nm-898.80nm. The results of RXD and RXD-UTD indicate this is not an efficient method at highlighting areas of disturbed soils or surface bodies. The false colour display had better results through visual assessment; the brighter sites do not correlate to any specific grave site type being reference, shallow and deep burials (Figure 10).

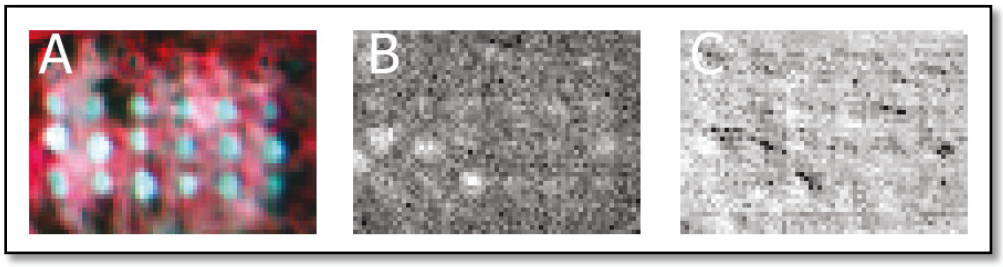

Figure 10. August 05 2011 CASI RDX results, A is false colour display (RGB:749nm, 646nm, 556nm) of easily distinguishable grave sites on image subset, B is same area after RDX analysis, C is RDX-UTD analysis. Bright pixels in the output image represent targets that are spectrally distinct from the image background. Pixel size is 0.79m

For the SASI images the September 09 2011 was subset to the study site area with spectral subsetting to 958-2389nm, the results were more useful, with both the RDX and the RDX-UTD highlighting not only the disturbed soil sites but also the surface bodies (Figure 11).

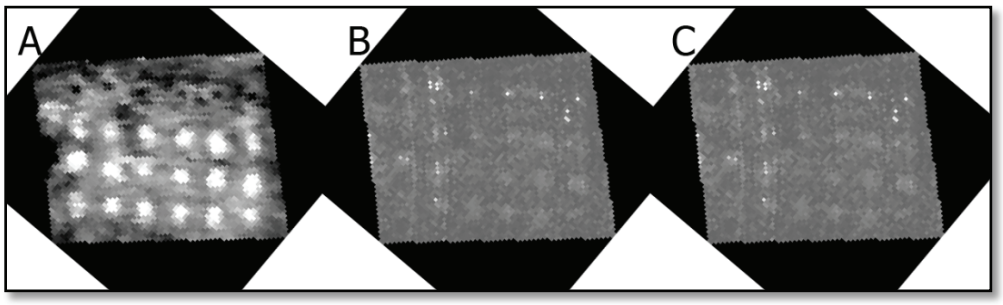

Figure 11. September 09 2011 SASI image RX anomaly detection on 958-2389nm. A is image displayed at 2203.5nm with Linear 2% enhancement, B is RDX result, C is RDX-UDT result. Bright pixels here indicate the surface bodies along the top row, the less bright pixels do show the grave site outlines but are not as apparent as in the plain display of the 2203.5nm band.

The same analysis was performed on the November 15 2011 SASI image. Because the November image is no geocorrected it is harder to locate spatially the pixels to the study site (Figure 12).

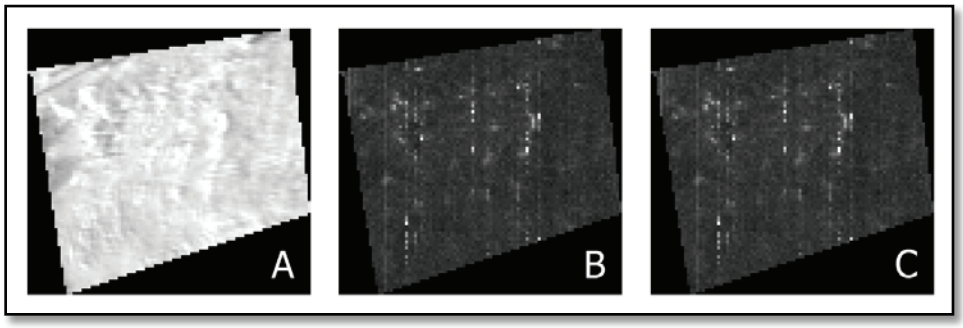

Figure 12. November 15th 2011 SASI image spectral subset to 958-2389nm RX anomaly detection. A is image displayed at 2203.5nm with Linear 2% enhancement, B is RXD results with Linear enhancement, C is RXD-UTD results with Linear enhancement. Bright pixels indicate anomalous pixels

The surface bodies were the brightest pixels indicating they were the most anomalous to the background, the best use of this analysis would be to focus it for surface body detection rather than disturbed soil since there are more efficient and easier to assess ways to look at the disturbed soils. Additionally this analysis did not differentiate between the three disturbed soils site types.

5.2. Vegetation Indices

Due to the limited availability of the CASI sensor I was not able to attempt the more complex analysis I had initially planned to do. Only on one collection date, August 05 2011, did I run any analysis on, this was the last fly over that included the CASI sensor, and since vegetation indices rely on VIS-NIR bands it was impossible to do any analysis using the September 09 and November 15 SASI images. Out of the original 18 vegetation indices, nine were shown to be useful for rapid visual assessments of the airborne data for an area in regards to disturbed soil detection (Figure 13) .These were Normalized Difference Vegetation Index (NDVI), Red Edge Normalized Difference Vegetation ($NDVI_{705}$), Modified Red Edge Normalized Difference Vegetation Index ($m(NDVI_{705})$, and Simple Ratio (SR), Vogelmann Red Edge Index 1 (VOG1), Enhanced Vegetation Index (EVI), Modified Red Edge Simple Ratio (mSR_{705}), Sum Green (SG) Index, and Plant Senescence Ratio Index (PSRI).

However none of the 18 indices were good for detection of the surface bodies. Though given the results of the November 15 vegetation spectra, it is likely that the vegetation indices would be a critical part of gravesite and surface body detection, and therefore any future data collection should include a VIS-NIR sensor.

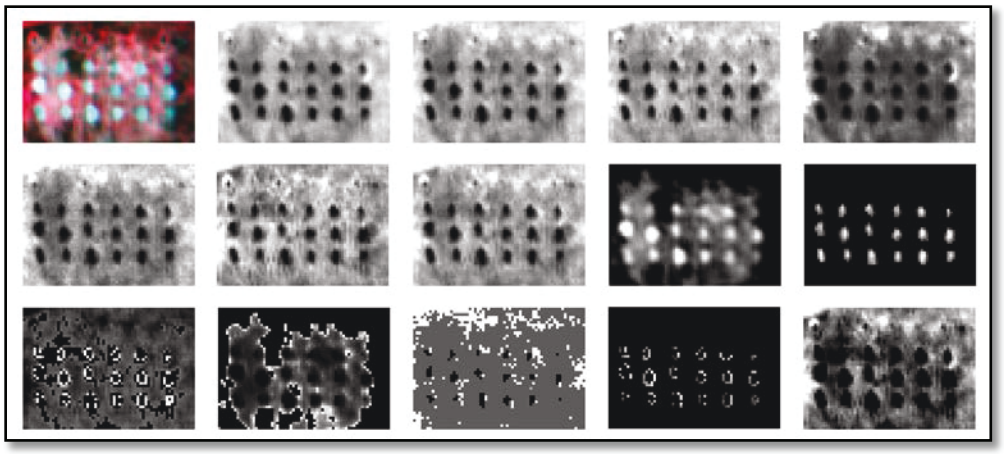

Figure 13. August 05 2011 CASI Vegetation Indices results visualized. Top row: False Colour of site (RGB 749nm,646nm,556nm), Normalized Difference Vegetation Index (NDVI), Red Edge Normalized Difference Vegetation ($NDVI_{705}$), Modified Red Edge Normalized Difference Vegetation Index (m($NDVI_{705}$), and Simple Ratio (SR). Middle row: Vogelmann Red Edge Index 1 (VOG1), Enhanced Vegetation Index (EVI), Modified Red Edge Simple Ratio (mSR_{705}), Sum Green (SG) Index, and Plant Senescence Ratio Index (PSRI). Bottom Row: Structure Insensitive Pigment Index (SIPI), Red Green Ratio (RG), Red Edge Position (REP) Index, Photochemical Reflectance Index (PRI), Atmospherically Resistant Vegetation Index (ARVI)

5.3. SASI Hydroxyl (OH^-)ions

This analysis examines the reflectance data for the 2200 nm region, specifically the 2203.5 nm band in all the SASI images. Relative enhancement of this band was used to highlight the disturbed soils. As can be seen on the pre site set up (July 19, 2010) SASI image (Figure 14), there is little variation in the surface soil.

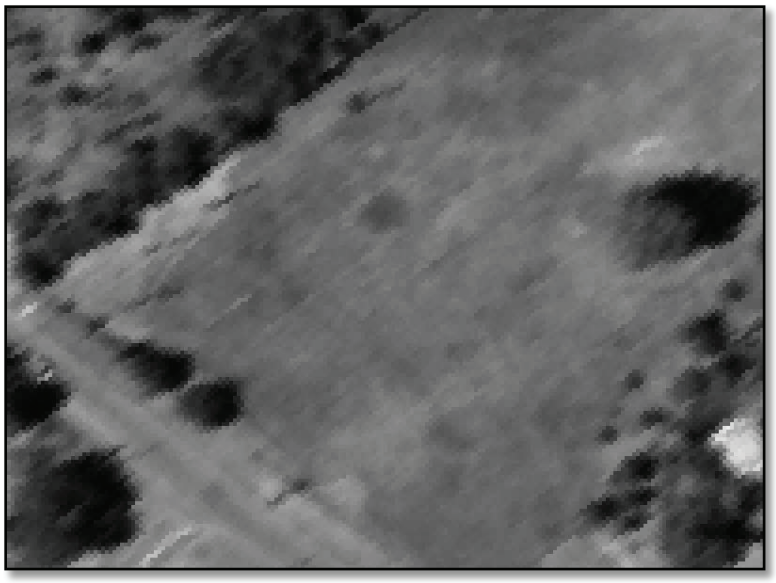

Figure 14. Site pre-set up on July 19, 2011 SASI displayed at 2,203.5 nm showing little variation in surface, relative enhancement using Linear 2%

This is in contrast to the amount of variation seen immediately after site set up with the disturbed soil surface on the gravesites clearly visible marking the individual graves (Figure 15). The linear enhancement seems to provide for easier visual assessment of the site.

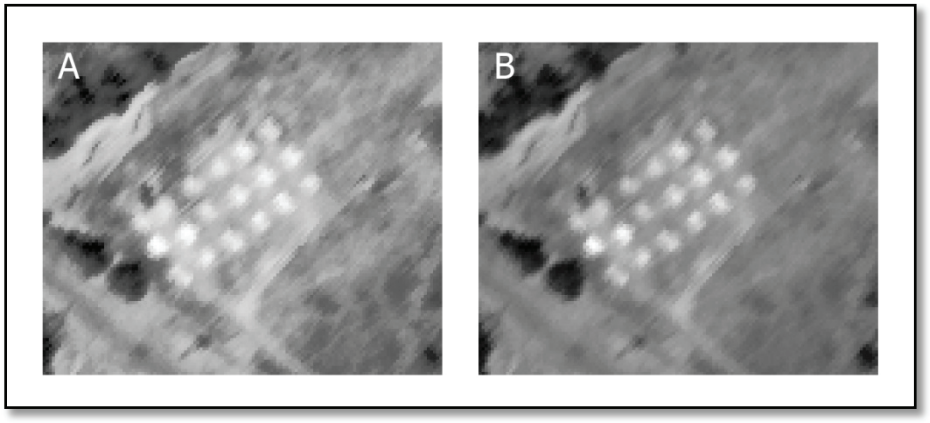

Figure 15. July 20, 2011 SASI image. Site immediately after set up, the backhoe is visible in the upper left corner of the site (dark grey). Image A is Gaussian enhancement, image B is linear enhancement.

The August 5, 2011 SASI demonstrates the effects of the six available image enhancements on the visual assessment of the site (Figure 16). With the exception of the Equalization enhancement, the bright areas of the other enhancements make the locations of the disturbed soils clear.

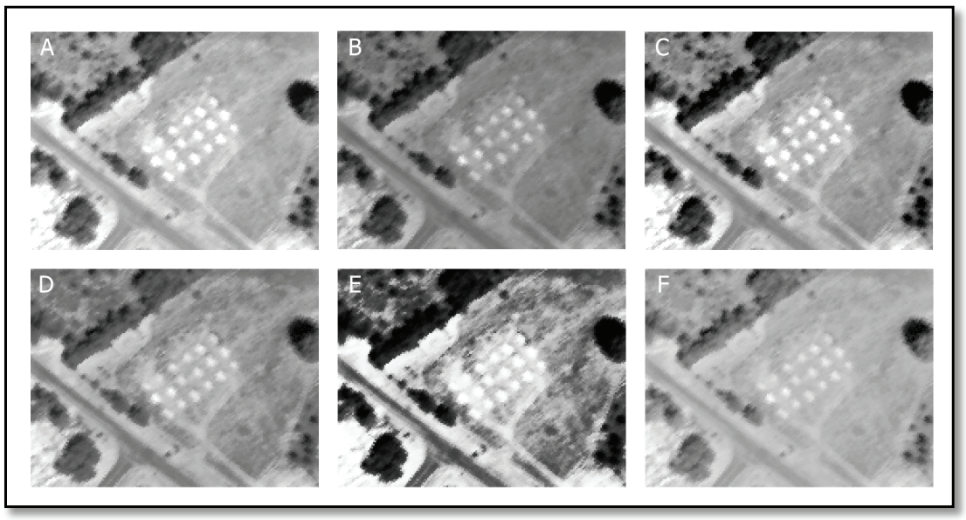

Figure 16. August 5, 2011 SASI images displayed at 2203.5 nm demonstrating the effects of the various relative enhancements; A – none, B- Linear, C- Linear2%, D- Gaussian , E-Equalization, and F-Square means. The bright areas correspond to disturbed soil surface and in this case makes the burial locations clears.

Examination of just the values from the September 9, 2011 image at 2203.5 nm (Figure 17) across the four site types through ANOVA indicates that there is a significant difference in at least one means of the four ($p= 0.001$). The Student T test indicated that the surface bodies were significantly different from the disturbed soil sites (p-value <0.001). The values between the shallow and deep, and reference sites are not significantly different ($p= 0.27$-0.32).

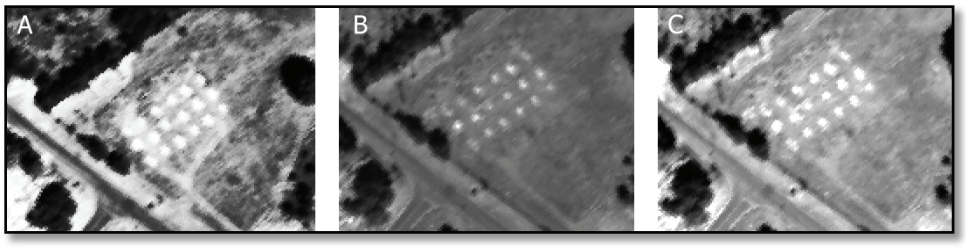

Figure 17. September 2011 SASI images displayed in 2203.5 nm demonstrating the visibility of the disturbed soil of the grave sites as well as the effects of the three relative enhancements; A- Gaussian, B-Linear, and C-Linear 2%

Visualization of the spectra of the four site types shows that the surface bodies have very different spectra from disturbed soil surface (Figure 18). However, the shapes of the soil spectra among the three disturbed soil types are not statistically different.

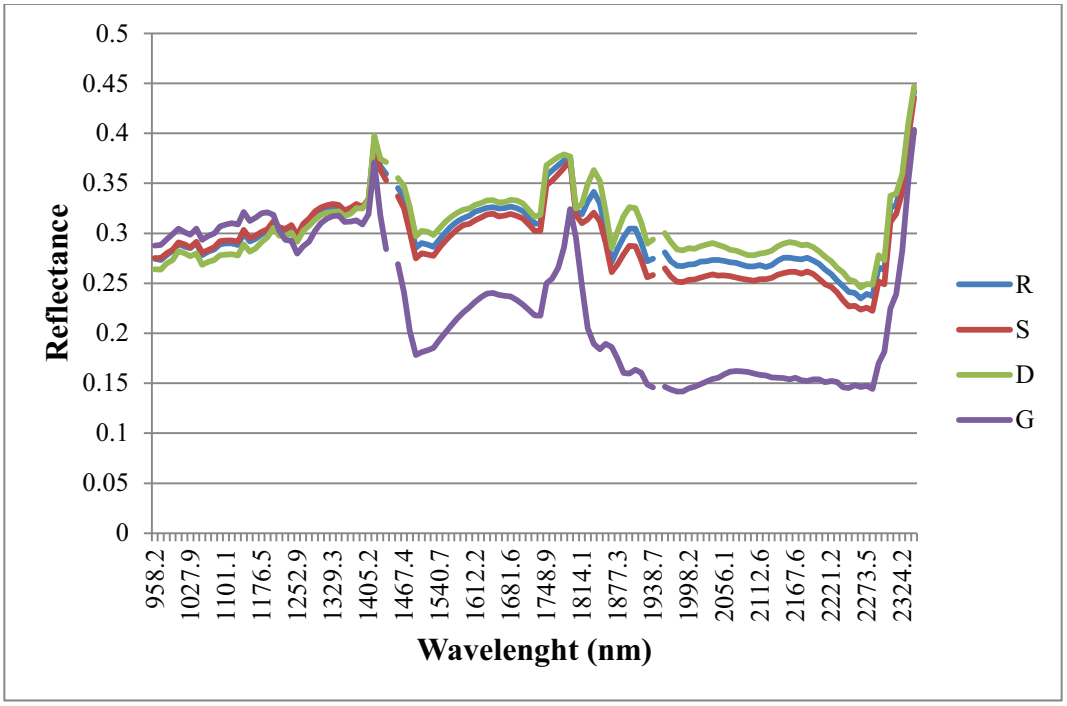

Figure 18. Sept 2011 SASI spectra of the four site types displaying a significantly different shape in surface (G) sites than in the deep(D), shallow (S) or Reference (R) sites. Gaps in spectra are the water absorption bands.

In its simplest application, a relative enhancement at 2203.5 nm could be used to rapidly and visually narrow down areas of interest for further analysis using a different method. Utilizing the SASI imagery with visual assessments at the 2203.5 nm band with a linear 2% enhancement proved to be very efficient at highlighting disturbed soils and while not possible differentiate between reference, shallow and deep burials, this could be used in conjunction with the RXD to highlight the surface bodies to narrowing down areas for investigation.

6. References:

Carter, D. O., Yellowlees, D., & Tibbett, M. (2007). Cadaver decomposition in terrestrial ecosystems. *Naturwissenschaften, 94*(1), 12-24.

Carter, D. O., Yellowlees, D., & Tibbett, M. (2008). Temperature affects microbial decomposition of cadavers (Rattus rattus) in contrasting soils. *Applied Soil Ecology, 40*(1), 129-137

Hall, R. E. (2007). *Soil essentials : managing your farm's primary asset*. Collingwood, Vic.: CSIRO Publishing.

Hopkins, D. W., Wiltshire, P. E. J., & Turner, B. D. (2000). Microbial characteristics of soils from graves: an investigation at the interface of soil microbiology and forensic science. *Applied Soil Ecology, 14*(3), 283-288.

Jones, J. B. (2003). *Agronomic handbook : management of crops, soils, and their fertility*. Boca Raton, Fla.: CRC Press.

Kabata-Pendias, A. (2011). *Trace elements in soils and plants* (4th ed.). Boca Raton: CRC Press.

Sall, J., Creighton, L., & Lehman, A. (2007). *JMP start statistics : a guide to statistics and data analysis using JMP* (4th ed.). Cary, NC: SAS Pub.

Subbarao, G. V., Ito, O., Berry, W. L., & Wheeler, R. M. (2003). Sodium—A Functional Plant Nutrient. *Critical Reviews in Plant Sciences, 22*(5), 391-416.

Towne, E. G. (2000). Prairie Vegetation and Soil Nutrient Responses to Ungulate Carcasses. *Oecologia, 122*(2), 232-239.

Vass, A. A., Bass, W. M., Wolt, J. D., Foss, J. E., & Ammons, J. T. (1992). Time since death determinations of human cadavers using soil solution. *J Forensic Sci, 37*(5), 1236-1253.

Wetterlind, J., Stenberg, B. , & Rossel, R. A. V. (2013). Soil Analysis Using Visible and Near Infrared Spectroscopy In F. Maathuis (Ed.), *Plant mineral nutrients : methods and protocols* (pp. xi, 297 p.). New York: Humana Press.

Conclusion

The study looked at the effects of carcass decomposition on vegetation and soil spectra in a temperate climate zone within the first year of depositing. This study brought together five different types of data to produce a picture of how cadaver decomposition affects the environment around them and how, by knowing what effect to look for, these could be utilized for finding surface bodies or disturbed soil sites that may contain bodies. This research makes a original contribution by developing a framework which may enable investigators to more accurately narrow their search for bodies, conserving resources, money, and time.

As this thesis has shown, soil chemistry analysis is the first step in ascertaining how much these cadaver decomposition chemicals were present (in the form of elements) and how these levels change over the course of the various stages of decomposition. Given the timeline, only the surface bodies had decayed sufficiently enough to impact the soil chemistry directly. Some of the observed changes were due to the disturbance of the soil and surface weathering such as those in magnesium, calcium and iron levels; however others such as sulphur, potassium, and phosphorus were influenced by the nutrients released from the carcasses as they decomposed. These temporal limitations suggest future studies, which would observe the research site over a 2 or 5 year period. Such a elongated period should yield interesting results in terms of monitoring changes in soil chemistry as skeletal demineralization, and more advanced stages of decomposition of the shallow and deep burials take place. This may change which cadaver decomposition chemicals are present in the soil and in what quantities, which in turn would have an effect on the soil and vegetation spectra.

Looking at vegetation pigment extraction and analysis provided interesting results that complement the soil chemistry data, since the vegetation absorbs most of its nutrients from the soil. Vegetation regrowth after soil disturbance was not expected in the first year given the late burial date, however warmer than normal temperatures, particularly in October and November 2011, traditionally a time for plant senescence, enabled collection of healthy vegetation samples from almost all

grave sites. Analysis of the vegetation pigments indicated that there was something occurring on the disturbed sites that affected the chlorophyll and carotenoid levels. Some of these changes were caused by disturbance of the soil, which explains the separability of the background vegetation from the disturbed sites; nonetheless it is clear that carcass decomposition played a key role in enabling separability between the surface bodies and the remainder of the disturbed soil sites. Given the minimal decomposition of the shallow and deep burials at the time of sample collection, it is not surprising there were no statistically significant differences between reference, shallow and deep graves sites.

The soil and vegetation spectra form a connection between cadaver decomposition and airborne images. For the soil spectra, some methods of analysis provided more consistent results. Spectral shape (theta) values were shown to be valuable for isolating surface sites from reference, shallow and deep burial sites. Utilizing classifiers to attempt to classify the data into the four categories yielded mixed results. Most classifiers were able to classify the surface bodies as separate from the disturbed soil sites. None of the classifiers were able to consistently classify the reference, shallow and deep sites from each other. Overall some classifiers performed better than others. Because low error rates the quadrc, klldc and bpxnc classifiers are strongly suggestive of their value as key areas to focus on in future analysis.

The vegetation spectra analysis followed a similar pattern as the soil spectra, however since a different instrument with a more limited spectral range was used to collect the data, the results are not directly comparable. Using the same classifiers and analysis for soil spectra suggested that it is possible to classify the background vegetation from the other sites and to then to distinguish surface bodies from the disturbed soil sites. For future analysis I would utilize the parzenc and klldc classifiers since both had consistently low error rates across all the questions and datasets. The quadrc and bpxnc classifiers may prove to be

useful later on. Ideally any future data collection will be done with the same sensor as the soil spectra collection so that the results can be more comparable.

This leads to the last data section, the hyperspectral data was collected via CASI and SASI sensors aboard a Twin Otter aircraft between July 2011 and November 2011. In many ways the airborne data is the critical aspect of this research project. The analysis of the airborne images turned out to be different from the rather more complex analysis scenarios I had initially planned on utilizing. My focus in analysis shifted from it initial path of identifying and differentiation between background, surface bodies, shallow burials, deep burials and reference sites to a simpler inquiry: whether it was possible to identify and narrow down areas where the soil may contain a body (human or not), and if it is possible to locate surface bodies using airborne sensors. Three relatively simple analysis and assessments were tried and found to be of use.

Out of the original 18 vegetation indices, nine were shown to be useful for rapid visual assessments of the airborne data for an area in regards to disturbed soil detection; however these were not so good for detection of surface bodies. Part of the reason for the shift in analysis was that the later data collections in August 22nd and November 15th 2011 were flown with the SASI sensor only, and therefore the ability to utilize vegetation indices which are dependent on the VIS-NIR wavelengths collected by the CASI sensor was lost. The vegetation indices are a critical part of surface body and gravesite detection and any future data collection should include a VIS-NIR sensor.

The RX anomaly detection was not very efficient at highlighting areas of disturbed soils in either CASI or SASI when compared to the other methods; however is RDX highlighted the surface bodies in the SASI images. Using SASI RXD in conjunction with either vegetation indices or SASI hydroxyl band should highlight both disturbed soils and surface bodies and could be a powerful, and simple to use tool with respect to narrowing down areas for investigation. Similarly, utilizing the SASI imagery with visual assessments at the 2203.5nm band with a linear 2% enhancement proved to be very efficient at highlighting

disturbed soils, but again it was not possible differentiate between reference, shallow and deep burials with that one band alone. This analysis could be utilized as a method to narrow down search areas.

The results of the analysis of the five data groups indicate that cadaver decomposition chemicals play a role in the ability to classify the surface sites from the other sites but that disturbance of the soil plays a greater role in terms of being able to classify between the background and other sites in recent burials. A future potential contribution to our understanding of these processes will be to track how the decomposition of the shallow and deep burials will affect the vegetation pigments, vegetation and soil spectra, and soil chemicals.

This research project successfully demonstrated the potential benefits of using hyperspectral remote sensing as a tool, for narrowing down search areas rather than directly in detecting recent burials and surface bodies. This has significant potential for the strategic deployment resources. Building on this research may allow for the future refining of this as a tool to more narrow focus, such as sites that do contain bodies rather than just disturbed soil areas that may have a body. Such a tool would be of great assistance in investigations to help find missing persons or clandestine grave sites.

Appendix A – ARSL Lab Excel Template

Surface S1	
Spectrum file name	1108080001.asd
ASD Serial number	16478
ASD Program Version	6
ASD File Version	7
Species name	*Soil*
Species code	
Measurement type	Probe
Field photo	NA
Target photo	NA
Photo directory	NA
Raw spectra directory	…\Thesis\Data\Soil\Spectra\Raw
Target type	Soil
Target description (Leaf No.)	S1
Spectrum collection date	Aug 08 2011
Reference time (WR)	9:10:16
Target time	9:10:51
Dark correction time	9:10:13
GPS latitude	NA
GPS longitude	NA
GPS Error (PDOP)	NA
Spectral units	Reflectance
Scaling factor	1
Integration time	30
SWIR1 gain	460
SWIR1 offset	2152
SWIR2 gain	845
SWIR2 offset	2334
No. of dark scans	25
No. of reference scans	25
No. of target scans	25
Wavelength	1108080001.asd
350	0.051262712
351	0.061388676
352	0.064023917
353	0.054771182
…	…

Appendix B

Extraction and Determinations of Chlorophyll a, b and total

The following is a guideline only for the extraction of Chlorophyll from leaf tissue using dimethyl sulfoxide (DMSO) as extractant, and determination of Chlorophylls a, b, and total by visible spectrophotometry. It includes a step-by-step outline of the method, equations, references and a Material Safety Data Sheet (MSDS) for dimethyl sulfoxide.

Prior to reading the absorbances of the samples, the wavelengths should be optimized for the particular spectrophotometer, since they may vary slightly from those listed here.

The toxicity of dimethyl sulfoxide is relatively low; however, its skin penetration properties are similar to those of ethanol, toluene, benzene, carbon tetrachloride and dimethyl formamide, and thus, should be handled with care. Latex or vinyl gloves or finger cots should be worn whenever the liquid is handled, and as much work as possible should be done in a fume hood. All samples collected at the experimental site are placed into 2.5mL Micro tubes, labeled with all of the pertinent information, wrapped in aluminum foil and bagged. When they arrive to the laboratory they are immediately placed in a -20° C freezer until time to analyze them.

Requirements for analysis of leaf/grass samples

1. Fume hood.
2. Variable temperature water bath.
3. Spectrophotometer capable of reading two wavelengths simultaneously.
4. 10ml (or greater) Dispensette (available from Fisher Scientific).
5. DMSO: Dimethylsulfoxide (available from Fisher Scientific): 10ml per sample.
6. 15mL Polypropylene centrifuge tubes (available from Fisher Scientific): one per sample.
7. racks for centrifuge tubes (available from Fisher Scientific).

8. racks for 2.5mL micro tubes (available from Fisher Scientific).
9. Disposable cuvettes, 1cm Path length (available from Fisher Scientific): one per sample.

Procedure for samples not requiring preparation

1. Pre-heat water bath to 65°C
2. Add standard size of plant leaf sample to each 15ml tube
3. Dispense 10ml DMSO into each tube.
4. Place rack into water bath with water level to top of liquid in tube.
5. Lay a piece of aluminum foil over all to exclude light
6. Allow to steep for 20 minutes, then remove from bath and cover with foil.
7. When cooled, carefully transfer, using a disposable plastic pipette, ~3mL of sample to disposable cuvette, keeping covered at all times. Fill only to within ~5mm of top of cuvette to prevent 'creep' of sample down the sides.
8. Read the absorbances for chlorophyll a and b – dependent on instrument calibration.
9. Calculate chlorophyll a, b, and total: the results are reported as mg a, b and total per sample.

Calculations:

Arnon's 1949 equation:

Chl a (g/L) = 0.0127A663 -
0.00269A645

Chl b (g/L) = 0.0229A645 -
0.00468A663

Chl total (g/L)= 0.0202A645 + 0.00802A663

Note: Results are reported as mg/sample = g/L x lL/1000mL x l0mL x l000m

Richardson A.D., S.P, Duigan and G.P, Berlyn. 2002. An evaluation of noninvasive methods to estimate foliar chlorophyll content. New Phytologist.
153:185-194

Hiscox, J.D., and G.F. Israelstam. 1979. A method for the extraction of chlorophyll from leaf tissue without maceration. Can. J. Bot. 57:133

Appendix C

Table 1. Detection Limits and units used for selected elements in the ACME Aqua Regia Digestion analysis

Analyte	Unit	MDL
Mn	PPM	2
Fe	%	0.01
Ca	%	0.01
P	%	0.001
Mg	%	0.01
Na	%	0.01
K	%	0.01
S	%	0.05

Appendix D Raw Results

Table 1. Research Questions for all classifiers across the nine questions. Background (B), reference (R), Surface bodies (S), and Graves containing shallow and deep burials (G).

Question	Components
Q1	B vs G vs R
Q2	B vs G+S vs R
Q3	B vs G vs S vs R
Q4	B vs G+S
Q5	B vs R
Q6	G vs S
Q7	B vs G
Q8	R vs G+S
Q9	R vs G

Table 2. Vegetation Training Classifier Results

Question	knnc	ldc	qdc	bpxnc	klldc	quadrc	parzenc	rnnc
Q1	0.39	0.87	0.86	0.39	0.04	0	0.09	0.57
Q2	0.27	0.27	0.27	0.30	0	0	0.06	0.39
Q3	0.40	0.57	0.57	0.56	0	0	0.06	0.61
Q4	0.10	0.89	0.88	0.11	0	0	0.03	0.47
Q5	0.30	0.67	0.67	0.07	0	0	0	0.33
Q6	0.20	0.41	0.41	0.34	0.08	0	0.04	0.51
Q7	0.14	0.83	0.81	0.11	0	0	0.05	0.49
Q8	0.20	0.20	0.20	0.20	0	0	0.05	0.37
Q9	0.30	0.70	0.70	0.30	0.03	0	0.08	0.39

Table 3. Vegetation Classifier Testing Results

Question	knnc	ldc	qdc	bpxnc	klldc	quadrc	parzenc	rnnc
Q1	0.38	0.88	0.88	0.38	0.22	0.15	0.43	0.45
Q2	0.28	0.27	0.27	0.28	0.17	0.21	0.36	0.48
Q3	0.56	0.57	0.57	0.62	0.27	0.28	0.56	0.61
Q4	0.10	0.90	0.90	0.10	0.01	0	0.09	0.30
Q5	0.21	0.69	0.69	0.24	0.07	0	0.14	0.24
Q6	0.43	0.41	0.41	0.41	0.16	0.10	0.40	0.49
Q7	0.18	0.84	0.84	0.11	0	0	0.18	0.34
Q8	0.21	0.20	0.20	0.22	0.19	0.19	0.30	0.49
Q9	0.30	0.70	0.70	0.36	0.27	0.22	0.40	0.46

Table 4 Soil Spectra Questions for all classifiers across the 11 questions. R = reference sites, D = deep graves, S = shallow graves, G = surface bodies, X = subsurface bodies (deep and shallow combined) selected classifiers results.

Question	Components
Q1	R vs D
Q2	R vs S
Q3	R vs G
Q4	R vs X
Q5	R vs X + G
Q6	R vs X vs G
Q7	R vs S vs G vs D
Q8	D vs S
Q9	D vs G
Q10	G vs S
Q11	X vs G

Table 5. July 28 Soil Training

Question	knnc	ldc	qdc	bpxnc	klldc	quadrc	parzenc	rnnc
Q1	0.24	0.57	0.57	0.05	0.05	0.00	0.57	0.48
Q2	0.22	0.50	0.50	0.00	0.00	0.00	0.50	0.44
Q3	0.00	0.50	0.50	0.00	0.06	0.00	0.50	0.50
Q4	0.23	0.70	0.70	0.00	0.00	0.00	0.70	0.47
Q5	0.18	0.77	0.77	0.00	0.03	0.00	0.77	0.51
Q6	0.33	0.77	0.77	0.00	0.00	0.00	0.77	0.77
Q7	0.33	0.77	0.77	0.00	0.05	0.00	0.77	0.77
Q8	0.24	0.43	0.43	0.00	0.14	0.00	0.43	0.38
Q9	0.29	0.43	0.43	0.00	0.10	0.00	0.43	0.29
Q10	0.00	0.50	0.50	0.00	0.06	0.00	0.50	0.44
Q11	0.20	0.30	0.30	0.03	0.17	0.00	0.30	0.33

Table 6. July 28 Soil Testing

Question	knnc	ldc	qdc	bpxnc	klldc	quadrc	parzenc	rnnc
Q1	0.25	0.55	0.55	0.15	0.30	0.00	0.55	0.30
Q2	0.33	0.50	0.50	0.33	0.39	0.00	0.50	0.50
Q3	0.17	0.50	0.50	0.11	0.22	0.00	0.50	0.61
Q4	0.34	0.69	0.69	0.03	0.21	0.00	0.69	0.38
Q5	0.24	0.76	0.76	0.08	0.26	0.00	0.76	0.42
Q6	0.45	0.76	0.76	0.03	0.34	0.00	0.76	0.76
Q7	0.47	0.76	0.76	0.11	0.45	0.00	0.76	0.76
Q8	0.35	0.45	0.45	0.10	0.05	0.00	0.45	0.35
Q9	0.35	0.45	0.45	0.00	0.05	0.00	0.45	0.40
Q10	0.17	0.50	0.50	0.11	0.11	0.00	0.50	0.56
Q11	0.24	0.31	0.31	0.10	0.17	0.00	0.31	0.45

Table 7. August 08 Soil Training

Question	knnc	ldc	qdc	bpxnc	klldc	quadrc	parzenc	rnnc
Q1	0.00	0.50	0.50	0.00	0.00	0.00	0.50	0.28
Q2	0.50	0.50	0.50	0.17	0.00	0.00	0.50	0.56
Q3	0.00	0.50	0.50	0.00	0.00	0.00	0.50	0.22
Q4	0.00	0.67	0.67	0.04	0.00	0.00	0.67	0.41
Q5	0.17	0.75	0.75	0.19	0.00	0.00	0.75	0.44
Q6	0.00	0.75	0.75	0.00	0.00	0.00	0.75	0.75
Q7	0.00	0.75	0.75	0.25	0.00	0.00	0.75	0.75
Q8	0.17	0.50	0.50	0.00	0.00	0.00	0.50	0.22
Q9	0.00	0.50	0.50	0.00	0.00	0.00	0.50	0.17
Q10	0.17	0.50	0.50	0.00	0.00	0.00	0.50	0.28
Q11	0.11	0.33	0.33	0.00	0.00	0.00	0.33	0.26

Table 8. Aug 08 Soil Testing

Question	knnc	ldc	qdc	bpxnc	klldc	quadrc	parzenc	rnnc
Q1	0.50	0.50	0.50	0.06	0.28	0.11	0.50	0.44
Q2	0.50	0.50	0.50	0.33	0.06	0.00	0.50	0.39
Q3	0.00	0.50	0.50	0.00	0.00	0.00	0.50	0.22
Q4	0.41	0.67	0.67	0.19	0.07	0.04	0.67	0.56
Q5	0.31	0.75	0.75	0.28	0.08	0.03	0.75	0.36
Q6	0.33	0.75	0.75	0.11	0.08	0.03	0.75	0.75
Q7	0.42	0.75	0.75	0.42	0.11	0.11	0.75	0.75
Q8	0.39	0.50	0.50	0.17	0.17	0.06	0.50	0.56
Q9	0.11	0.50	0.50	0.00	0.00	0.00	0.50	0.22
Q10	0.17	0.50	0.50	0.06	0.00	0.00	0.50	0.33
Q11	0.11	0.33	0.33	0.00	0.00	0.00	0.33	0.26

Table 9. August 22 Soil Training

Question	knnc	ldc	qdc	bpxnc	klldc	quadrc	parzenc	rnnc
Q1	0.00	0.50	0.50	0.00	0.00	0.00	0.50	0.28
Q2	0.50	0.50	0.50	0.17	0.00	0.00	0.50	0.56
Q3	0.00	0.50	0.50	0.00	0.00	0.00	0.50	0.22
Q4	0.00	0.67	0.67	0.04	0.00	0.00	0.67	0.41
Q5	0.17	0.75	0.75	0.19	0.00	0.00	0.75	0.44
Q6	0.00	0.75	0.75	0.00	0.00	0.00	0.75	0.75
Q7	0.00	0.75	0.75	0.25	0.00	0.00	0.75	0.75
Q8	0.17	0.50	0.50	0.00	0.00	0.00	0.50	0.22
Q9	0.00	0.50	0.50	0.00	0.00	0.00	0.50	0.17
Q10	0.17	0.50	0.50	0.00	0.00	0.00	0.50	0.28
Q11	0.11	0.33	0.33	0.00	0.00	0.00	0.33	0.26

Table 10. Aug 22 Soil Testing

Question	knnc	ldc	qdc	bpxnc	klldc	quadrc	parzenc	rnnc
Q1	0.50	0.50	0.50	0.06	0.28	0.11	0.50	0.44
Q2	0.50	0.50	0.50	0.33	0.06	0.00	0.50	0.39
Q3	0.00	0.50	0.50	0.00	0.00	0.00	0.50	0.22
Q4	0.41	0.67	0.67	0.19	0.07	0.04	0.67	0.56
Q5	0.31	0.75	0.75	0.28	0.08	0.03	0.75	0.36
Q6	0.33	0.75	0.75	0.11	0.08	0.03	0.75	0.75
Q7	0.42	0.75	0.75	0.42	0.11	0.11	0.75	0.75
Q8	0.39	0.50	0.50	0.17	0.17	0.06	0.50	0.56
Q9	0.11	0.50	0.50	0.00	0.00	0.00	0.50	0.22
Q10	0.17	0.50	0.50	0.06	0.00	0.00	0.50	0.33
Q11	0.11	0.33	0.33	0.00	0.00	0.00	0.33	0.26

Table 11. November 15 Soil Training

Question	knnc	ldc	qdc	bpxnc	klldc	quadrc	parzenc	rnnc
Q1	0.33	0.50	0.50	0.00	0.17	0.00	0.50	0.33
Q2	0.17	0.50	0.50	0.00	0.00	0.00	0.50	0.17
Q3	0.17	0.50	0.50	0.00	0.17	0.00	0.50	0.17
Q4	0.22	0.67	0.67	0.00	0.00	0.00	0.67	0.22
Q5	0.08	0.75	0.75	0.00	0.00	0.00	0.75	0.17
Q6	0.42	0.75	0.75	0.00	0.00	0.00	0.75	0.75
Q7	0.58	0.75	0.75	0.00	0.00	0.00	0.75	0.75
Q8	0.00	0.50	0.50	0.00	0.17	0.00	0.50	0.50
Q9	0.33	0.50	0.50	0.00	0.17	0.00	0.50	0.50
Q10	0.50	0.50	0.50	0.00	0.00	0.00	0.50	0.33
Q11	0.33	0.33	0.33	0.00	0.11	0.00	0.33	0.44

Table 12. November 15 Soil Testing

Question	knnc	ldc	qdc	bpxnc	klldc	quadrc	parzenc	rnnc
Q1	0.67	0.50	0.50	0.67	0.67	0.83	0.50	0.67
Q2	0.67	0.50	0.50	0.83	0.83	1.00	0.50	0.83
Q3	0.67	0.50	0.50	0.67	0.33	0.50	0.50	0.67
Q4	0.56	0.67	0.67	0.67	0.67	0.56	0.67	0.56
Q5	0.42	0.75	0.75	0.58	0.58	0.58	0.75	0.58
Q6	0.67	0.75	0.75	0.67	0.50	0.58	0.75	0.75
Q7	0.83	0.75	0.75	0.67	0.75	0.92	0.75	0.75
Q8	0.50	0.50	0.50	0.83	0.50	0.83	0.50	0.67
Q9	0.33	0.50	0.50	0.17	0.17	0.50	0.50	0.67
Q10	0.50	0.50	0.50	0.17	0.17	0.17	0.50	0.50
Q11	0.33	0.33	0.33	0.44	0.22	0.22	0.33	0.56